Mixed Oxide Silica Aerogels Synthesised Through Non-Supercritical Route for Functional Applications
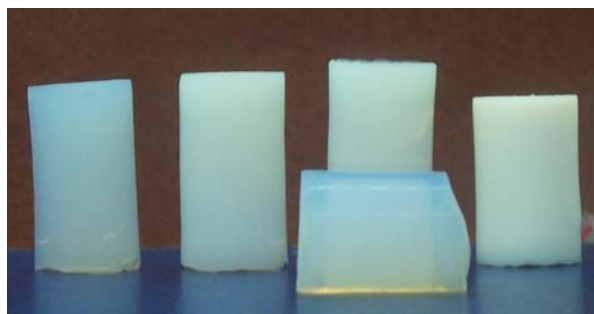
THESIS SUBMITTED TO

COCHIN UNIVERSITY OF SCIENCE AND TECHNOLOGY
IN PARTIAL FULFILMENT OF THE REQUIREMENTS
FOR THE DEGREE OF
DOCTOR OF PHILOSOPHY IN CHEMISTRY

UNDER THE FACULTY OF SCIENCE

By
Aravind P. R.

Under the Supervision of
Dr. K. G. K. Warrier

Materials and Minerals Division
NATIONAL INSTITUTE FOR INTERDISCIPLINARY SCIENCE AND TECHNOLOGY
(Formerly Regional Research Laboratory)
Council of Scientific and Industrial Research
Thiruvananthapuram, Kerala, India - 695019

July 2008

Dedicated to my Loving Parents and Teachers

DECLARATION

I hereby declare that the work embodied in the thesis entitled **"*Mixed Oxide Silica Aerogels Synthesised Through Non-Supercritical Route for Functional Applications*"** is the result of the investigations carried out by me at Materials and Minerals Division, National Institute for Interdisciplinary Science and Technology (NIIST, formerly Regional Research Laboratory, RRL-T), CSIR, Thiruvananthapuram, under the supervision of **Dr. K. G. K. Warrier** and the same has not been submitted elsewhere for any other degree.

Aravind P. R.

Thiruvananthapuram

July 2008

CERTIFICATE

This is to certify that the work embodied in the thesis entitled "*Mixed Oxide Silica Aerogels Synthesised Through Non-Supercritical Route for Functional Applications*" has been carried out by Mr. Aravind P. R. under my supervision at Materials and Minerals Division, National Institute for Interdisciplinary Science and Technology, (formerly Regional Research Laboratory), CSIR, Thiruvananthapuram, in partial fulfilment of the requirements for the award of the Degree of Doctor of Philosophy in Chemistry, under the faculty of science, Cochin University of Science and Technology, Kochi and the same has not been submitted elsewhere for any other degree.

K. G. K. Warrier

(Thesis Supervisor)

Thiruvananthapuram

July 2008

iii

ACKNOWLEDGEMENTS

CONTENTS

Preface

Aerogels are unique solid materials since they have extremely low densities (up to 95% of their volume is air), large open pores of 1-100 nm range and high surface area. The bulk density of aerogels is in the range of 0.03 g/cm^3 to 0.8 g/cm^3 with a surface area of about 1500m^2/g. Silica Aerogels are normally prepared by the hydrolysis and condensation of silicon alkoxides. The gels are normally dried under supercritical conditions since this is the most important step in the synthesis of aerogels.

The increasing industrial application of aerogels in the fields of catalysts, thermal and acoustic insulators, dielectric substrates and in space applications have generated considerable interest in developing aerogels through novel methods in addition to supercritical drying. Active research programme are recently reported for identifying alternative process for supercritical drying as well as for new compositions which will result in high temperature pore stability and functionality. The present work addresses two salient features of aerogels such as a novel synthesis technique involving non-supercritical drying and new mixed oxide aerogels having improving thermal pore stability and functionality.

A general introduction to porous materials, and aerogels and their synthesis makes up the first chapter. The second chapter deals with the synthesis and characterization of Silica-Alumina aerogels by hybrid sol-gel route followed by non-supercritical drying. The thermal pore stability of the mixed oxide aerogels is also presented. The third chapter deals with the synthesis of silica-silica aerogels and their application for simulated nuclear waste confinement. The synthesis of silica-titania aerogels and application as photocatalyst are described in the fourth chapter. The overall conclusion as well as structure-property correlation is presented at the end.

Abbreviations

BET	Brunauer-Emmet-Teller
DTA	Differential Thermal Analysis
FTIR	Fourier Transform Infrared
TEM	Transmission Electron Microscopy
TPD	Temperature Programmed Desorption
XRD	X-ray Diffraction
TEOS	Tetraethylorthosilicate
CA	Composite Aerogels
MTMS	Methyltrimethoxysilane
TMCS	Trimethylchlorosilane

Chapter 1: Introduction

1.1 High Temperature Inorganic Materials

High temperature inorganic materials generally include metallic oxides, silicates, nitrides, carbides, borides, aluminosilicates etc. that are stable towards high temperature. [1-4]. Such materials are generally known as ceramic materials which have its origin from the Greek word "keramos" which means "potters earth". Ceramic products vary from pottery, porcelain, refractories, structural clay products, abrasives, porcelain enamels, cements and glass, nonmetallic magnetic materials, ferroelectrics to glass ceramics. Ceramics can be broadly classified into traditional and advanced ceramics. Traditional ceramics comprises of clay products, cements and silicate glass essentially the starting materials being natural in origin. Advanced ceramics possessing higher temperature resistance, superior mechanical properties, special electrical properties and greater chemical resistivity have been developed in order to fulfill particular needs. The range of inorganic compounds from burnt clays which are natural aluminosilicates find applications in structural, electrical, magnetic, optical and electronic fields. Out of this various oxide ceramic materials, aluminium oxide, silicon oxide, zirconium oxide, titanium oxide etc are most widely used. Electro optic ceramics such as lithium niobate ($LiNbO_3$) and lanthanum modified lead zirconate (PLZT) provide a medium by which electrical information can be performed on command of an electrical signal. Magnetic ceramics form the basis of magnetic memory units in large computers. Metal-Ceramic composites are an important part of the machine-tool industry. Ceramic carbides such as silicon carbide and boron carbide are good abrasive materials. Silicon oxides have

applications as high temperature structural parts, catalysts, in composites and as electronic substrates and packages.

Ceramics can again be classified into dense and porous ceramics according to the extent of porosity in the material. Dense ceramics are relatively pore free and are mainly used for load bearing applications. Porous ceramics can be reticulate materials with open honey comb structure foams with very low densities, membranes with controlled porosity and aerogels with very high surface area having 90% porosity and low densities.

1.2 Porous Materials

A solid material that contains cavities channels or interstices can be regarded as porous. Porous solids are widely used in numerous technological applications such as absorbant, catalysts and membranes [5]. The behaviour and performance of such materials may be determined by many characteristics. Important among which are surface area, porosity and pore size distribution. Physical properties such as density, thermal conductivity and strength are also dependent on the pore structure of that solid. Porosity also influences the chemical reactivity of solid and the physical interaction of solids with gases and liquids [6]. High surface area porous materials are of great importance especially as catalyst, catalyst supports, thermal insulators, sensors, filters, electrodes and burner materials [7]. The science and technology of porous materials has progressed steadily and is expanding in many new directions with respect to processing methods and applications.

The surface area of a given mass of solid is inversely proportional to the size of the constituent particles. In a porous body, in addition to the external surface, there is an internal surface [6]. External surface is contributed by all the prominence and all of those

cracks which are wider than they are deep. The internal surface comprises the walls of all cracks, pores and cavities which are deeper than their width. The particles of a fine powder will stick together more or less firmly under the action of surface forces to form secondary particles. The voids between the primary particles within a secondary particle, together with those between a secondary particle and its neighbours, constitute a pore system [6].

1.2.1 Description of Porous Material

There are a number of terms to describe the porous solid as recommended by IUPAC [7] and are listed in Table1.1.

Table 1.1. Description of porosity terms as recommended by IUPAC

Porous solid	A solid with pore, i.e. cavities, channels, or interstices, which are deeper than their width
Pore volume	Volume of the pore, as measured by a given method which must be stated
Pore size	The distance between two opposite walls of the pores, diameter of cylindrical pores width of slit shaped pores
Pore size distribution	Represented by the derivatives d_{ap}/d_{vp} or d_{vp}/d_{rp} as a function of rp, where ap, vp and rp are the wall area , volume and radius of the pore
Porosity	Ratio of the total pore volume to the apparent volume v of the particle or powder
Surface area	Extent of total surface as determined by a given method under stated conditions
True density	Density of the material excluding pores and inter particle voids
Apparent density	Density of the material including closed and inaccessible pores
Bulk density	Density of the material including pores and inter particle voids

1.2.2 Classification of Pores
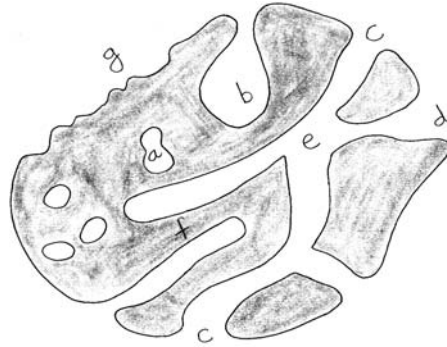
Fig. 1.1. Classification of pores

According to the availability of an external fluid, pores can be classified to closed pores and open pores. Closed pores are totally isolated from their neighbours and surface of the particle. They influence macroscopic properties such as, bulk density, mechanical strength and thermal conductivity but are inactive in such process as fluid flow and adsorption of gases. Pores which have a continuous channel of communication with external surface of the body are called open pores. In Fig.1.1, region (a) represents the closed pores and regions such as (b), (c), (d), (e) and (f) represents open pores. The pores may also be of one end like (b) and (f) and are described as blind or saccate pores

Table 1.2. Classification of pores

Type of material	Pore size
Macroporous	>50 nm
Mesoporous	2-50 nm
Microporous	<2 nm

Based on the size of the pores, they can be classified to microporous, mesoporous and macroporous as described in Table 1.2.

1.2.3 Synthesis of Porous Ceramic Oxides

Porous ceramic materials are synthesised by various methods such as polymer sponge method, foam method, leaching, sintering of particles having a range of sizes, emulsion templating, gel casting, injection moulding, sol-gel synthesis and heat treatment of a ceramic precursor containing carbon rich compound. In all these cases, sintering of porous ceramics is in the temperature range at which the densification is slow so that the porosity is retained and adequate neck growth between particles is obtained. Systems, where slow densification kinetics is possible at high temperatures, will be most ideal for the synthesis of desirable porous ceramics.

Silica porous glasses (SPG) are products of etching of heat treated alkali-borosilicate glasses which are widely used as adsorbents, ion exchange membranes and chemical filters, in applied optics for hologram recording and fabrication of gradient refractive glasses. Two phase sodium borosilicate glass is treated with 0.5 N HCl at 50-60 °C over a period of 5-50 min. The leached sodium borosilicate glass is washed with water and dried at 140 °C to obtain silica porous glass [8].

Introduction of organic phase, which burns off during calcination/sintering in a blend of ceramic oxides, has been another approach to prepare porous ceramics. A few such pyrolysable pore forming agents (PFA) are starch and polyethylene [9]. Such methods have advantages such as control over porosity development and formation of open pore networks because of the percolation of these pyrolysable particles in the green body. Use of polyelectrolytes such as ammonium poly(metha)acrylic acid has shown

excellent pore size distribution [10, 11] creating gradient porosity and has been reported for synthesis of functionally gradient ceramic membrane supports for waste water treatment and similar applications. Porous alumina containing uniform capillaries having an interconnected morphology has been reported by Tomandl [12] where by a gelation method involving alginate gel followed by calcination/binder burn out is carried out. Another organic phase, which is worth indicating, is rice flour which is used along with boehmite to prepare porous alumina [13].

There are two methods for the preparation of cellular ceramics such as polymer sponge method and gel casting foam technique [14]. Polymer sponge method is usually used for the preparation of open cell macrostructures of ceramics. In the gel casting foam technique, the cellular structure results from the controlled generation of foam in an aqueous ceramic suspension containing organic monomers and foaming agents. After the foam formation, polymerization of the monomers promotes setting. Polymer burnout and sintering are carried out to give mechanical strength to the ceramic body. Ceramic-Polymer method [15] has an advantage over the earlier methods in imparting directionality and uniformity of pores in the porous ceramic. Directionality can also be incorporated using simple long chain polymers such as PVA, which are characterized by fewer problems in binder burnout, but has networking long chain structure [16].

Macroporous ceramics with excellent uniformity of pores and distribution could be achieved through emulsion templating [17]. This method is reported to be efficient to obtain porosities as high as 90% with uniform distributed narrow sized pores. Pillared layered structures obtained by intercalation are another class of porous materials. Poly nuclear cations are introduced into the interlayer region of layered structures in order to

increase the spacial gap between the layers to achieve porosity at elevated temperatures [18]. Zeolites, periodic three dimensional framework aluminosilicates containing voids, exemplify microporous solids.

Sol-gel processing can produce much finer pore sizes, as well as narrower particle size distribution compared to conventional methods. Sol-gel technology can also provide simpler processing as well as capability of tailoring microstructure including pore volume, pore size and thickness.

1.3 Sol-Gel Synthesis of Ceramic Oxides

Sol-Gel process is a colloidal route used to synthesise ceramics with an intermediate stage of a sol or a gel state. It generally consists of the preparation of a colloidal suspension of a solid into liquid; viz (sol) and then three dimensional structures of solid enclosing the liquid (gel). The gel on further removal of liquid results in the final material which will be in the hydroxylated state [19, 20]. The starting material used in the preparation of the sol is usually inorganic metal salts or metal organic compounds such as metal alkoxides. In a typical sol gel process the precursor is subjected to a series of hydrolysis and polymerization reactions to form a colloidal suspension or sol. The sol when cast into mould results in the formation of a gel. With further drying and heat treatment, the gel is converted into dense ceramics or glass articles. If the liquid in a wet gel is removed under supercritical conditions; a highly porous and extremely low density material called aerogel is obtained. Applying sol-gel process, it is possible to fabricate ceramic or glass materials in a wide variety of forms, ultra fine or spherical shaped, powders, thin film coatings, ceramic fibers, microporous inorganic membranes, monolithic ceramics and glasses or extremely porous aerogel materials.

1.3.1 Sol

A sol is a stable suspension of colloidal solid particles within a liquid [21]. Particles of a sol are small enough to remain suspended indefinitely by Brownian motion. Sols are classified as lyophobic if there is a relatively weak solvent particle interaction and lyophilic if the interaction is relatively strong. Lyophobic sols exhibit well defined Tyndall effect. In lyophilic sols the particles are largely solvated and this lowers the differences in refractive indices of two phases. The Tyndall effect is due to the scattering of light from the surface of colloidal particles.

1.3.1.1 Stability of sols

Sol particles are held by Van der Waals forces of attraction or dispersion energy. Van der Waals force is propotional to the polarisabilities of the atoms and inversely related to the sixth power of their separation. This Van der Waals force results from transitory dipole-transitory dipole interactions (London forces). It is this London forces that produce long range attraction between the colloidal particles.

The attractive potential for two infinite slabs separated by distance, h is given by

$$V_A = -A/\ 12\ \pi\ h^2$$

$$\text{For atoms,}\ \ V_A\ \alpha\ -1/\ h^6$$

Where A is a material property called Hamaker's constant. Since this attractive force extends over distances of nanometers, sols are thermodynamically unstable [1, 4]. Aggregation can be prevented by erecting necessary barriers of comparable dimensions. This can be done by

i) Electrostatic stabilization

Electrostatic stabilization is explained by DLVO theory. According to this theory the net force between particles in suspension is assumed to be the sum of the attractive Van der Waals forces and electrostatic repulsion created by charges adsorbed on particles. The repulsive barrier depends on two types of ions that make up the double layer, charge determining ions that controls the charge on the surface of the particle and counter ions that are in solution in the vicinity of the particle and act to screen charges of potential determining ions [20]. A schematic representation of electrostatic stabilization is provided in Fig. 1.2.
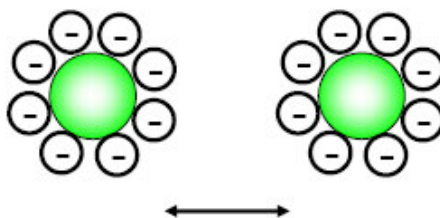
Fig. 1.2. Electrostatic stabilisation

For hydrous oxides the charge determining ions are H^+ and OH^- which establish the charge on the particle by protonating or deprotonating the MOH bonds on the surface of the particle.

$$M\text{-OH} + H^+ \longrightarrow M\text{-OH}_2^+ \qquad (1)$$

$$M\text{-OH} + OH^- \longrightarrow M\text{-O}^- + H_2O \qquad (2)$$

The ease with which the protons are added or removed from the oxide depends on the metal atom. The pH at which the particle is neutrally charged is called the Point of Zero Charge (PZC). At pH greater than PZC equation (2) predominates and the particle is

negatively charged, whereas at pH less than PZC equation (1) gives the particle a positive charge. The magnitude of the surface potential depends on the departure of the pH from the PZC, and that potential attracts oppositely charged ions (counter ions) that may be present in the solution.

According to the standard theory, from Fig.1.3. the potential drops linearly through the tightly bound layer of water and counter ions, called the Stern layer. Beyond the Helmholtz plane h=H, that is, in the Gouy layer, the counter ions diffuse freely. In this region the repulsive electrostatic potential of the double layer varies with distance from the particle, h, approximately according to

$$V_R \propto e^{-K(h-H)}, h \geq H$$
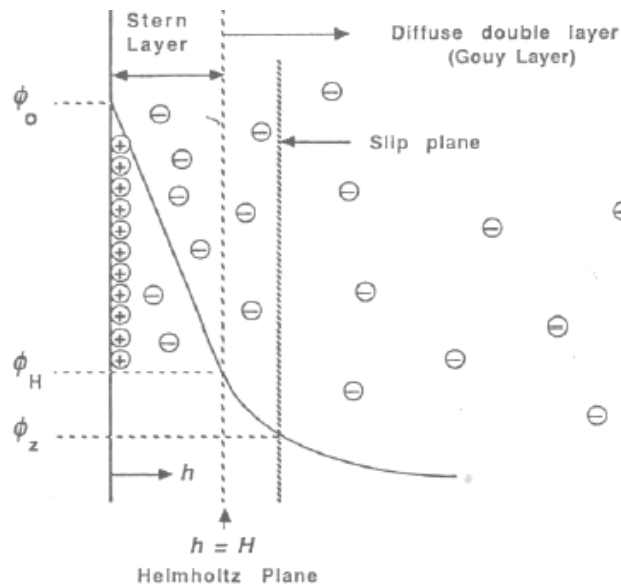
Fig. 1.3. Schematic of Stern and Guoy layers. Surface charge on particle is assumed to be positive

Where1/K is called the Debye Huckel screening length. When the screening length is large (i.e. K is small), the repulsive potential extends far from the particle. This happens when the counterion concentration is small. When counterions are present, the potential

drops more rapidly with distance. Since the repulsive force is propotional to the slope of the potential,

$$F_R = d\,V_R\,/\,d_h \propto K\,e^{-K\,(h-H)}$$

The repulsive force increases with small additions of electrolyte. (i.e F_R increases with K). Large amounts of counterions collapse the double layer. As the concentration of counterions increases, the double layer is compressed because the same numbers of charges are required to balance the surface charge and they are now available in a smaller volume surrounding the particle. On further increase in the concentration of counterions , the double layer repulsions are reduced to the point that net particle potential is attractive and the colloid will coagulate immediately.

When an electric field is applied to a colloid, the charged particles move towards the electrode with the opposite charge. This phenomenon is called electrophoresis. When the particle moves it carries along the adsorbed layer and part of the cloud of counterions, while the more distant portion of the double layer is drawn towards the opposite electrode. The slip plane or plane of shear separates the region of fluid that moves with the particle from region that flows freely. The rate of movement of particles in the field depends on the potential at the slip plane, known as zeta potential. The pH at which zeta potential is zero is called the isoelectric point (IEP). The stability of the colloid correlates with zeta potential to be around 30-50 mV [20].

ii) Steric stabilization

Sols can be stabilized by steric hindrance. For example when short chain polymers are adsorbed onto the surface of particles. There are two components to this stabilization energy. As the sol particles approach one another, the adsorbed polymer

11

loses configurational entropy. This raises the Gibb's free energy of the system, which is equivalent to the development of a repulsive force between the particles. In addition, as the polymer layers overlap the concentration of the polymer in the overlap region increases. This leads to local osmotic pressure and a repulsive force between the particles [22]. A schematic representation of steric stabilization is provided in Fig. 1.4.
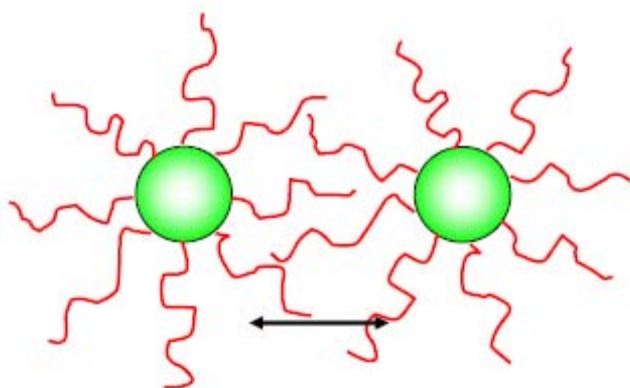
Fig. 1.4. Steric Stabilisation

iii) Stability by solvation

Sol stability coming from energy of solvation is most effective in aqueous system. Energy of solvation is the energy required to disrupt the ordered layer of solvent surrounding the sol particles and to desolvate the surface to allow the particles to come into contact with one another. Because of the energy of solvation, lyophilic sols tend to be more stable than lyophobic sols [23].

1.3.2 Gel

A gel is a porous three dimensionally inter-connected solid network that expands in a stable fashion throughout the liquid medium and is only limited by the size of the container [8]. Gel results when the sol loses its fluidity. An important criterion for gel

formation is that at least part of the solvent is bound. If the solid network is made up of colloidal particles, the gel is said to be colloidal (particulate). If the solid network is made up of sub colloidal chemical units the gel is called polymeric. In particulate gels, the sol gel transition is caused by physio-chemical effect and in the latter by chemical bonding [23].

1.3.3 Sol-Gel Precursors

Metal salts and alkoxides are the two main groups of precursors. The general formula of metallic salts is M_mX_m where M is the metal, X is the anionic group. $M(OR)_n$ is the general formula of alkoxides. Sol-Gel precursors undergo chemical reactions both with water and other species present in the solution.

1.3.4 Application of Sol-Gel Process

Monoliths, fibers, films and nano-sized powders obtained directly from the gel state combined with compositional and microstructural control and low processing temperatures finds applications in various fields.

❖ Thin films and coatings find applications for optical, electronic, protective and porous thin films or coatings.

❖ Monoliths find applications as optical components, transparent super insulation and ultra low expansion glasses.

❖ Powders, grains and spheres used as ceramic precursors or abrasive grains.

❖ Fibers drawn from viscous sols are used primarily for reinforcement or fabrication of refractory textiles.

❖ Gels can be used as matrices for particle-reinforced composites and as hosts for organic, ceramic or metallic phases.

❖ Porous gels and membranes found application in filtration, separations, catalysis and chromatography.

1.3.4.1 Advantages of sol-gel process

Advantages of sol-gel process are given below [24].

❖ Increased chemical homogeneity in multicomponent system.

❖ High surface area for the gels or powders produced.

❖ High purity can be maintained because of the absence of grinding and pressing steps.

❖ A range of products in the form of fibers, powders, coatings and spheres can be prepared with relative ease starting from simple solutions.

❖ Low temperatures for sol-gel process, saving energy and minimizing evaporation losses.

❖ Gels can be molded in the shape of the final desired object, with dimensions enlarged to allow for shrinkage during drying and sintering.

1.3.4.2 Disadvantages of sol-gel process

❖ Hydrolysable organic derivatives of the metals used in sol-gel processing are expensive [24].

❖ The moulded body tends to crack during drying and sintering due to considerable shrinkage [24].

❖ Long processing times [25].

1.4 Sol-Gel Synthesis of Silica

1.4.1 Silica Gels from Aqueous Silicates

The growth of colloidal silica gels from aqueous solutions occurs in three stages [20].

1) Polymerisation of monomers

2) Growth of particles

3) Linking of particles in to chains, the network extends throughout the liquid medium which thickens to form a gel.

The polymerization process can be divided into three approximate pH domains, pH 2, pH 2-7 and pH 7 [20]. pH 2 can act as a boundary since it is the point of zero charge. Above pH 2 condensation rate is proportional to $[OH^-]$ and below pH 2 it is proportional to $[H^+]$.

1.4.2 Hydrolysis and Condensation Reactions of Silicon Alkoxides

Silicate gels are most often synthesised by hydrolysing monomeric tetrafunctional alkoxide precursors employing a mineral acid or base as a catalyst. The most common catalysts are mineral acid or base. The most common alkoxysilane used in sol-gel process are Tetraethylorthosilicate (TEOS) and Tetramethylorthosilicate (TMOS). At the functional group level three reactions are generally used to describe the sol-gel process.

$$\equiv Si\!-\!OR + H_2O \underset{\text{Esterification}}{\overset{\text{Hydrolysis}}{\rightleftharpoons}} \equiv Si\!-\!OH + ROH$$

$$\equiv Si\!-\!OR + HO\!-\!Si\equiv \underset{\text{Alcoholysis}}{\overset{\text{Alcohol condensation}}{\rightleftharpoons}} \equiv Si\!-\!O\!-\!Si\equiv + ROH$$

$$\equiv Si\!-\!OH + HO\!-\!Si\equiv \underset{\text{Hydrolysis}}{\overset{\text{Water condensation}}{\rightleftharpoons}} \equiv Si\!-\!O\!-\!Si\equiv + H_2O$$
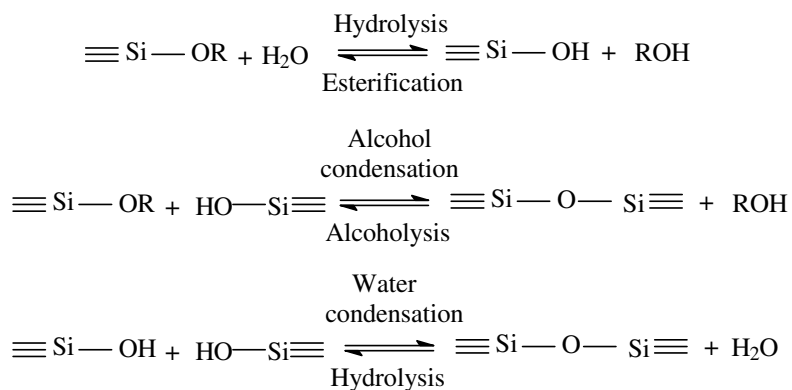
a) Hydrolysis

Hydrolysis occurs by the nucleophilic attack of the oxygen contained in water on the silicon atom as evidenced by the reaction of isotopically labelled oxygen containing

water with TEOS that produces only unlabelled alcohol in both acid and base catalysed systems [20].

$$Si\text{--}OR + H\text{--}O^{18}H \rightleftharpoons Si\text{--}O^{18}H + ROH$$

Hydrolysis is classified into acid catalyzed hydrolysis and base catalyzed hydrolysis. In acid catalysed hydrolysis a mineral acid such as HCl or HNO_3 is used as a catalyst. Under acidic conditions alkoxide group is protonated in a rapid first step. Electron density is withdrawn from silicon making it more electrophilic and thus more susceptible to attack by water. The water molecule attacks from, the rear and acquires a partial positive charge. The positive charge of the protonated alkoxide is correspondingly reduced making alcohol a better leaving group. The transition state decays by displacement of alcohol, accompanied by the inversion of silicon tetrahedron. The hydrolysis rate is increased by substituents that reduce steric crowding around silicon. Electron- providing substituents help to stabilise the developing positive charges also increase the hydrolysis rate.
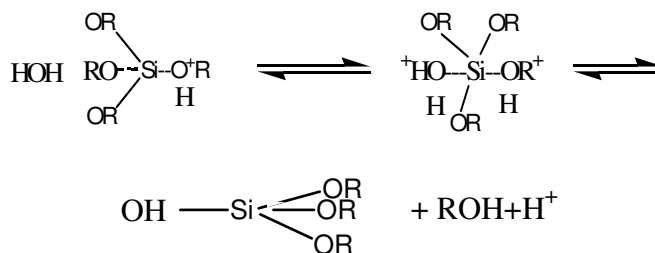
In base catalyzed hydrolysis ammonia is used as a catalyst. The step is the rapid dissociation of water to form hydroxyl anions. The second step involves an SN2–Si mechanism in which -OH displaces -OR with inversion of the silicon tetrahedron.

The mechanism is affected by both steric and inductive factors; however steric factors are more important since silicon acquires little charge in the transition state.

b) Condensation

Polymerisation to form siloxane bonds occurs by either an 1) alcohol producing condensation reaction or 2) by a water producing condensation reaction [20].

$$Si\text{--}OR + HO\text{--}Si \longrightarrow Si\text{--}O\text{--}Si + ROH \quad (1)$$

$$Si\text{--}OH + HO\text{-}Si \longrightarrow Si\text{--}O\text{--}Si + H_2O \quad (2)$$

The overall condensation rate is found to be minimized at around pH 1.5 and maximised at intermediate pH. Protonated and deprotonated silanols are involved in the acid and base catalysed condensation mechanism at pH<2 and pH>2 respectively. Under conditions in which depolymerisation is suppressed, condensation may lead to molecular networks, whereas in which depolymerisation is promoted, restructuring occurs ultimately resulting in the formation of highly condensed colloidal particles.

It is generally accepted that base catalysed condensation, occurs by an SN2-Si mechanism involving a penta or hexa coordinated silicon intermediates or transition states as in the case of the polymerization of silicic acid

The acid catalysed condensation mechanism involves a protonated silanol species. Protonation of silanol makes the silicon more electrophilic and they are more susceptible to nucleophilic attack. The most basic silanol species contained in monomers or weakly branched are the most likely to be protonated. Therefore condensation reactions may occur preferentially between neutral species and protonated silanols situated on monomers end groups of chains etc.

Acid catalysed condensation is a slower transformation than hydrolysis. However silanols protonate more easily when it is at the end of a polymer chain. The polymers obtained are therefore linear with scarcely any branching points.

c) Sol-Gel Transition

The hydrolysis and condensation reactions continue and the resultant clusters grow by condensation of polymers or aggregation of particles until the links form between the clusters to produce a single giant cluster, gel. Nuclear magnetic resonance spectroscopy, Raman and Infrared spectroscopy and X- ray, neutron and light scattering are the different methods for determining the structural evolution during sol-gel transition [13]. Sol-gel transition can also be followed by rheological characterization. In the microanalysis, the gel point is defined as the time at which the viscosity is observed to increase abruptly. The structural evolution in the silicate species in solution is explained in scales of different length. On the short length scale, the nearest neighbour of silicon may be an alkoxide group, a hydroxyl group or bridging oxygen (OSi). On intermediate length scales, oligomeric species (dimers, trimers, tetramers etc) may be linear, branched or cyclic. On length scales large with respect to monomers and small with respect to

polymers, structures may be dense with well defined solid-liquid interface, uniformly porous or tenuous network.

There are both equilibrium growth models and kinetic growth models to describe the gelation process. Flory-Stockmayer is the first among the equilibrium growth models which attempted to describe diverges in cluster, mass and average radius accompanying the gelation [20]. This model is qualitatively successful as it correctly describes the emergence of an infinite cluster at some critical extent of the reaction and provides good prediction of gel point. However it does not provide an entirely realistic picture of polymer growth.

Kinetic growth process produces objects with self-similar fractal properties. Schafer and Keefer [26, 27] postulated Kinetic models for the growth of gel network based on SAXS data. Two most important models are shown in Fig. 1.5. The pH value is the decisive parameter for the relative rates of hydrolysis and condensation of tetra alkoxysilanes [Si $(OR)_4$]. Under acidic conditions (pH 2-5) hydrolysis is favoured, and condensation is the rate-determining step. A great number of monomers or small oligomers with reactive Si-OH groups are simultaneously formed. Under these conditions, reactions at terminal silicon atoms are favoured for electronic reasons. This results in polymeric gels which are formed from chains with few branches; that is small clusters condenses to give a polymer like network with small pores. This process is called reaction limited cluster aggregation (RLCA).

In contrast, hydrolysis is the rate-determining step under basic conditions. Due to different mechanism, reaction at the central silicon atoms of an oligomer unit is not favoured. The resultant network is characterized by big particles and large pores

("colloidal" gels). Hydrolysed species are immediately consumed because of the faster condensation. Condensation of clusters with each other is relatively unfavourable because it requires inversion of configuration at one of the silicon atoms involved in the reaction. There, the clusters grow mainly by condensation of monomers. This model is called reaction limited monomer cluster growth (RLMC) or Eden growth.
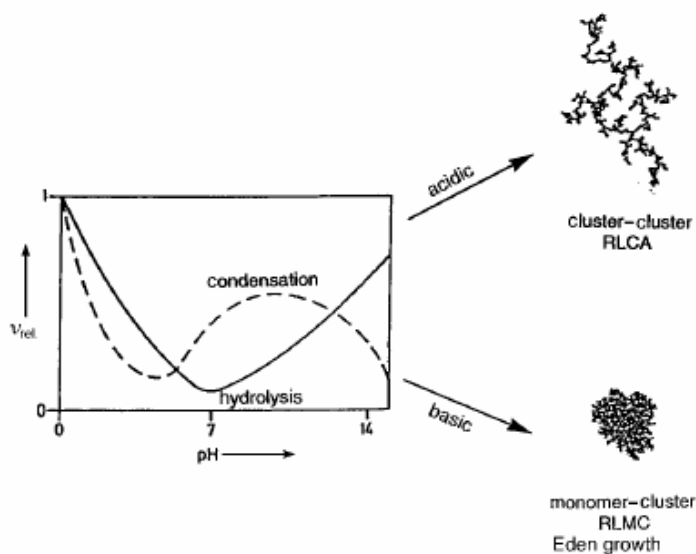
Fig. 1.5. Dependency of the hydrolysis and condensation reaction on the pH, and derived growth models

1.4.2.1 Factors affecting the hydrolysis and condensation

The parameters which influence the hydrolysis and condensation are

- ❖ The kind and concentration of precursors
- ❖ The relative concentration of components in the precursor mixture
- ❖ Kind of solvent
- ❖ The ratio of water to alkoxy group
- ❖ Temperature
- ❖ The pH value

1.5 Aging of Gels

The composition, structure and properties of gels continue to change with time even after the gel point, in a process called aging. The subsequent drying of the gel is strongly influenced by the structure developed during aging. Particulate or polymeric gels are aged essentially to increase their strength prior to drying in order to avoid cracking and/or to alter the microstructure of the wet gels and subsequently the xerogel. Processes involved in aging are categorised as

a) Polymerisation, i.e. increase in connectivity of the gel network

b) Syneresis, i.e. spontaneous shrinkage of the gel with the expulsion of solvent

c) Coarsening, i.e. increase in pore size and reduction in surface area through dissolution and re-precipitation

a) Polymerisation

In silica gels made from hydrolysis of alkoxides, it has been shown by NMR and Raman Spectroscopy that the number of bridging bonds increases long after gelation. The condensation reaction,

$$Si\text{--}OH + HO\text{-}Si \longrightarrow Si\text{--}O\text{--}Si + H_2O$$
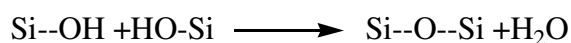
proceeds, because of the large concentration of the silanol groups. As new bonds are formed the flexibility of the network decreases. Further hydrolysis and re esterification can also occur.

$$Si\text{--}OR + H_2O \longrightarrow Si\text{--}OH + ROH$$

$$Si\text{--}OH + ROH \longrightarrow Si\text{--}OR + H_2O$$
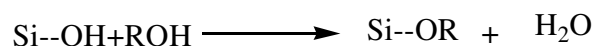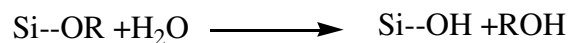
b) Syneresis

As condensation reaction proceeds, the increase in bridging bonds causes contraction of the gel network. The shrinkage of the gel and the resulting expulsion of liquid from the pores is called syneresis. The same condensation reaction that produces gelation leads to syneresis.

$$Si\text{--}OH + HO\text{--}Si \longrightarrow Si\text{--}O\text{--}Si + H2O$$
$$Si\text{--}OR + HO\text{--}Si \longrightarrow Si\text{--}O\text{-}Si + ROH$$
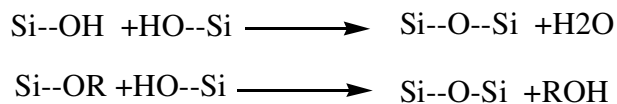
This type of syneresis is called macrosyneresis while microsyneresis is the process of phase separation in which the polymers cluster together creating regions of free liquid and the driving force for this is the greater affinity of polymer for itself than the pore liquid. In organic polymers more syneresis produces turbidity owing to the scattering of light by separate phase. The porosity in dried organic gels is attributed to microsyneresis.

c) Coarsening

Coarsening is a process of dissolution and reprecipitation driven by difference in solubility between surfaces of different radii of curvature. The result of dissolution-reprecipitation is to reduce the net curvature of the solid phase, small particles disappear and small pores are filled in. So the interfacial area decreases and the average pore size increases. However this will not produce any shrinkage because the centers of particles do not move towards one another.

Dissolution and reprecipitation causes growth of necks between particles, increasing the strength and stiffness of the gel. Under aqueous conditions the particle growth is such that the initial aggregates restructure through dissolution reprecipitation to

form larger, more stable particles, thereby consuming the small primary particles. The mechanism by which this occurs is termed as Ostwald ripening mechanism.

The rate of coarsening is affected by factors that affect solubility such as temperature, pH, concentration and type of solvents. The amount of shrinkage that occurs during drying is dependant on the stiffness of the network.

1.6 Drying of Gels

The stages of gel drying are schematically illustrated in Fig. 1.6.
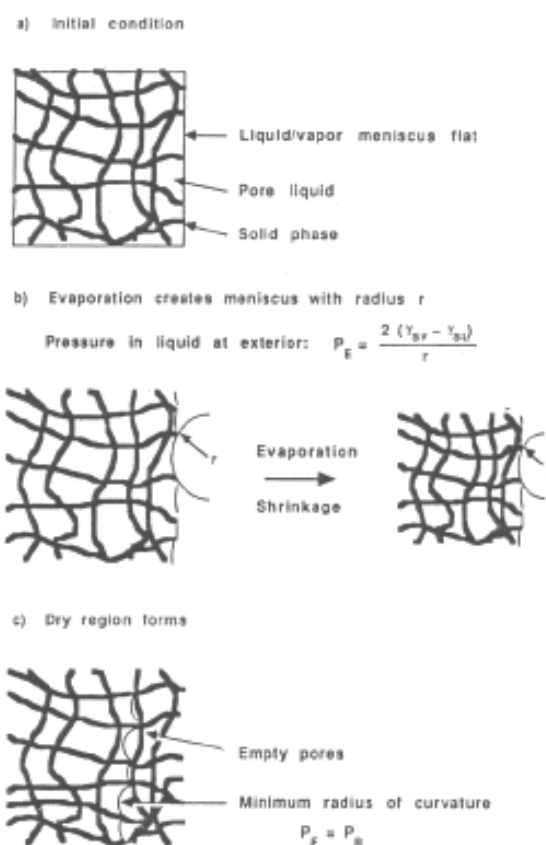
Fig. 1.6. Schematic depiction of drying of a gel

The gel consists of a solid network enclosing a continuous liquid phase. Initially the liquid/vapour interface (meniscus) is flat. Evaporation of liquid from the pores of a gel exposes the solid phase. Since the solid/vapour interfacial energy (γ_{SV}) is larger than

the solid/liquid interfacial energy (γ_{SL}), the liquid tends to squeeze out from the interior

of the gel to cover the exposed solid. As the liquid stretches to cover the solid, tensile

stress develops in the liquid and compressive stress is imposed on to the solid phase. The

meniscus begins to develop a curvature; the pressure in the liquid at the exterior surface

(Pc) is related to the radius of curvature of the meniscus (r) by,

$$Pc = 2(\gamma_{SV}\text{-}\gamma_{SL})/\ r$$

Initially the gel is so compliant that the compressive stress causes viscoelastic

deformation of the solid, drawing it under the surface of the liquid. The network shrinks

as fast as the liquid evaporates, and the liquid/vapour meniscus remains at the exterior

surface of the gel. This is known as the constant rate period.

As the gel shrinks its stiffness increases, because the solid network becomes more

tightly packed and the aging process occurs concurrently. As the gel stiffens, the pressure

(Pc) at the surface of the liquid rises until the meniscus reaches its maximum curvature,

and the capillary pressure,

$$P_R = (\gamma_{SV}\text{-}\gamma_{SL})\ Sp/Vp$$

Where Sp and Vp are the surface area and volume of the (liquid filled) pore space.

When the gel is too stiff to contract under that pressure, the shrinkage stops. This is

known as the leather hard point. The amount of shrinkage that occurs up to that point

depends on the amount of aging. After the Leather hard point the shrinkage drops

abruptly. The leather hard point is also referred to as critical point of drying, as the

chance of cracking of the gel is high at this point. The extend of shrinkage, collapse of

gel structure and structural changes during drying of a gel greatly depends on the initial

gel structure, the aging steps involved before drying, the nature of pore fluid and the method of desiccation.

The dependence of silica sol on pH and different water concentration are shown in Fig. 1.7. The Fig. 1.7 (a) represents a silicate gel made at low pH (<3) and low water concentration (<4 mol water per mol of alkoxide), which has low cross link density. Fig. 1.7 (b) shows a silica gel made at moderate pH (5-7) and water content which consist of more densely cross linked clusters. Fig. 1.7 (c) illustrates coarsening that can occur if a gel is aged in a solution in which the solid phase is slightly soluble, dissolution and reprecipitation causes necks to develop between particles, the aged gel is stiffer and shrinks less when dried. Fig.1.7 (d) represents a colloidal gel, which could be made using a high pH and water content. In all cases drying causes shrinkage. However the extend of shrinkage is maximum for a gel prepared at low pH conditions.

Aging helps to reduce cracking of gels. The cracking of gels can also be reduced by employing surfactants, drying control chemical additives, hypercritical drying and dialysis. Surfactants reduce the interfacial energy and drying control chemical additives (DCCA) like formamide and oxalic acid produce larger and uniform pores. DCCAs also improve the strength of the gel.
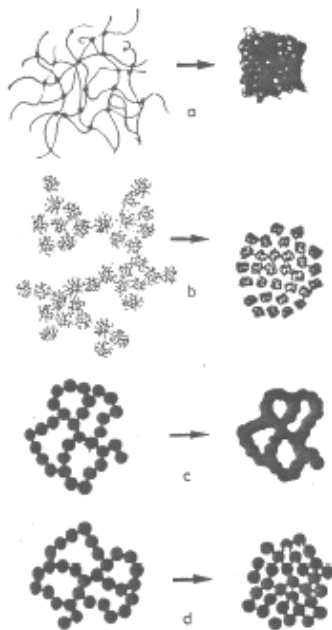
Fig. 1.7. Schematic illustration of gel desiccation with different characteristics

1.7 Aerogels

Aerogel was first developed by S.S. Kistler at the Stanford University in 1931 [28]. They are unique solid materials since they have extremely low densities (up to 95% of their volume is air), large open pores and high surface area. The pore structure extends from scale length 1-100 nm, showing micro as well as macroporosity. The bulk density of aerogels is in the range of 3 mg/cm^3 to 0.8 g/cm^3 with a surface area of about 1500 m^2/g. The properties of silica aerogels are provided in Table 1.3. Aerogels are prepared from molecular precursors by sol-gel processing. Hydrolysis and condensation of metals or semimetal alkoxides or other hydrolysable metal compounds results in the formation of gel whose pore liquid mainly consists of water and/or alcohols. When the pore liquid is replaced by air without altering the network structure or the volume of the gel body, aerogels are obtained. A xerogel is formed upon conventional drying of the wet gels, that

is, by increase in temperature or decrease in pressure with concomitant large shrinkage of the initial uniform gel body.

Table 1.3. Properties of silica aerogel

Property	Range
Bulk density (gcm^{-3})	0.003-0.800
Skeletal density (gcm^{-3})	1.700-2.100
Porosity (%)	80-99.8
Mean pore diameter (nm)	20-150
Inner surface area (m^2g^{-1})	100-1600
Refractive index	1.007-1.24
Thermal conductivity λ (In air 300)($Wm^{-1}K^{-1}$)	0.017-0.021
Modulus of elasticity E (MPa)	0.002-100
Sound velocity C_L (ms^{-1})	<20-800
Dielectric constant	1-2
Loss tangents	10^{-4}-10^{-2} (3-40 GHZ)

The principle for network formation of silica gels also holds for non-silicate inorganic gels. Aqueous solutions of salts as molecular precursors in organic solvents, again usually alkoxides, can be employed for sol-gel processing. The preferred precursors

27

for the synthesis of Al_2O_3 aerogels are Al (OsBu) $_3$ and Al (OtBu) $_3$. Teichner et al. investigated the basic chemistry of aluminium alkoxides in the context of preparing alumina aerogels [29-31]. The first Titania and Zirconia aerogels were prepared by Teichner et al. as early as 1976 [29]. V_2O_5 aerogels [32, 33], Cr_2O_3 aerogels [34, 35], Fe_2O_3 [34-36], MoO_2 [29] and Nb_2O_5 [37] aerogels are also reported. Recently Yanping P Gao et al. synthesised Zinc Oxide aerogels by alcoholic sol-gel processing of an alcoholic Zinc Nitrate solution with propylene oxide as gelation inhibitor [38].

1.7.1. Mixed Oxide and Metal Doped Aerogels

Binary and Ternary oxide aerogels are also reported. TiO_2-SiO_2 and Al_2O_3-SiO_2 aerogels were reported by D.C.M. Dutoit et al. [39] and F. Chatput et al. respectively [40]. T. Heinrich et al. reported Mullite aerogels [41]. Aerogels of Fe_2O_3-SiO_2 [42], V_2O_5-MgO [43] and NiO-SiO_2-MgO [44] are also reported.

D.C.M. Dutoit et al. [45] prepared vanadia-silica mixed oxide aerogels via sol-gel method, involving acid catalysis together with prehydrolysis in order to achieve matching reactivities of vanadium (V) oxide triisopropoxide and tetraethoxy silane. The gels were supercritically dried by CO_2 supercritical drying at 313 K. The effect of composition, aging and textural properties of the solids were investigated.

J. B. Miller et al. [46] described preparation and characterisation of zirconia-silica aerogels having different ratios of Zr:Si. The samples were prepared both with and without silica precursor prehydrolysis and the authors found out that prehydrolysed samples display improved molecular scale homogeneity as evidenced by total acidity and Bronsted populations.

S. Blacher et al [47] discussed methods to extract information on the texture from nitrogen adsorption-desorption data of mixed SiO_2-ZrO_2 aerogels prepared under different conditions. The data have been analysed following two methods a) the classical Brunnar-Emmett-Teller theory and extensions and fractal FHH theories.

P. Pirard et al. [48] in another work obtained silica-zirconia aerogels by supercritical conditions. The modifications of the aerogel porous texture as a function of chemical composition and thermal treatments are investigated using adsorption-desorption isotherm analysis, mercury porosimetry, electron microscopy and X-ray diffraction.

Vanadia-silica mixed oxides derived from sol-gel preparation were tested in the partial oxidation of n-butane and 1,3-butadiene to furan [49]. The dependency of furan selectivity on morphological properties and vanadium dispersions in the silica matrix has been studied. Butane was mainly transformed to carbon oxides and the best furan selectivity was only 3.6%. In butadiene transformation, 25% furan selectivity was achieved at 20% conversion, but the coke formation was significant.

T. Osaki prepared NiO-Al_2O_3 aerogel from a mixture of cyclic nickel glycoxide, $(CH_2O)_2$ Ni and boehmite sol by increasing the pH gradually [50]. The gel was later supercritically dried and subsequently calcined.

P. Fabrizioli et al. [51] prepared Manganese oxide-silica mixed oxide aerogels with different morphological and chemical properties using sol-gel method and ensuing extraction of the solvent with supercritical CO_2. Two types of manganese precursor, varying hydrolysis condition of silica and manganese precursor, influence of base addition for gelation and calcination temperature were investigated. Base addition

strongly affects the textural properties and the catalytic performance of the aerogels in the selective oxidation of ammonia. The state of manganese also strongly affects the reaction.

D. J. Rosenberg et al. [52] prepared sulfated silica-zirconia mixed oxides containing 33 mol% Zr by sol-gel routes with sulfate/zirconia molar ratio varying between 0.2 :1 and 0.3 :1. The influence of the added sulfate introduced by both insitu and exsitu methods on the bulk and surface properties were examined.

Zhi-Gang Wu et al. [53] prepared a series of mesoporous SiO_2-ZrO_2 aerogels with various zirconia content (10–90 wt %) by the sol–gel method followed by supercritical drying. The characterization of aerogels was performed by XRD, FT-IR, 29Si liquid-state NMR, and BET N_2 adsorption. The results showed that (i) the aerogels have type IV (BDDT) profile which is the typical of mesopores in the interval between $2 < Dp < 50$ nm; (ii) the specific surface areas varied from 340 to 730 m^2/g with (SBET) $_{MAX}$ = 735:5 m^2/g for the aerogel with 10 wt% zirconia and the surface areas decreased with the increase of zirconia; (iii) all the aerogels with different zirconia content remained amorphous or poorly crystallized after calcination in air at 500 °C; (iv) a large number of Si-O-Zr bands existed in the aerogels indicating a homogeneous distribution of the components on the atomic scale. In addition, using inorganic salt as zirconium source instead of the expensive and toxic zirconium alkoxide was very economic

N. Moussa et al. [54] prepared Vanadia-silica xerogel and aerogel catalysts, with various V/Si molar ratios (0.05, 0.1, and 0.2), by sol–gel processing. Gels were obtained under acid catalysed conditions (HNO_3) from vanadium (III) acetylacetonate (V (acac) $_3$) and tetraethoxysilane (TEOS). Under these conditions, it was found that the gelation time increased with V/Si molar ratio. The structure and catalytic properties of the mixed

oxides were found to be mainly influenced by the V/Si molar ratio and drying mode. The catalytic behaviour of the xerogels and aerogels was tested in the epoxidation reaction of trans-2-hexen-1-ol. Using a molar ratio TBHP/alcohol = 4/7, the epoxide yield was about 50% in the presence of xerogels, with ca. 8 h required to achieve stationary-conversion conditions in this heterogeneous-catalysis system. In contrast, the aerogel catalysts required only 2 h to reach stationary conversion conditions, due to partial leaching of the vanadium species from the solid and the associated contribution of a relatively rapid homogeneous catalysis mechanism to the overall conversion. These differences in catalytic behaviour were related to the vanadium species and the texture of the catalysts.

Chien-Tsung Wang et al. prepared Nanostructured pure and silica-supported iron oxide materials by the aerogel approach [55]. They were then evaluated for methanol oxidation in an ambient fixed-bed flow reactor from 225 to 300°C.

Filippo Somma et al. synthesised Niobia–silica mesoporous materials (xerogel, aerogel and MCM type) by sol–gel techniques using different co-solvents as templates [56]. All materials are active catalysts in the epoxidation of cyclohexene with hydrogen peroxide, but only meso–macroporous aerogels give a stable and recyclable catalyst.

M.I. Kim et al. [57] prepared a series of V_2O_5–TiO_2 aerogel catalysts by sol–gel method with subsequent supercritical drying with CO_2. The aerogel catalysts showed much higher surface areas and total pore volumes than V_2O_5–TiO_2 xerogel and impregnated V_2O_5–TiO_2 catalysts. The selective oxidation of hydrogen sulfide in the presence of excess water and ammonia was studied over these catalysts and the aerogel catalysts showed very high conversion of H_2S without harmful emission of SO_2.

Chien-Tsung Wang et al. [58] prepared Nanoparticle gold/iron oxide (maghemite) aerogels and were used as photocatalysts to degrade Disperse Blue 79 azo dye in water under ultraviolet light illumination. Addition of gold species caused the light absorption to shift towards the red visible region, and thus the band gap energy reduced. Photocatalytic activity enhanced with increasing Au loading up to 8 wt%, and the activity increase was dependent upon catalyst pretreatment.

To incorporate metal components into the gel matrix, the formed aerogels can be impregnated with solutions of the corresponding metal salt. Alternatively, suitable metal salt can be added to precursor soln. which results in the incorporation of the metal compounds into the gel during sol-gel processing. Cu/SiO_2 [59], Cu/Mgo [60], $Cu/ZnO/Al_2O_3$ [60], Pt/TiO_2 [61], and Pt/Al_2O_3 [62] are reported. The spectrum of properties of aerogels is widened or improved without influencing the existing positive properties, such as good heat insulation, transparency and high surface area [63].

An interesting alternative to the inorganic aerogels was developed by Pekala et al. [64]. Purely organic aerogels were synthesised by polymerisation of multifunctional organic monomers in dilute Solution followed by supercritical drying. Resorcinol-Formaldehyde and Melamine-Formaldehyde were the first precursor mixtures for organic sol-gel chemistry [65].

1.7.2 Silica Aerogels

Silica aerogels (Fig. 1.8) are nanostructured solids usually synthesised by sol-gel process. They have many fascinating properties such as high surface area (500-1000 m^2/g), low bulk density and low thermal conductivity (~ 0.02 $Wm^{-1}K^{-1}$) (A description is provided in Fig. 1.9 A) [66-69].

Fig. 1.8. The wonder material "AEROGEL"

A

B
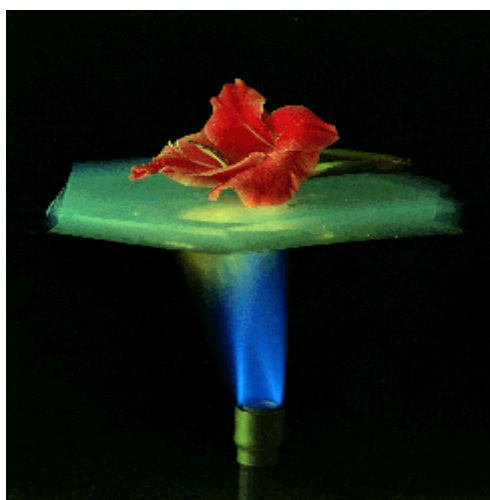
Fig. 1.9 A. Aerogels have excellent insulating properties, as shown here for a silica aerogel tile.

Fig. 1.9 B. In an experiment using a special air gun, particles are shot into aerogel at high velocities. Close up of particles that have been captured in aerogel are shown here. The particles leave a carrot-shaped trail in the aerogel.
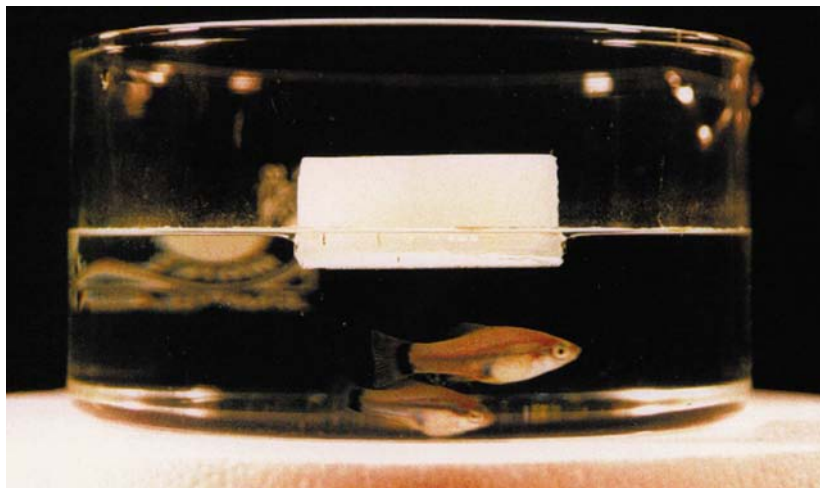
Fig. 1.10. Hydrophobic Silica aerogels

These features have led the aerogels for various scientific and industrial applications such as super thermal insulation [70, 71], acoustic insulation [72], Cherenkov radiation detectors [73, 74], low dielectric constant aerogel films in ultra large scale integrated circuits [75], super hydrophobic aerogels for oil spill clean up (See Fig. 1.10) [76], window applications [77], catalysts [78], Internal Confinement Fusion (ICF) targets in thermonuclear fusion reactions [79], cosmic dust capture (See Fig. 1.9 B) [80] and waste management (gas absorption, radioactive waste confinement) [81-84].

1.7.3 Structure of Aerogels

Aerogels are supposed to retain the wet gel structure. Nitrogen adsorption studies, mercury porosimetry, microscopic techniques and scattering techniques (SAXS and SANS) [85] are used to explore the structure of aerogels. The structure of particulate silica is shown in Fig. 1.11. The aerogels consists of three levels of structure [86, 87]. In the range up to 1nm, a primary structure which consists of compact silica (Density- 2200 kg/m^3) is present. These massive particles gradually build up to a porous secondary structure (5-10nm) as shown in Fig. 1.11A. The further build up leads to branching and

cross linking of chains until for length scales of about 50 to100 nm as shown in Fig. 1.11B. When a silica aerogel monolith breaks under force only secondary particle lose contact with one another while primary particle remains undisturbed. So the mesoporous space between these particles would be maintained. The silica aerogels exhibit microstructures consisting of loosely interconnected silica particles, which form an open network.

A   B
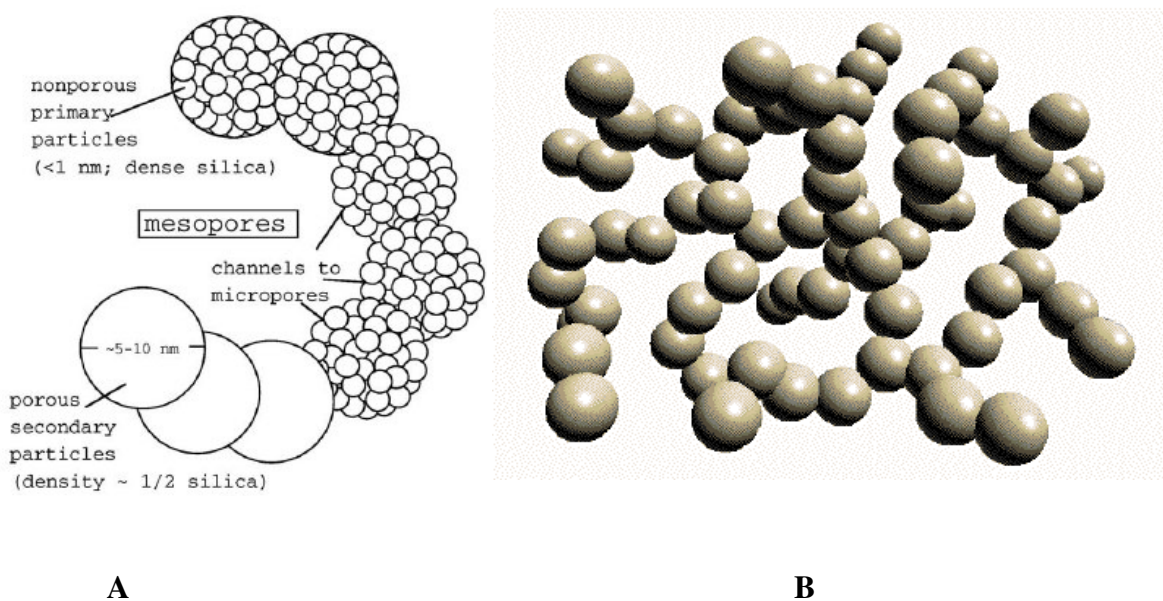
Fig. 1.11. Structure of Silica aerogels

1.7.4 Synthesis of Aerogels

Aerogels are normally prepared by the hydrolysis and condensation of silicon alkoxides. The silicon alkoxides on hydrolysis and condensation gives a gel. The drying of the gels is the most important step in the synthesis of aerogels.

Drying

Drying is governed by capillary pressure and the shrinkage of the gels during drying is driven by the capillary pressure, P_c according to the equation,

$$P_c = 2\gamma \, Cos \, \theta / \, r_p$$

Where γ is the surface tension of the pore liquid, r_p is the pore radius, which is represented by

$$r_p = 2Vp/Sp$$

where V_p and S_p are pore volume and surface area, respectively. They are critical parameters. The capillary tension developed during drying may reach 100-200 MPa.

i) Supercritical drying

Under supercritical conditions, that is, above critical temperature (Tc) and critical pressure (Pc) there is no distinction between the liquid and vapour phases, i.e., there is no liquid/vapour interface and therefore no capillary pressure [88]. The wet gel is put into the supercritical state, and therefore there are no liquid/gas interfaces in the phases during drying. The wet gel is placed in an autoclave and covered with additional solvent. Drying out of the samples (which would lead to the formation of cracks), is thus avoided, and the critical volume V_c is reached. After the autoclave is closed, the temperature is slowly raised in an increase of pressure (Pathway A in Fig. 1.12). Both the temperature and the pressure are adjusted to values above the critical point of the corresponding solvent (Tc, Pc) and kept there for a certain period of time. This ensures that the autoclave is completely filled with supercritical fluid. The fluid is then slowly vented at constant temperature, which results in a drop in pressure. When ambient pressure is reached, the vessel is cooled to room temperature and then opened. Drying is often performed in a way that the vessel is prepressurised with nitrogen to avoid evaporation of the solvent (Path B in Fig. 1.12). The phase boundary between the liquid and the gas must not be crossed during drying [88-90].

In principle, different organic solvents can be used for drying. The critical constants of the most common drying fluids are listed in Table. 1.3. Shrinkage can be eliminated almost completely by the use of supercritical drying. Unfortunately supercritical processing is energy intensive dangerous and expensive, and therefore has severely restricted the commercial production of aerogels [91, 92].
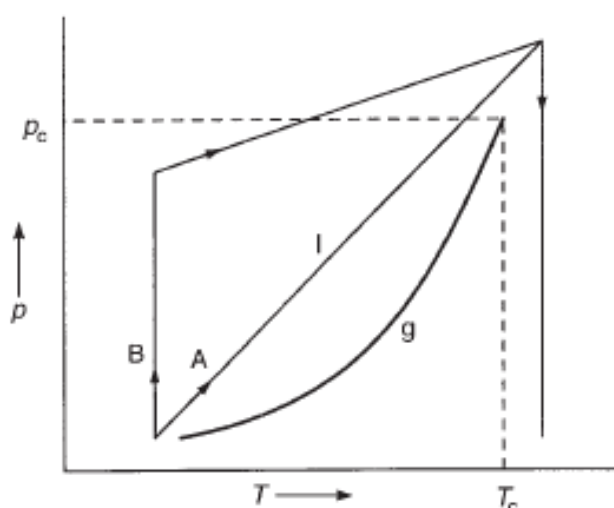
Fig. 1.12. Schematic representation of the principle of supercritical drying. At the critical point (T_c, P_c) the densities of the liquid (l) and the gas (g) are equal. Supercritical drying can be performed along pathway A or B.

Table 1.3. Critical constants for some solvents

Solvent	$T_c[°C]$	$p_c[Mpa]$	$V_c[cm^3 mol^{-1}]$
methanol	240	7.9	118
ethanol	243	6.3	167
acetone	235	4.7	209
2-propanol	235	4.7	
H_2O	374	22.1	56
CO_2	31	7.3	94
N_2O	37	7.3	97

ii) Supercritical drying with carbon dioxide

An alternative to drying in organic solvents is the use of liquid carbon dioxide [93]. The major safety concerns associated with supercritical drying was considerably reduced by the replacement of fluid by liquid carbon dioxide (very low critical temperature and moderate pressure). But this method adds cost and brings in the necessity of extensive and time consuming solvent exchange [94].

iii) Freeze drying

Here the phase boundary between the liquid and gas is avoided as in the case of supercritical drying. The pore liquid is freezed and is sublimed under vacuum [20]. However aging periods have to be extended to stabilize the gel network and the solvent must be exchanged with another having low expansion coefficient. A high pressure of sublimation and low freezing temperatures should also be achieved by the addition of salts. Another disadvantage of this method is that the network may be destroyed by crystallisation of the solvent in the pores. Cryogels are only therefore obtained as powders.

iv) Ambient pressure drying

To make aerogels interesting for larger scale commercial application, one must avoid the most expensive and risky part of the preparation: supercritical drying. Therefore, the interest in alternative ways for exchanging the pore liquid in the gels by air is very high. R. Deshpande et al. studied the effect of surface tension of a wide variety of aprotic solvents on the two-step acid/base catalysed silica gel that has been aged in alcohol and water baths followed by various aprotic solvents [95]. P.J. Davis et al. infiltrated the gel network by sodium silicate or Tetraethoxysilane (TEOS) prior to drying

[96]. In another work, the authors aged the gels in a series of alcohol and water bath and the physical and chemical structure of the gels were measured [97]. The authors noticed that the alcohol aging lead to small pore size distributions. The alcohol aged gels had a surface area of 1500-2000 m^2/g in the wet gel state, which decreased to 1000 m^2/g after drying. The water aged gel had a surface area of 1000 m^2/g in the wet state which subsequently deceased to 500 m^2/ g in the dry stage. S. Haereid et al. aged the TMOS derived gels in solutions of TEOS and dried at ambient pressure. The authors proved that the shrinkage during drying can be reduced and hence low density gels were obtained [98]. M.-A. Einarsrud et al. aged Tetramethoxy silane (TMOS) based alcogels in solutions of TEOS/ MeOH which increased the strength and stiffness of the alcogels which reduced the shrinkage during drying. Load relaxation experiments were performed to shear modulus (G), Poisson's ratio (r) and the permeability of wet gel as a function of aging time in TEOS/ MeOH soln. Aging the gels in 70 vol% of TEOS/MeOH increases the G from 0.48 MPa to 1.8 MPa and 7.4 MPa after aging for 24 hour and 144 hours respectively [99]. S. Haereid et al. aged the TEOS based gels in solutions of TEOS/EtOH and low density gels were obtained by changing the aging parameters such as time and temperature [100].

Deshpande, Smith and Brinker put forward a new process (DSB process), in which the wet gels are washed with an aprotic solvent, reacted with Trimethylchlorosilane (TMCS) and then dried at ambient pressure [101]. D.M. Smith et al. prepared aerogels by methylating the surface of the wet gel through a reaction with chlorotrimethyl silane followed by drying [102]. F. Schwertfeger et al. prepared silica hydrogels from cheap precursor, water glass. The hydrogels were then placed together

with Hexamethyldisiloxane (HMDSO) in a beaker. Then different amounts of TMCS were added to the suspension. By this technique expensive solvent exchange part was avoided as well as the processing speed was higher [92]. Mari-Ann Einarsrud and Eid Nilsen prepared gels from cheap water soluble sodium silicate and colloidal silica sols. These gels were subsequently aged in TEOS soln. where a ten fold increase in shear G modulus was obtained within 27 h, showing a vary high reactivity of this system compared to alkoxide based gels. The authors also observed a lower density for gels prepared from 6mm sols compared to 3mm sol for gels aged in TEOS [103]. In another related work, the gels derived from water glass were soaked in to a washing soln. of 20 vol% H_2O/EtOH for 24 h at 60 °C, followed by aging in a soln. of 70 vol% TEOS/EtOH at 70 °C for various lengths of time. The gels were also aged in water glass solution. The authors noted that aging in TEOS soln. is more effective in order to increase stiffness [104].

A two step derived silica doped with titania powder dissolved in ethanol was prepared by Young-Geun Kwon et al. [105]. The surface modification was performed with TMCS and gels dried at ambient pressure. The gels heated at 350 °C exhibited thermal conductivities of 0.0136 W/m.K and 0.0284 W/m.K at room temperature and 400 °C resp. The effect of solvents, type of precursor and surface chemical modification on physiochemical properties of silica aerogels prepared by ambient pressure drying was studied by A.V. Rao et al [106]. Rao et al. investigated the properties of ambient pressure dried silica aerogels with water glass precursor using various silylating agents [107]. The physical properties of the aerogels such as density, porosity, pore volume, thermal conductivity and contact angle measurements were studied by using various mono, di and

tri alkyl or aryl silylating agents. The best quality gels were obtained with tri alkyl silylating agent such as Hexadecadisilazane (HMDZ). V.D. Land et al. studied the feasibility of utilising azeotropic distillation to exchange the solvent and substitute TMCS with a more stable silylating reagent TMMS. The TMMS treated gels provided significantly higher porosity than the DSB process [108].

Nicholas Leventis reported a typical polymer crosslinked silica aerogels which are stronger, less hydrophilic and can withstand the capillary forces exerted upon their nanostructured framework and thus dried under ambient conditions [109]. The experimental results by various exchanging solvents in the preparation of two step processed ambient pressure dried hydrophobic silica aerogels were reported by A. Parvathy Rao et al. [110]. Hexamethyldisilazane was used as methylating agent and the physical and hydrophobic properties of silica aerogel strongly depend on nature of solvent and EtOH/TEOS molar ratio (R).

Using cheap water glass as silica source, silica aerogels were synthesised via a novel fast ambient drying using an ethanol/Trimethylchlorosilane (TMCS)/Heptane soln. One step solvent exchange and surface modification were simultaneously progressed by immersing the hydrogel in EtOH/TMCS/Heptane soln. in which TMCS reacts with pore water and Si-OH groups on the surface of the gel, with ethanol and heptane helping to decrease the rate of TMCS reacting with pore water [111]. Sharad. D. Bhagat et al. reduced the processing time of ambient pressure dried silica aerogel beads derived from water glass by utilising the co-precursor method for the surface modification in the hydrogel [112]. Silicic acid was prepared by co-precursor method in which the surface modifying reagents such as TMCS and HMDS were added to the ion exchanged silicic

acid at various proportions. The surface modified silica sol was then added to n-Hexane under constant stirring and to accomplish gelation, pyridine was added drop by drop. The hydrogels was then dried at ambient pressure to obtain aerogel beds. The aerogel beads are mesoporous with pore diameters ranging from 32 to 49 Å and specific surface area as high as 591 m^2/g. Silica aerogel with thermal conductivity as low as 0.036 Wm^{-1}K^{-1} and porosity as high as 97% were successfully prepared by ambient pressure drying through a multiple modification approach [113]. The multiple treatments were found to be necessary to achieve sufficient modification of the wet gel for reduction in drying induced surface tension force.

P.B. Sarawade et al. prepared silica aerogels by acid-base sol-gel polymerisation of TEOS followed by drying at ambient pressure [114]. In order to minimise drying shrinkage, the surface of the gels was modified by TMCS before ambient drying. The effect of base catalyst (NH$_4$0H) addition to the sol, at different time intervals (T), on physical and textural properties of aerogels was investigated. The time interval (T) greatly influenced the physical and textural properties of aerogels. The bulk densities decreased as T value increased and there was also significant increase in the surface area and pore volume for increased value of T. A.V. Shlyakhtina et al. prepared silica alcogels by two step sol-gel process [115]. The solvent isopropanol was exchanged with n-butanol and gel surface was modified using TMCS in n-butanol. The solvent was exchanged in several steps with saturated hydrocarbons in order to obtain pore fluids containing azeotropic mixtures of water, n-butanol and a hydrocarbon. Ambient pressure drying was performed in two steps, at the boiling points of the ternary isotope and hydrocarbons respectively. S.D. Bhagat developed a novel route for the synthesis of silica aerogels by

employing sol-gel polymerisation of Methyltrimethoxysilane (MTMS) precursor and utilising ambient pressure drying [116]. The process yields silica aerogels exhibiting very low bulk density and high specific surface area. The aerogels were superhydrophobic with contact angle as high as 152°. In another work, Sharad D. Bhagat et al. employed the fluidisation technique for the drying of wet gel slurry at ambient pressure [117]. The fluidisation column was fed with the silylated wet gel slurry in a continuous mode and the fluidisation was carried out at 220 °C. Using this process, hydrophobic silica aerogel powders exhibiting tap density as low as 0.05 g/cm^3, high specific surface area and cumulative pore volume of 1.79 cm^3/g was obtained. A. Fidelgo et al. developed a novel sol-gel route to prepare monolithic hybrid polymer aerogels [118]. The synthesis of the hybrid wet gels followed a two-step hydrolysis/polycondensation of TEOS with excess water, in 2-propanol. Cohydrolysis with Trimethoxy silyl-modified poly (butyl methacrylate-co-butyl acrylate) cross linked nanoparticles was carried out. The gels were then subcritically dried in quasi-saturated solvent atmosphere and the aerogels possessed good mechanical properties.

1.8 Definition of the Present Problem

The increasing industrial application of aerogels in the fields of catalysts, thermal and acoustic insulators, dielectric substrates and in space applications have generated considerable interest in developing aerogels through novel methods in addition to supercritical drying. To make aerogels interesting for larger scale commercial application, one must look for alternative process for the most expensive and risky part of the preparation: supercritical drying. Further one should look for compositions which will result in high temperature pore stability and functionality.

The present work has been designed based on the following

1) Pure silica aerogels have limited pore stability since they sinter at temperatures above 600 °C and this is detrimental for its use as high temperature insulation materials. Increased thermal pore stability will be beneficial for its application at high temperature. So Silica-Alumina mixed oxide aerogels through non-supercritical drying using boehmite as a precursor for alumina is to be synthesised. During the preparation of mixed oxide aerogels involving silica, if the hydrolysis of the metal alkoxide is faster than that of silicon alkoxide, a non uniform sol results because sedimentation takes place before gelation. So we have chosen boehmite (Condea, Germany) sol as one of the precursors for the preparation of silica alumina aerogels and hybrid sol-gel route ensures nano-metric scale mixing in heterogeneous systems. The percentage of alumina in the silica matrix is to be varied and the gels are to be calcined at various temperatures to study the thermal pore stability.

2) To synthesise Silica-Silica composite aerogels by non-supercritical method by the addition of pyrogenic silica into silica sol. The percentage of pyrogenic silica is to be

varied in the silica matrix. The application of composite aerogels as a confining media for high level nuclear waste storage is also to be explored. The use of silica alcogels as a confining media for waste storage will also be tested and compared.

3) Silica-Titania mixed oxide aerogels to be synthesised by non-supercritical drying using chelated Ti $(O^iPr)_4$ precursor for titania. The chelating agents such as acetic acid and acetyl acetone will be employed for the preparation of titania sol which will later be added to hydrolysed silica sol for the preparation of Silica-Titania aerogels. Silica-Titania aerogels will also be prepared by impregnation. The application of these aerogels as photocatalyst will be looked in to.

References

[1] C.K. Narula, Ceramic Precursor Technology and its Application, Marcel Dekker, New York, 1995.

[2] W.D. Kingery, H.K. Bowen and D.R. Uhlmann, Introduction to Ceramics, John Wiley and Sons, New York, 1975.

[3] T.A. Ring, Fundamentals of Ceramic Powder Processing and Synthesis, Academic Press, Inc. San Diego, 1996.

[4] G.Y. Onoda and L.L. Hench eds. Ceramic Processing Before Firing, John Wiley and Sons, New York, 1978.

[5] J.D.F. Ramsay, in "Characterisation of Porous Solids" ed. By K.K. Unger, J. Rouquerol, K.S.W. Sing and H. Kral, Elsevier, Amsterdam, 1998, p. 23.

[6] S.J. Gregg and K.S.W. Sing, Adsorption, Surface area and Porosity, 2nd edn. Academic Press, London, 1995.

[7] Recommendations for the characterization of Porous Solids, Pure and Appl. Chem., 66 (8) (1994) 1739.

[8] Y.O. Roizin, S.A. Gevelyuk, L.P. Prokopovich, D.P. Savin, J. Porous Mater 4 (1997) 151

[9] S.T. Corbin, P.S. Apte, J. Am. Ceram. Soc. 82(7) (1999) 1693.

[10] O. Lyckfeldt, J.M. Ferreira, J. Eur. Ceram. Soc. 18(2) (1998) 131.

[11] Y.N. Sun, M.D. Sacks and J.W. Williams in "Ceramic Powder Science II' ed. By G.L. Messing, E.R. Fuller and H. Hausner, Ceramic Transaction, 1(1998) 538.

[12] G. Tomandl, Ceramic Forum Int. 75 (1998) 22.

[13] S. Komarneni, L. Pach, R. Pidugu, Adv. Por. Mat. Res. Soc. Symp. Proc. 371 (1995) 285.

[14] M.D.M. Innocentini, P. Sepulveda, V.R. Pandolfelli, J.R. Coury, J. Am. Ceram. Soc. 81(12) (1998) 3349.

[15] N.W. Androff, L.E. Francis, B.V. Velamakanni, Ceram. Processing 43 (11A) (1997) 2878.

[16] M.A. Gulgun My, H. Nyguyen, W.M. Kriven, J. Am. Ceram. Soc. 82 (3) (1999) 556.

[17] A. Imhof, D.J. Pine Ad. Mater. 10(9) (1998) 697.

[18] S. Sivakumar, Novel Synthesis Route for High Surface Area Metal Oxide Pillared Montmorillonite, PhD. Thesis, University of Kerala, 1997.

[19] A.C Pierre, Introduction to Sol-Gel Processing, Kluwer Academic publishers, The Netherlands, 1998

[20] C.J. Brinker and G. W. Scherer, Sol-Gel Science, The physics and chemistry of Sol-Gel processing, Academic press, New York, 1990.

[21] P.C. Hiemenz, Principles of Colloidal and Surface Chemistry, Marcel Dekker, New York 1997

[22] C.W. Turner, Am. Ceram. Soc. Bull. 70(9), 1991 pp1487

[23] C.F. Baes Jr., R. E. Mesmer, The Hydrolysis of Cations Wiley, New York 1976

[24] H. Schmidt, A. Kaiser, M. Rudolph and A Lentz in "Science of Ceramic Chemical Processing", ed. By L. L. Hench and D. R. Ulrich, Wiley, New York 1996

[25] B.E. Yoldas, J. Mater. Sci. 21 (1986) 1080.

[26] D.W. Schaefer, MRS Bull. 19 (4) (1994) 49.

[27] K.D. Keefer, D.W. Schaefer, Phys. Rev. Lett. 53 (1984)1383.

[28] S.S. Kistler, Nature (London) 127 (1931) 741.

[29] S.J. Teichner, G.A. Nicolaon, M.A. Vicarini, G.E.E. Gardes, Adv. Colloid. Interface Sci. 5 (1976) 245.

[30] S.J. Teichner in "Aerogels": Springer Proc. Phys. 1986, 6.

[31] Preparation of Catalysts: G. Tournier, M. Lacroix-Repellin, G.M. Pajonk, S.J. Teichner in Studies in Surface Science and Catalysis, Vol. 31 (Eds. B. Delmon, P.granga, P.A. Jacobs, G. Poncelet), Elsevier, Amsterdam, 1987, p. 333.

[32] F. Chaput, B. Dunn, P. Fugua, K. Sallonx, J. Non-Cryst. Solids 188 (1995) 11.

[33] K. Sudoh, H. Hiroshima, J. Non-Cryst. Solids 147/148 (1992) 386.

[34] K. Kearby, S.S. Kistler, S. Swann, Ind. Eng. Chem. 30 (1938) 1082.

[35] J.N. Armor, E.J. Carlson, Appl. Catal. 19 (1985) 327.

[36] F. Blanchard, B. Pommier, J.P. Reymond, S.J. Teichner, Stad. Surf. Sci. Catal. 16 (1983) 395.

[37] S.M. Maurer, E.I. Ko, J. Catal. 135 (1992) 125.

[38] Y.P. Gao, C.N. Sisk, LJ. Hope Weeks, Chem. Mater. 19 (2007) 6007.

[39] D.C.M. Dutoit, M. Schneider, A. Baiker, J. Catal. 153 (1995) 165.

[40] F. Chatput, A. Laconte, A. Dauger, J.P. Boilot, Rev. Phys. Appl. 1989, 137 (Proc. 2nd Int. Symp. Aerogels, Colloque C4, Les Editions de Physique, Les Ulis Cedex.

[41] T. Heinrich, F. Raether, H. Marsmann, J. Non-Cryst. Solids 168 (1994) 14.

[42] F. Blanchard, J.P. Reymond, B. Pommier, S.J. Teichner, J. Mol. Catal. 17 (1982) 171.

[43] R. Marinangelli, G.M. Pajonk, S.J. Teichner, Proceedings of the 7th Simposio Iberoamericano de catalisis (La Plata, Argentina) 1980, 126.

[44] A. Sayari, A. Ghorbel, G.M. Pajonk, S.J. Teichner, Bull. Soc. Chim. Fr. (1981) 220.

[45] D.C.M. Dutoit, M. Schneider, P. Fabrizioli, A. Baiker, Chem. Mater. 8 (1996) 734.

[46] J.B. Miller, E.I. Ko, J. Catal. 159 (1996) 58.

[47] S. Blacher, R. Pirard, J.P. Pirard, Langmuir 13 (1997) 1145.

[48] P. Pirard, D. Bonhomme, S. kolibos, J.P. Pirard, A. Lecloux, J. Sol-Gel Sci. Technol. 8 (1997) 831.

[49] M.D. Wildberger, T. Mallat, U. Gobel, A. Baiker, Appl. Catal. A: Gen. 168 (1998) 69.

[50] T. Osaki, T. Horinchi, T. Sugiyma, K. Suzuki, T. Mori, J. Non-Cryst. Solids 225 (1998) 111.

[51] P. Fabrizioli, T. Burgi, A. Baiker, J. Catal. 207 (2002) 88.

[52] D.J. Rosenberg, F. Coloma, J.A. Anderson, J. Catal. 207 (2002) 88.

[53] Zhi-Gang Wu, Yong-Xiang Zhao, Dian-Sheng Liu, Micropor. Mesopor. Mater. 68 (2004) 127.

[54] N. Moussa, A. Ghorbel P. Grange, J. Sol-Gel Sci. Technol. 33 (2005) 127.

[55] Chien-Tsung Wang , Shih-Hung Ro Appl. Catal. A: Gen. 285 (2005) 196.

[56] F. Somma, Strukul, Catal. Lett. 107 (2006) 511.

[57] M.I. Kim, D.W. Park, S.W. Park, X. Yang, J.S. Choi, D.J. Suh, Catal. Today 111 (2006) 212.

[58] Chien-Tsung Wang, J. Non-Cryst. Solids 353 (2007) 1126–1133

[59] M.B. Taghavi, G.M. Pajonk, S.J. Teichner, J. Colloid Interface Sci. 71 (1979) 451.

[60] B. Pommier, S.J. Teichner, Proc. Int. Congr. Catal. 9th 2 (1988) 610.

[61] M. Schneider, D.G. Duff, T. Mallat, M. Wildberger, A. Baiker, J. Catal. 147 (1994) 500.

[62] K. Balakrishnan, R.D. Gonzales, J. Catal. 144 (1993) 395.

[63] F. Schwertfeger, W. Glaubitt, U. Schubert, J. Non-Cryst. Solids 145 (1992) 82.

[64] R.W. Pekala, J. Mater. Sci. 24 (1989) 3221.

[65] R.W. Pekala, F.W. Kong, Poly. Prepn. (Am. Chem. Soc. Div. Poly. Chem.) 31 (1991) 167.

[66] L.W. Hrubesh, Chem. Ind. 17 (1990) 824.

[67] G.C. Bond, S. Flamerz, Appl. Catal. 33 (1987) 219.

[68] J. Fricke, A. Emmerting, Struct. Bond. 77 (1992) 27.

[69] C.A.M. Mulder, J.G. Van Lierop, in: J. Fricke (Ed.), Aerogels, Springer, Berlin, 1986, p. 68.

[70] M. Schmidt, F. Schwertfeger, J. Non-Cryst. Solids 225 (1998) 364.

[71] V. Gibiat, O. Lefeuvre, T. Woignier, J. Pelous, J. Phalippou, J. Non-Cryst. Solids 186 (1995) 244.

[72] Janusz Chwastowski, Jan Figiel, Andrzej Kotarba, Krystyna Olkiewicz, Leszek Suszycki, Nucl. Instrum. Methods Phys. Res. A 504 (2003) 222.

[73] T. Bellunatoa, A. Braem, A.R. Buzykaev, M. Calvi, E. Chesi, A.F. Danilyuk, S. Easo, S. Jolly, C. Joram, E.A. Kravchenko, D. Liko, C. Matteuzzi, M. Musy, P. Negri, N. Neufeld, A.P. Onuchin, J. Sleguinot, S. Wotton, Nucl. Instrum. Methods Phys. Res. A 504 (2003) 290.

[74] Yun Liu, Liangying Zhang, Xi Yao, Chaonan Xu, Mater. Lett. 49 (2001) 102.

[75] J.L. Mohanan, S.L. Brock, J. Non-Cryst. Solids 350 (2004) 1.

[76] J.G. Reynolds, P.R. Coronado, L.W. Hrubesh, J. Non-Cryst. Solids 292 (2001) 127.

[77] K.I. Jensen, J.M. Schultz, F.H. Kristiansen, J. Non-Cryst. Solids 350 (2004) 351.

[78] S. Maury, P. Buisson, A.C. Pierre, J. Mol. Catal. B: Enzymatic 19-20 (2002) 269.

[79] K.Y. Jang, K. Kim, R.S. Upadhye, J, Vac. Sci. Technol. A 8 (3) (1990) 1732.

[80] P. Tsou, J. Non-Cryst. Solids 186 (1995) 415.

[81] T. Woignier, J. Reynes, J. Phalippou, J. L. Dussossoy, N, N Jacquet- Francillon, J. Non-Cryst-Solids 225 (1998) 353

[82] T. Woignier, J. Reynes, J. Phalippou, J. L. Dussossoy, J. Sol-Gel Sci. Technol. 19 (2000) 833.

[83] J. Reynes, T. Woignier, J. Phalippou, J. Non Cryst. Solids. 285 (2001) 323

[84] T. Woignier, J. Primera, M. Lamy, C. Fehr, E. Anglaret, R. Sempere, J. Phalippou. J. Non-Cryst. Solids 350 (2004) 292.

[85] B. Himmel, H. Burger, Th. Gerber, A. Olbertz, J. Non Cryst. Solids. 185 (1995) 56.

[86] J. Fricke, A. Emmerling, J. Am. Ceram. Soc. 75 (8) (1992) 2027.

[87] G. Zhang, A. Das, A. Rawashdeh, J. Thomas, J. A. Counsil, C. S- Leventis, E. F. Fabrizio, F. Ilhen, P. Varsilaras, D. A. Schaiman, L. Mc Corkle, A. Palzer, J. Chris Johnson, M. A. Meador, N. Leventis, J. Non-Cryst. Solids 35 (2004) 152.

[88] G.W. Sherrer, J. Am. Ceram. Soc. 73 (1) (1990) 3.

[89] J.G. Van Lerop, A. Huizing, W.C.P.M. Meerman, C.A.M. Mulder, J. Non-Cryst. Solids 350 (2004) 152

[90] R.A. Laudere and D.W. Johnson Jr., J. Non-Cryst. Solids 79 (1986) 155.

[91] S.S. Prakash, C.J. Brinker, A. J. Hued, S.M. Rao, Lett. Nature 374 (1995) 439

[92] F. Schwertfeger, D. Frank, M. Schmidt, J. Non-Cryst solids 225 (1998) 24.

[93] P.H. Tewari, A.J. Hund, K.D. Lofftus, Mater. Lett. 3 (1985) 363.

[94] Aerogels-Airy materials: Chemistry structure and properties Nicola Husing and Ulrich Schubert, Angew. Chem. Int. Ed. 37 (1998) 22.

[95] R. Deshpande, Duen-Wu-Hua, D. M. Smith, C. J. Brinker, J. Non-Cryst. Solids 144 (1992) 32.

[96] P.J. Davis, C.J. Brinker, D.M. Smith, J. Non-Cryst. Solids 142 (1992) 189.

[97] P.J. Davis, C.J. Brinker, D.M. Smith, R. Assink, J. Non-Cryst. Solids 142 (1992) 197.

[98] S. Haereid, M-A. Einarsrud and G. W. Scherrer, J. Sol-Gel Sci. Technol. 3 (1994) 199

[99] M-A. Einarsrud and S. Haereid, J. Sol-Gel Sci. Technol. 2 (1994) 903.

[100] S. Haereid, M. Dahle, S. Lima, M-A. Einarsrud, J. Non-Cryst. Solids 186 (1995) 96.

[101] R. Deshpande, D. Smith, C.J. Brinker, US patent No. 5, 565,142 issued 1996.

[102] D.M. Smith, D. Stein, J.M. Anderson, W. Ackerman, J. Non-Cryst solids 186 (1994) 104.

[103] M-A. Einarsrud, E. Nilsen, J. Non-Cryst. Solids. 226 (1998) 122.

[104] M-A. Einarsrud, E. Nilsen, J. Sol-Gel Sci. Technol. 13 (1998) 317.

[105] Young-Geun Kwon, Se- Young Choi, J. Mater. Sci. 35 (2000) 6075.

[106] A. Venkateswara Rao, E. Nilsen, M-A. Einarsrud, J. Non-Cryst Solids 296 (2001) 165.

[107] A. Venkateswara Rao, G.M. Pajonk, S.D. Bhagat, P. Barboux, J. Non-Cryst Solids 350 (2004) 216.

[108] V.D. Land, T.M. Hareis, Dale C. Teeters, J. Non-Cryst Solids 283 (2001)11.

[109] N. Leventis, A. Plazer, L. McCorkle, J. Sol-Gel Sci. Technol. 35 (2005) 99.

[110] A. Parvathy Rao, A. Venketeswara Rao, J. Sol-Gel Sci. Technol. 36 (2005) 285.

[111] Fei Shi, Ligiu Wang, Jing Xiao Liu, Mater. Lett. 60 (2006) 3718.

[112] S.D. Bhagat, Yong-Ha Kim, Young-Soo Ahn, Jeong-Gu Yeo, Micropor. Mesopor. Mater. 96(2006) 237.

[113] Te-Yu Wei, Tso-Fu Chang, Shih-Yuan Lu, J. Am. Ceram. Soc. 90(2007) 2003.

[114] P.B. Sarawade, Jong-Kil Kim, Ho-Kun Kim, Hee-Tack Kim, App. Sur. Sci. 254 (2007) 574.

[115] A.V. Shlyakhtina, Young-Jei Oh, J. Non-Cryst Solids 354 (2008)1633.

[116] S.D. Bhagat, Chang-Sup Oh, Yong-Ha Kim, Young-Soo Ahn, Jeong-Gu Yeo, Micropor. Mesopor. Mater. 100(2007) 350.

[117] S.D. Bhagat, Kyung-Tae Park, Yong-Ha Kim, Jongg-Soon Kim, Jong-Hun Han Solid state sciences (2007) doi:10.1016/j.solidstatesciences.2007.11.016.

[118] A. Fidelgo, J.P.S. Farinha, J.M.G. Martinho, M.E. Rosa, L.M. Ilharco, Chem. Mater. 19 (2007) 2603.

Chapter 2: Mesoporous Silica-Alumina Aerogels Through Hybrid Sol-Gel Route Followed by Non-Supercritical Drying

2.1 Synthesis and Characterisation of non-supercritically dried Silica-Alumina aerogels

2.1.1 Abstract

Silica-alumina mixed oxide aerogels have been synthesised by non-supercritical method, having compositions of 5, 10, 15, 20 and 25 wt% of alumina in silica through a hybrid sol-gel technique. Boehmite was used as the precursor for alumina and TEOS for silica. Subcritical drying method involving repeated solvent exchange and gel wall strengthening is followed in place of supercritical method. The aerogels are calcined at 500, 700, 900 and 1200 °C. Nitrogen sorption studies indicate that the mixed oxide aerogels are mesoporous in nature with high surface areas comparable to supercritically dried aerogels and also possess excellent thermal pore stability. Fourier Transmission Infrared (FT-IR) spectroscopy has been used to study the effect of alumina addition to silica. The linear shrinkage of aerogels upon heat treatment is also reported. The acid strength distribution was measured by temperature programmed desorption of ammonia (TPD). The present method involving hybrid sol-gel route followed by subcritical drying could be further developed for synthesis of many mixed oxide mesoporous hybrids for catalyst and gas adsorption applications.

2.1.2 Introduction

Aluminosilicate aerogels with porous structures reveal very interesting physical properties and have many practical and potential industrial applications, including their

use as acid catalysts due to their good chemical resistance [1-6] as membranes for the separation of gas phases [7] purification of water and reactors [8] as adsorbents [9] as humidity control materials [10] and as starting materials for the synthesis of mullite ceramics [11, 12]. The sol-gel process is an attractive method to synthesise metal catalysts and mixed metal oxide catalysts [5]. The most important step for obtaining a porous ceramic from the precursor gel in a sol-gel process is the removal of solvent and volatiles. Usual drying methods lead to considerable shrinkage of the gel and this introduces stresses which result in the collapse of the gel. Supercritical conditions or critical point drying (CPD) result in aerogels which are characterized by low densities and extremely high porosity [13, 14]. Non-supercritical methods are investigated as an alternative to supercritical route which is generally known to be energy intensive, hazardous and expensive [15, 16]. But it is highly restricted by the large drying stresses developed during drying and the large shrinkages associated with it. The drying stress developed due to the capillary forces and the subsequent shrinkage can be minimized by reducing the capillary force [17-19]. Shrinkage during ambient pressure drying can also be minimized by increasing the stiffness of the gel network. This is achieved by reinforcing the gel network by infiltrating sodium silicate or Tetraethoxy silane (TEOS) prior to drying [20-26]. Deshpande, Smith and Brinker eliminated shrinkage during ambient pressure drying by surface modifying the silica gel by Trimethyl chloro silane (TMCS) prior to drying [27]. The reduction in shrinkage, attributed to 'spring back effect' of the gel structure due to repulsion between the hydrophobic caps of surface silanol groups has been used by many researchers [16, 19, 28-31].

During the preparation of mixed oxide aerogels involving silica, if the hydrolysis of the metal alkoxide is faster than that of silicon alkoxide, a non uniform sol results because sedimentation and associated separation take place before gelation. Tamon et al. prepared aerogels by hydrolysing TMOS first, ensuring that no water remains after hydrolysis [3]. Then the aluminium alkoxide was added to obtain uniform Si-O-Al linkages and finally hydrolysed the alkoxide again. Heinrich et al. used chelated aluminium alkoxides in order to reduce reaction rates of [Al (OBu)$_3$] in comparison with TEOS [32-34]. A double alkoxide was used by Pouxviel [35, 36]. We have used boehmite sol as one of the precursors for the preparation of silica alumina aerogels and hybrid sol-gel route ensures nano-metric scale mixing in heterogeneous systems [31-39].

Pure silica aerogels have limited thermal pore stability since they sinter at temperatures above 600 °C [46-48] and this is detrimental for its use as high temperature insulation materials. Saliger et al. added aluminium oxide and aluminium hydroxide powders to silica and studied the sintering process using dilatometry, viscosity and nitrogen sorption studies [49].

In this chapter the synthesis of silica-alumina aerogels by a hybrid sol-gel route followed by subcritical drying is presented. The aerogels were then calcined at 500, 700, 900 and 1200 °C and were characterized by BET, FT-IR, XRD, & TPD measurements. The bulk density of the as prepared aerogels is also presented. The linear shrinkage of the silica aerogels and the mixed oxide aerogels upon heat treatment were also studied.

2.1.3 Experimental

2.1.3.1 Materials & preparation procedure

Non-supercitical drying method has evolved as a simple method over supercritical drying method for the synthesis of aerogels [16-31]. This involves aging, solvent exchange and drying under controlled conditions. Previous experiments revealed that the mixed oxide gels prepared under high water/alkoxide ratio result in porous gels having high surface area [18]. The gels were immersed in water for 24 hours so as to hydrolyse any unreacted TEOS. Solvent exchange was done with isopropanol to remove water from the pores and was aged in 80% silane solution. The aging process provides strength to the gel network, since dissolution and reprecipitation of silica particles to the gel network takes place [22]. The aging process in 80% silane solution for 48 hours gave the highest surface area [50]. These gels were then solvent exchanged with isopropanol, since solvent exchange reduces capillary stresses [17], and further, liquids of low surface tension and high molecular volume favour the production of gels having high surface area [18].

Boehmite, (AlOOH) (99% purity, alumina content 70%, Condea Chemie, Germany) having BET surface area of 230 m^2/g and crystalline size 48-60 Å was used as the precursor for alumina and Tetraethoxy silane (Fluka, Switzerland) for silica. The concentration of alumina in the stock boehmite sol was 0.0107 g/ml. TEOS was mixed with isopropanol (S.D. Fine Chemicals, India) and HCl (pH=1.54) in a molar ratio of 1: 4: 16 [18]. In a typical experiment for preparing 25 wt% alumina in silica, 3.884g of TEOS in 4.475g isopropanol was hydrolysed using 5.45g of H^+ (HCl, pH=1.54). The clear sol was stirred for 30 min, 35 ml boehmite sol was added and the sol was again

stirred for 30 min. Subsequently, the pH was adjusted to 5 using 5% ammonia solution.

The visually homogeneous sol was then transferred to vials and kept at 50 °C for gelation.

```
                 ┌─────────────────────────────────────┐
                 │  TEOS + isopropanol + 0.001 M HCl   │
                 └─────────────────────────────────────┘
                                   │
                                   ▼
        ┌─────────────────────────────┐      ┌─────────────────┐
        │      Silica precursor sol   │ ◄─── │  Boehmite sol   │
        └─────────────────────────────┘      └─────────────────┘
                                   │
                                   ▼
                 ┌─────────────────────────────────┐
                 │     Silica-Alumina gel rods     │
                 └─────────────────────────────────┘
                                   │
                                   ▼
                 ┌─────────────────────────────────┐
                 │    Aging in water for 24 hours  │
                 └─────────────────────────────────┘
                                   │
                                   ▼
                 ┌─────────────────────────────────┐
                 │   Solvent exchange (isopropanol)│
                 └─────────────────────────────────┘
                                   │
                                   ▼
                 ┌─────────────────────────────────┐
                 │      Silane aging (48 hours)    │
                 └─────────────────────────────────┘
                                   │
                                   ▼
                 ┌─────────────────────────────────┐
                 │   Solvent exchange (isopropanol)│
                 └─────────────────────────────────┘
                                   │
                                   ▼
        ┌─────────────────────┐          ┌──────────────────────────┐
        │   Drying at 70 °C   │ ───────► │  Calcining at 500, 700,  │
        └─────────────────────┘          │     900 & 1200 °C        │
                                         └──────────────────────────┘
```
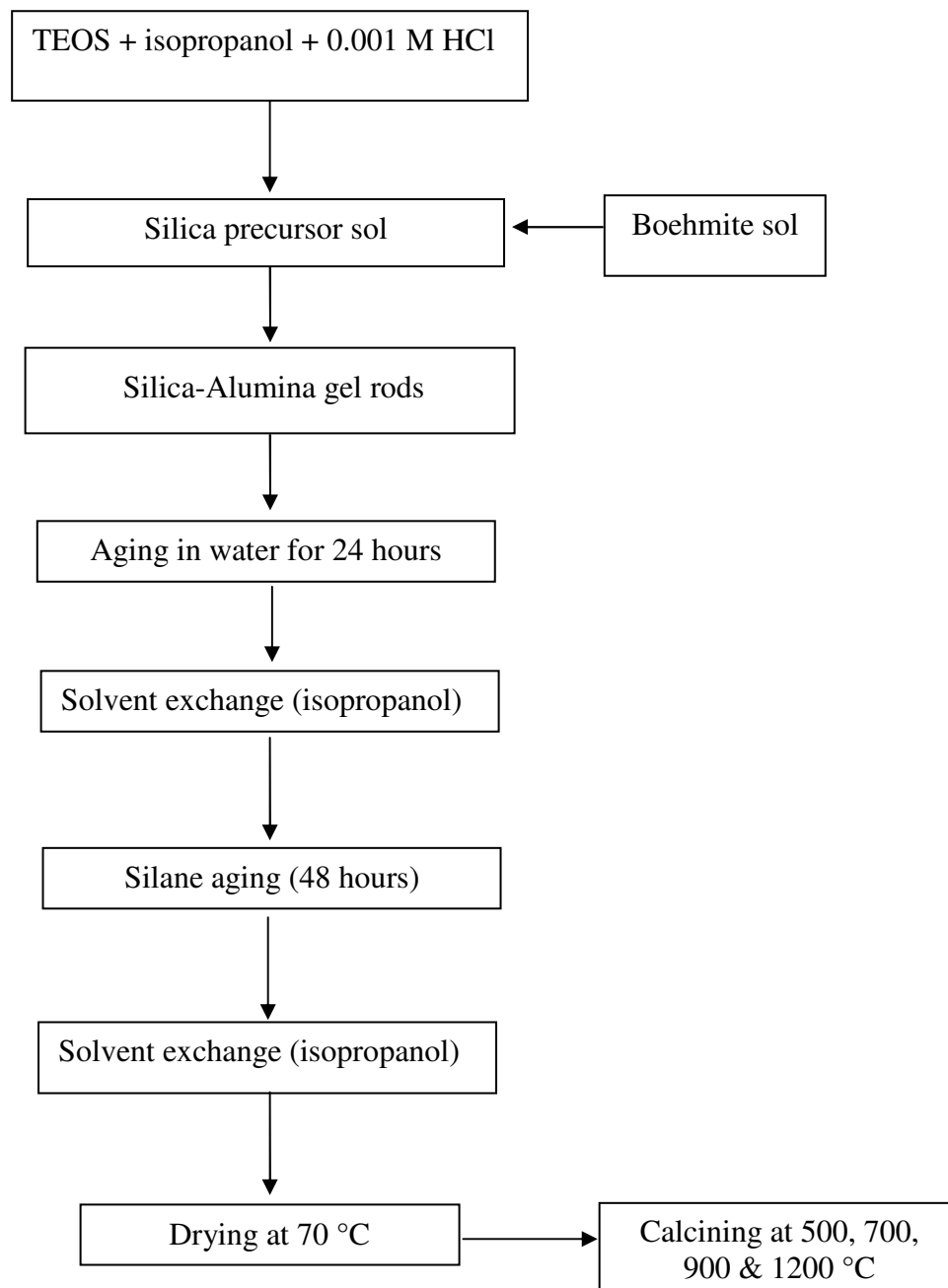
Fig. 2.1.1. Flowchart for the preparation of Silica-Alumina mixed oxide aerogels

The gelation time was noted. The gels were aged for 5 to 6 hours and transferred to water and was kept for 24 hours at 50 °C. It was then washed with isopropanol five times within 24 hours so as to remove water from pores. During the washing process the gels were kept at 50 °C. This was followed by aging the gels in 80% TEOS for 48 hours at 50 °C and the final solvent exchange with isopropanol maintaining the gels at 50 °C. The gels were then dried in tightly closed containers at 70 °C so that the porous structure is retained in the gels by the slow removal of solvent from the pore network. The aerogels obtained after drying at 70 °C were calcined for 3 hours at 500, 900, 700 and 1200 °C. The alumina content was varied from 5 to 25 wt%. The detailed flowchart for the preparation of Silica-Alumina aerogels is presented in Fig.2.1.1.

2.1.3.2 Characterisation of the aerogels

Bulk density of the dried gels was calculated by measuring their mass and volume.

$$\text{Volume, V} = \pi d^2 I \big/ 4$$

Where d is the diameter and I length of the gel.

$$\text{Bulk Density} = \text{Mass/Volume}$$

The Fourier Transform Infrared Spectroscopy of gels and calcined samples was recorded in Nicolet Magna-560-FT-IR Spectrometer (USA) using pellets made out of KBr and dispersed gel powder. The BET surface areas of calcined aerogels were determined by N_2 adsorption at 77K (Micromeritics, Gemini Model 2360, USA). The calcined samples were preheated in a flow of nitrogen for 3 hours at 200 °C to remove all the volatiles and chemically adsorbed water from the surface. Adsorption studies were carried out at liquid nitrogen temperature. The temperature-programmed desorption (TPD) was carried out by keeping 0.5 g of the aerogel sample in a microreactor followed

by degassing at 300 °C for half an hour. The reactor was then cooled to room temperature and 20 ml ammonia gas was injected through the sample. The gas emerging from the reactor outlet was scrubbed into known volume of standard sulphuric acid for 15 minutes. The eluted ammonia was estimated volumetrically using the equation,

Amount of ammonia adsorbed = $(N_{NaOH} * \Delta V) * 17 / W * 1000$ mmol/g.

The experiment was repeated at temperatures from 100 to 800 °C. Thermo mechanical analysis (TMA) of the aerogels was performed by heating the aerogel pellets at the rate of 10 °C/ min. under Nitrogen atmosphere using Shimadzu 60 H Thermo Mechanical Analyser. The X- ray powder diffraction patterns of the calcined samples were recorded in Philips Diffractometer (PW 1710), Netherlands, using Ni filtered CuKα radiation. The samples were scanned from 0 to 60° (2θ values) with a step speed of 2.4°/ min.

2.1.4 Results and Discussion

The gelation time for silica as well as those containing various alumina compositions is provided in Table 2.1.1. As the alumina content is increased in silica the gelation time is prolonged. Huang et al. studied the variation in gel time of silica sol as a function of either H_2O/TEOS molar ratio or amount of base catalyst added [51]. They found that increase of water content (as a reactant) would increase the gel time. Here the TEOS: isopropanol: water was kept constant at 1:4:16, but to obtain higher loadings of alumina, a larger volume of boehmite sol was required compared with lower alumina compositions. A composition greater than 25% was difficult to obtain since the alcogel became very fragile. The bulk density of aerogels ranges from of 0.003 to 0.8 g/cm^3 with high surface area extending up to about 1500 m^2/g [52]. The density measurements of the

silica-alumina aerogels and pure silica aerogel prepared are provided in Table 2.1.2. The silica aerogel has a density of 0.401 g/cm^3, and the 5, 10 and 15 wt% alumina aerogels possess densities of 0.40, 0.54 and 0.63 g/cm^3 respectively. The 20 wt% and 25 wt% alumina aerogels cracked during drying.

Table 2.1.1. Gelation time for mixed oxide gels

Alumina content in mixed oxide Sol (wt %)	Gelation time (min)
0	14
5	25
10	70
15	110
20	150
25	220

Table 2.1.2 Density measurements of silica-alumina aerogels

Alumina content in mixed oxide Sol (Wt %)	Density (g/cm^3)
0	0.401
5	0.400
10	0.54
15	0.63
20	Cracked gel
25	Cracked gel

For the preparation of silica-alumina mixed oxide aerogels the essential prerequisite for ensuring homogeneity is the decomposition of alkoxy and other anionic residues followed by cross-condensation between aluminium and silicon moieties [53]. The cross condensation is initiated around 400 °C [53] and the gels are calcined from 500 °C upwards.
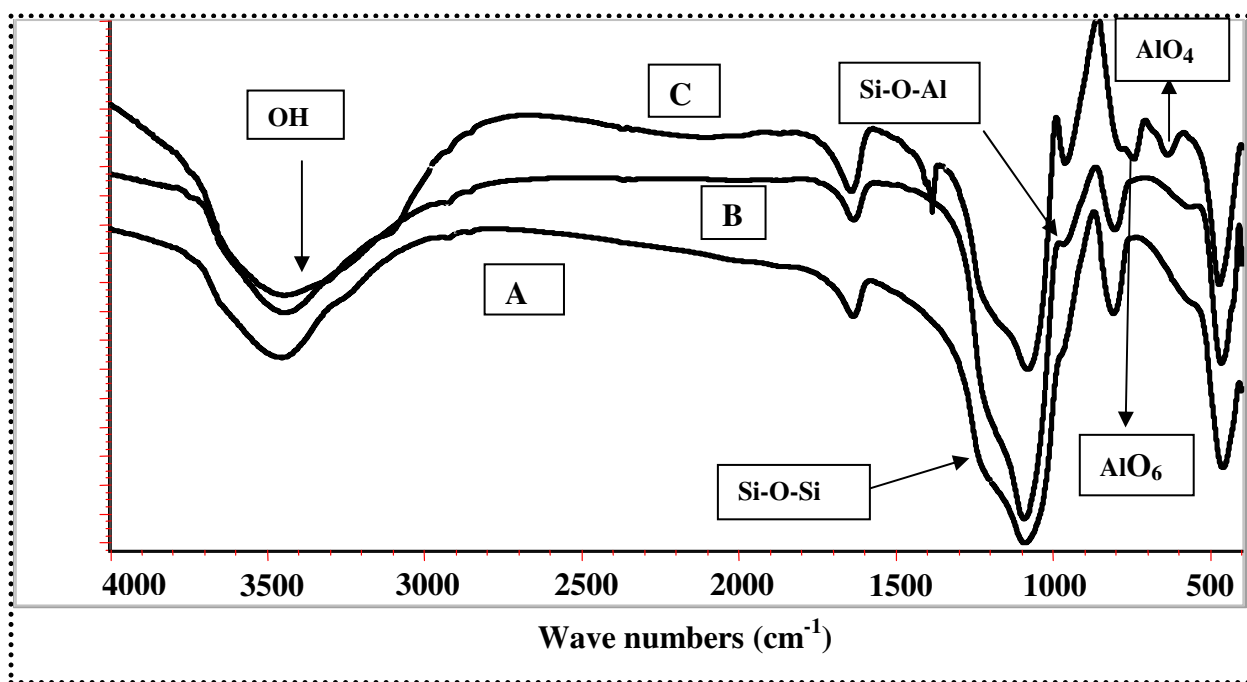
Fig. 2.1.2. FTIR spectra of (A) Silica aerogel calcined at 500 °C (B) 25 wt% alumina gel calcined at 500 °C (C) as prepared 25 wt% alumina gel

The FTIR spectra of the as prepared 25 wt% alumina gel and that calcined at 500 °C are provided in Fig. 2.1.2. The FTIR spectrum of 500 °C calcined silica aerogel is also provided. Boehmite is composed of AlO_6 octahedra and silica is composed of SiO_4 tetrahedra. All Al-O and Si-O related vibrations are known to appear only in the 1200-400 cm^{-1} region [47]. The peak at 3300 cm^{-1} indicates OH vibrations. The peak at 1069 cm^{-1} is characteristic of Si-O-Si vibration while the shoulders appearing at high and lower side of this absorption band indicate the presence of Si-O-Al bonds through cross

condensation of boehmite and silica [54]. When alumina is added to silica, the silica forces AlO_6 in boehmite to AlO_4 polyhedron [53]. The bands at 620 cm^{-1} and 731 cm^{-1} in the as prepared gels of 25 wt% alumina in silica are characteristic of octahedra Al and tetrahedral Al respectively [53]. This infers that the silica is forcing the AlO_6 polyhedra in boehmite to AlO_4 tetrahedra. The same aerogel sample calcined at 500 °C shows shoulder peaks appearing at high and lower side of the absorption peak at 1069 cm^{-1} indicating the presence of Si-O-Al bonds.
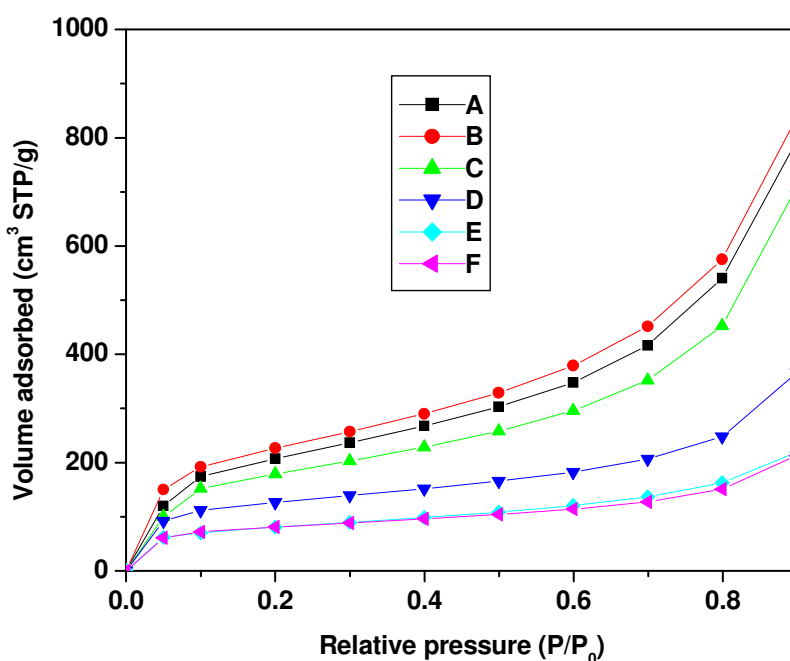
Fig. 2.1.3. Adsorption isotherms of (A) silica (B) 5 wt% (C) 10 wt % (D) 15 wt % (E) 20 wt % and (F) 25 wt % alumina calcined at 500 °C.

The isotherms of silica and mixed-oxide aerogels calcined at 500 °C are provided in Fig. 2.1.3. The isotherm is Type IV which is characteristic of mesoporous materials. The surface area and total pore volume of 500 °C calcined aerogels are provided in Fig.

2.1.4. The figure indicates clearly that as the percentage of alumina increases above 5 wt%, the surface area decreases.

D.R. Dunphy et al. prepared surfactant templated silica-alumina thin films by doping alumina into the pore walls during material synthesis or grafting on to the pore surface of preformed mesophases [55]. There was a decrease in total porosity and surface area with Al doping. On the basis of refractive index data, this decrease was attributed to reduction in pore accessibility and not pore collapse. Similar decrease in surface area was also reported by Hernandez et al. [56]. The authors studied the relationship between the porous texture, the co-ordination number of Al atoms, the type of surface acidity and the sol-gel acidic synthesis conditions at two pH values (pH≈ 2 and pH ≈ 0) in silica-alumina aerogels made with molar Si to Al ratio r $_{Si/Al}$ =100. K. Sinko et al. prepared alumino-silicate aerogels under various conditions and compared with respect to their nanostructures and porosity [57]. The authors found that the Al incorporation into the silicate network did not decrease the porosity in these series. The highly bonded Al content, the loose fractal structure and the very small elementary units derived from gelation of aluminium nitrate or isopropoxide and TEOS guarantee good porosity property hence a high surface area.

The decrease in surface area beyond 5 wt% alumina addition may be attributed to the crystallization of Al in the pores of the aerogel. B. Ameen et al. [58] prepared silver nanoparticles in silica aerogel matrix by subcritical drying. On increasing the silver concentration, the specific surface area decreased from 845 m^2/g to 307 m^2/g. The concomitant decrease in surface area with increase in silver concentration showed that fine silver particles crystallise within the pores of the aerogel matrix. Moreover the

largest pore volume was obtained for 1% Ag and it subsequently decreased as percentage of silver is increased. This characteristic was attributed to the partial replacement of silicon by silver atom in the silica framework and the associated vacancy created for the charge compensation. With increasing silver concentration, the silver atoms get crystallised in the pores of the aerogel matrix, reducing the total pore volume.

Fig. 2.1.4. Surface area and pore volume of silica and silica-alumina aerogels calcined at 500 °C.

For silica, a surface area of 736 m^2/g and a pore volume of 1.227 cm^3/g after calcining at 500 °C was obtained. The surface area of 25 wt% alumina was found to be 266 m^2/g, the pore volume was 0.329 cm^3/g. The surface area of 5 wt% alumina is higher than that of pure silica calcined at 500 °C. By the addition of 5 wt% alumina to silica, the aerogel network is strengthened and the shrinkage is therefore less when compared to silica aerogel.
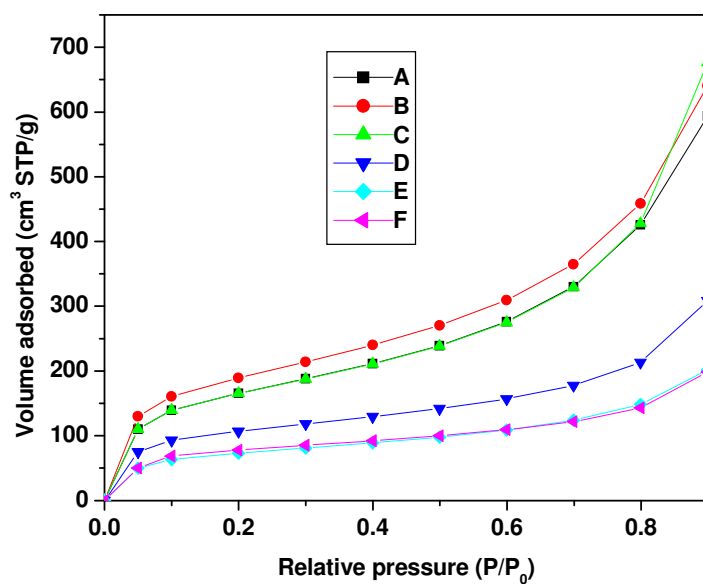
Fig. 2.1.5. Adsorption isotherms of (A) silica (B) 5 wt% (C) 10 wt% (D) 15 wt% (E) 20 wt% and (F) 25 wt% alumina calcined at 700 °C.
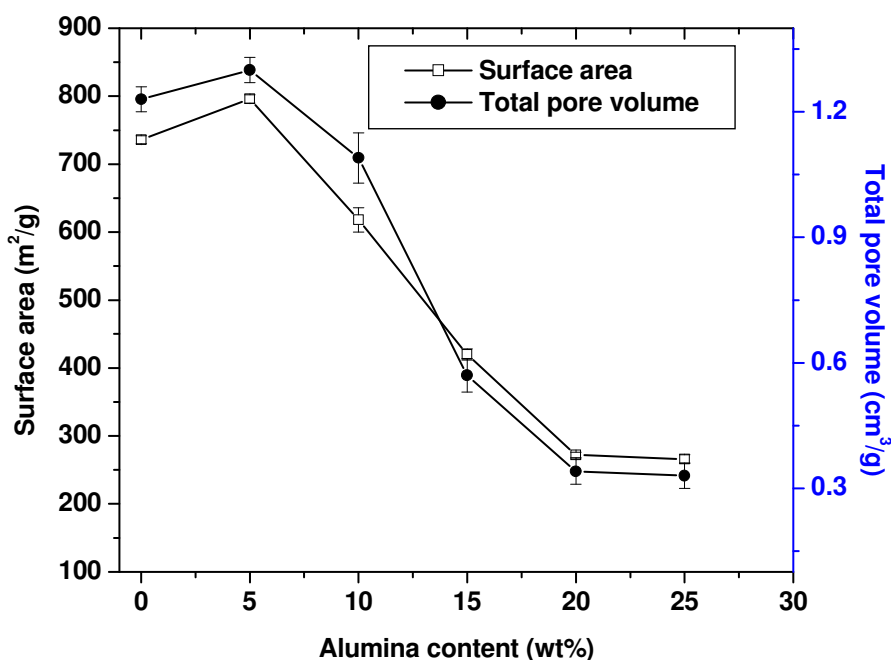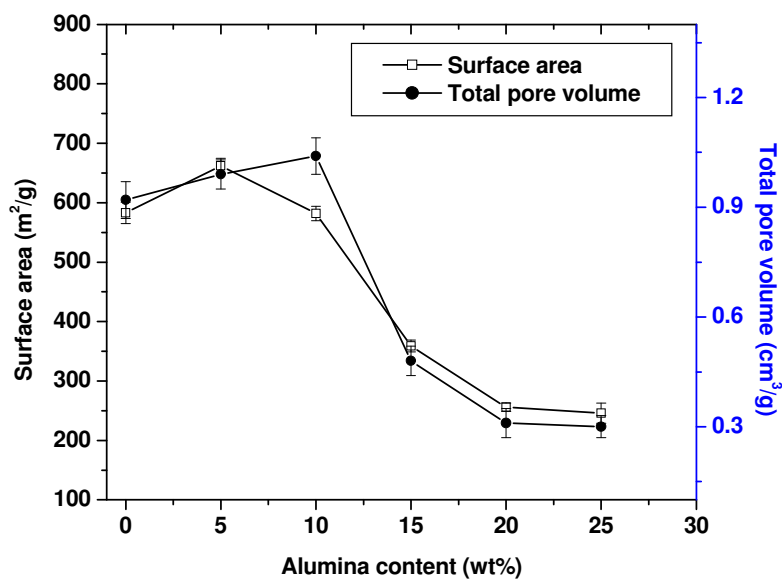

Fig. 2.1.6. Surface area and pore volume of silica and silica-alumina aerogels calcined at 700 °C.

This is confirmed by the fact that 5 wt% alumina possesses a total pore volume of 1.3 cm^3/g compared to a pore volume of 1.22 cm^3/g in the case of pure silica.

The isotherms of silica and mixed oxide aerogels calcined at 700 °C are provided in Fig. 2.1.5. The isotherm is Type IV which is characteristic of mesoporous materials. The surface area and total pore volume for the 700 °C calcined aerogels are provided in Fig. 2.1.6. The figure indicates clearly that as the percentage of alumina increases the surface area and total pore volume decreases. The surface area of 5 wt% alumina-silica is higher than that of pure silica calcined at 700 °C. By the incorporation of 5% alumina to silica, the aerogel network is strengthened and as we increase the calcination temperature the alumina sites shield adjacent Si-OH....Si-OH groups preventing the silanol condensation. The same phenomenon is also seen in the case of 10 wt% alumina aerogel. The surface area of 10 wt% alumina aerogel is almost same as that of silica. Silica aerogels calcined at 700 °C have a surface area of 583 m^2/g with a total pore volume of 0.92 cm^3/g. The 10% alumina-silica aerogel calcined at 700 °C has a surface area of 582 m^2/ g and a total pore volume of 1.04 cm^3/g. The surface area of 5 wt% alumina calcined at 700°C was found to be 662 m^2/g with a total pore volume of 0.99 cm^3 /g and that of 25 wt% alumina calcined at 700 °C was found to be 246 m^2/g with a pore volume of 0.31 cm^3/g.

The isotherms of silica and mixed-oxide aerogels calcined at 900 °C are provided in Fig. 2.1.7. The surface area and total pore volume of silica and silica-alumina aerogels calcined at 900 °C are provided in Fig. 2.1.8. As in the case of 500 °C aerogel sample the surface area decreases as the percentage of alumina in silica increases from 5 wt% to 25 wt%. For pure silica aerogel, the surface area was found to be 415 m^2/g with a pore

**Fig. 2.1.7.** Adsorption isotherms of (A) Silica (B) 5 wt% (C) 10 wt% (D) 15 wt% (E) 20 wt% and (F) 25 wt% alumina calcined at 900 °C.

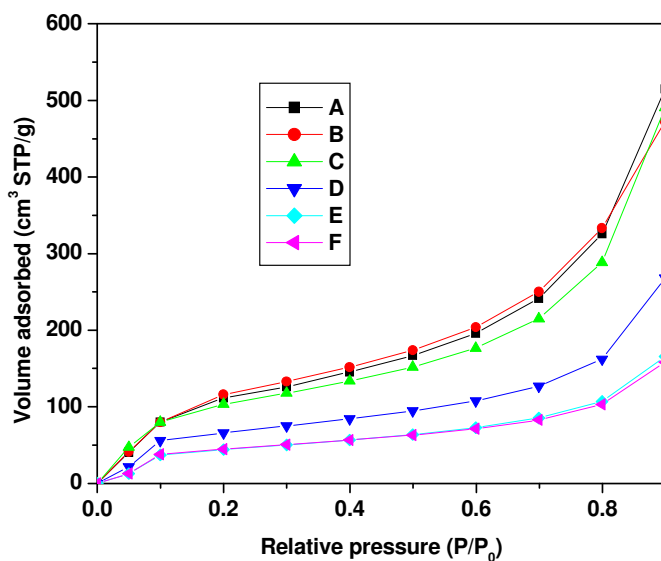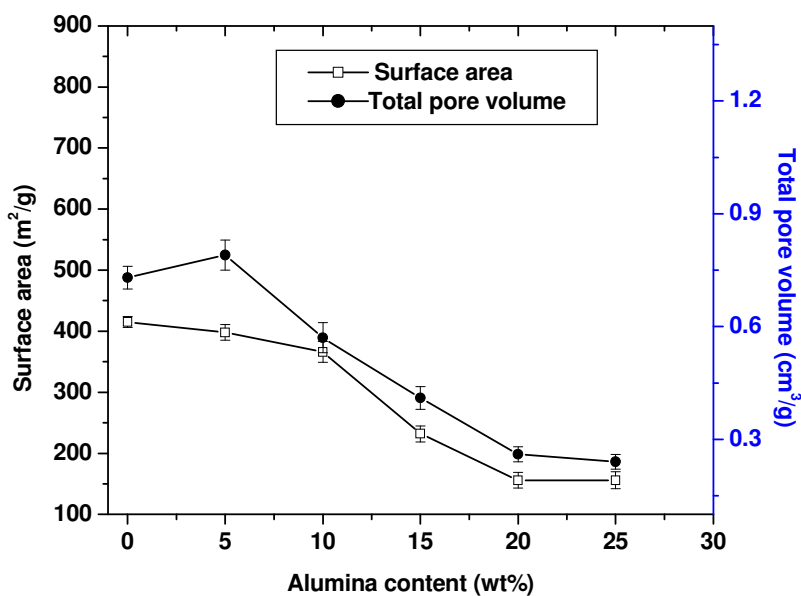**Fig. 2.1.8.** Surface area and pore volume of silica and silica-alumina aerogels calcined at 900 °C.

volume of 0.73 cm^3/g and for 25 wt% alumina the surface area was 156 m^2/g with a pore volume of 0.24 cm^3/g. The isotherms of mixed-oxide aerogels calcined at 1200 °C are provided in Fig. 2.1.9. The surface area and total pore volume of silica and silica-alumina aerogels calcined at 1200 °C are provided in Table 2.1.3. The silica and 5 wt% alumina-silica aerogel loses its surface area when calcined at 1200 °C and for 15 and 25 wt% alumina aerogels the surface areas are 88 and 70 m^2/g respectively. The pore volumes for 15 and 25 wt% alumina are 0.15 cm^3 /g and 0.11 cm^3/g respectively. Surface area and Pore volume of silica and silica-alumina aerogels calcined at 500, 900 and 1200°C are provided in Table 2.1.3. The specific surface area and pore volume for the gels decrease with increase in calcination temperatures. The most obvious physical change that occurs when an amorphous gel is heated above room temperature is shrinkage. The physical and chemical changes that occur during the heat treatment of the aerogels are studied in detail [59]. Above 600 °C viscous sintering starts in the silica gel network [46-48] and this will cause a further decrease in surface area at a temperature of 1000 °C. The silica and 5 wt% alumina aerogel completely lose surface area after calcining at 1200 °C. The reduction in surface area is due to the densification of secondary particles leading to pore collapse. The pore radius increases as the calcination temperature increases for silica and mixed oxide aerogels. The slight increase in pore size for aerogels as we increase the calcination temperature may be due to the fact that the primary particles collapse to form larger pores. The incorporation of aluminium atoms into the silica network has a significant influence on the macroscopic properties of the aerogels [60]. Pure silica aerogels calcined at 1200 °C has a surface area much below the value one, (nearly no adsorption).
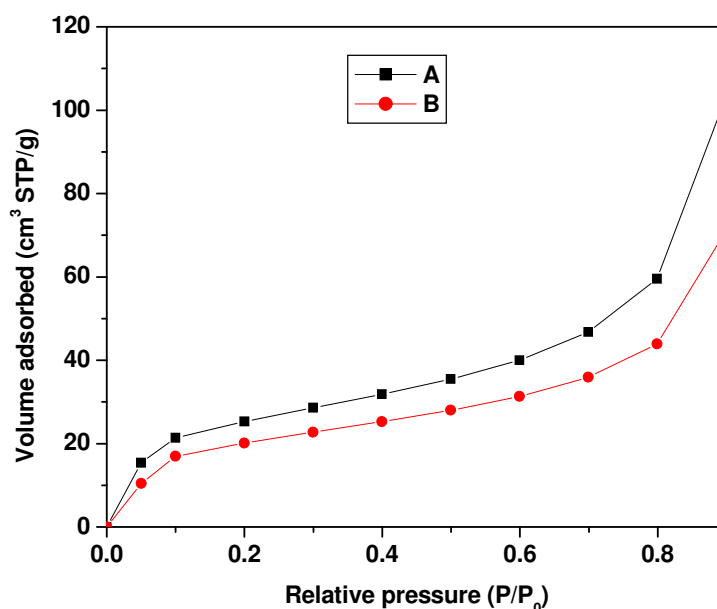
Fig. 2.1.9. Adsorption isotherms of (A) 15 wt% and (B) 25 wt% alumina calcined at 1200 °C.

By the incorporation of 15 wt% and 25 wt% of alumina, the surface area was increased from zero to 88 m^2/g and 70 m^2/g, respectively. The thermal pore stability of silica is increased by the addition of alumina. The aluminium sites shield adjacent Si-OH…OH-Si groups thus preventing the dehydroxylation and silanol condensation and also reduce the number of hydrogen bonds. The densification of secondary particles leading to pore collapse is prevented by the presence of alumina. Himmel et al. [60] investigated the linear shrinkage of subcritically dried 70% SiO_2-30% Al_2O_3 aerogel and found that the linear shrinkage was only 25% when compared with silica aerogel which showed a linear shrinkage of 48%. Saliger et al. gave a description of the shrinkage associated with supercritically dried silica aerogel into which dried aluminium oxide and aluminium hydroxide powders were integrated during sol-gel process [49].

Table 2.1.3. Surface area and pore volume of silica and silica-alumina aerogels calcined at 500, 700, 900 and 1200 °C.

Alumina content in mixed oxide Sol (wt %)	Calcination temp. (°C)	Surface area (m^2/g)	Pore volume (cm^3/g)	Pore radius (Å)
0	500	736	1.23	66
	700	583	0.91	62
	900	415	0.73	70
	1200	0	0	0
5	500	796	1.3	65
	700	662	0.99	59
	900	398	0.79	80
	1200	0	0	0
15	500	420	0.57	53
	700	359	0.48	53
	900	232	0.41	71
	1200	88	0.15	72
25	500	266	0.33	49
	700	246	0.31	50
	900	156	0.24	62
	1200	70	0.11	62

The authors found that addition of γ- Al_2O_3 improves the sinter stability of the aerogel network significantly and an admixture of only 6% of the powders reduces the shrinkage at 1000 °C by a factor of three. Cluzel et al. studied the structure of two different kinds of mullite aerogels obtained from CO_2 or methanol evacuation [61]. The thermal evolution was studied by dilatometric measurements. The temperature vs. linear shrinkage (%) is provided in Fig. 2.1.10. The linear shrinkage (%) for silica was found to be 30%, for 5 wt% alumina the shrinkage was found to be 20% and for 15 wt% alumina the shrinkage was only 20%. The shrinkage for 25 wt% alumina was found to be only 15%. This confirms that aluminium sites shield adjacent Si-OH…OH-Si groups thus preventing the dehydroxylation and silanol condensation.
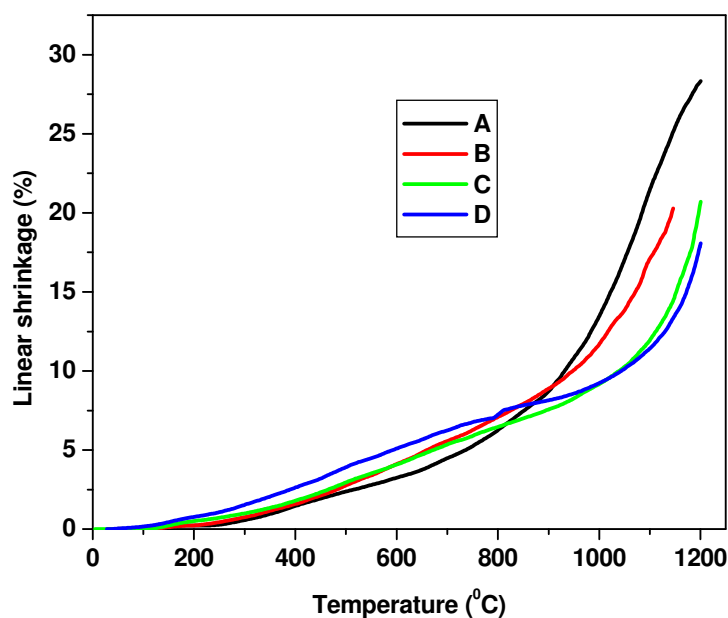
Fig. 2.1.10. Linear shrinkage (%) of (A) Silica aerogel (B) 5 wt% (C) 15 wt% and (D) 25 wt% alumina

The total acidity for 5 wt% alumina determined via TPD measurements was found to be 2.09 mmol/g and for 10% alumina it was found to be 2.13 mmol/g. When alumina is added to silica, there will be charge imbalance since alumina is octahedral and silica is tetrahedral. Substitution of Si by Al in to tetrahedral sites of SiO_2 creates a charge imbalance, which can be neutralized by H^+ cations from water molecules, which dissociate to give hydroxyl anions on the Al^{3+} cations. [53]. The total acidity for 25 wt% alumina was found to be 1.38 mmol/g and this is due to the decrease in the surface area for 25 wt% alumina aerogel.
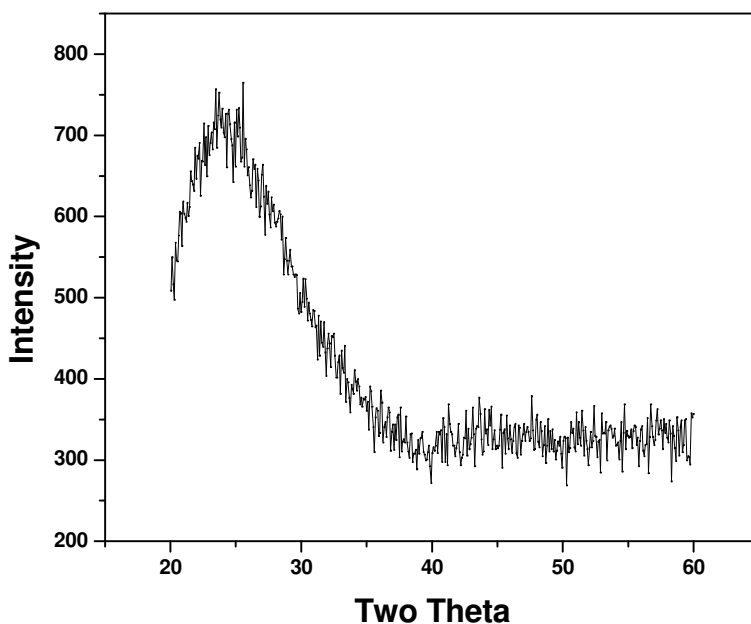
Fig. 2.1.11. XRD spectrum of 25% alumina calcined at 1200 °C.

The X-ray analysis of 25% alumina-silica aerogel calcined at 1200 °C (Fig. 2.1.11) samples showed no peaks corresponding to α-Al_2O_3 which suggests that the alumina in the aerogel is distributed homogeneously on a molecular scale.

74

2.1.5 Conclusion

A sol-gel route followed by non-supercritical drying was employed for the synthesis of silica-alumina mixed oxide aerogels. The aerogels which were calcined at different temperatures were characterised by Nitrogen sorption studies. The FTIR studies indicated the presence of Si-O-Al bonds in the mixed oxide system after calcining it at 500 °C. The resultant silica-alumina aerogel with an alumina content of 5 wt% showed a surface area of 796 m^2/g at 500 °C. With the incorporation of 15 and 25 wt% alumina, the thermal pore stability of silica aerogel was retained up to a temperature of 1200 °C. TMA indicated that the linear shrinkage (%) was only 15% for 25wt% alumina when compared with that of silica which had shrinkage of 30%. Temperature-programmed desorption studies revealed that the aerogels were acidic and the aerogel with 10 wt% alumina showed the highest acidity. The aerogels were homogeneous since there was no α-Al_2O_3 peak in the XRD pattern even after calcining at 1200 °C.

2.2 Non-Supercritically Dried Silica-Alumina Aerogels-Effect of Gelation pH

2.2.1 Abstract

Silica-alumina mixed oxide aerogels having compositions containing 5, 10, 15, 20 and 25 wt% of alumina in silica have been synthesised by a hybrid sol-gel technique followed by subcritical drying. The gelation has been carried out under pH of 3 and 5. The pH is a decisive parameter which affects the rate of hydrolysis and condensation of alkoxides. Moreover it also influences the surface area and porosity features of the final material. The gelation times have been found to be much longer for the gels which were gelled at pH 3. Nitrogen sorption studies of the aerogels calcined at 500 °C indicate that the mixed oxide aerogels are mesoporous in nature and the gel prepared under a gelation pH of 3 has been found to have higher surface area than the pH 5 counterpart. Transmission Electron Microscopy (TEM) and X- ray diffraction (XRD) analysis have been performed to verify the homogeneity of the mixed oxide aerogel.

2.2.2 Introduction

Silica–Alumina mixed oxide systems have attracted considerable academic and industrial attention owing to their application as catalyst [1-6]. An attractive method to synthesise metal catalysts and mixed metal oxide catalysts is the sol-gel method [5]. One of the most investigated forms of metal oxide catalysts is the aerogels. Aerogels are normally prepared by drying under supercritical conditions of the pore fluid. Attempts to replace the conventional drying technique for the preparation of silica-alumina mixed oxide aerogels was discussed in Chapter 2 section 2.1. The success of the drying technique, choice of the alumina precursor and its thermal pore stability were reported in this chapter. The hydrolysis conditions for the reported preparation had to be maintained

in a narrow pH window to eliminate segregation limiting the structural variations that could be achieved by changing the hydrolysis conditions in the method. But on the other hand the gelation pH is also an influential parameter that determines the final structure of the material which was not discussed in our previous report. The condensation reaction leading to gelation proceeds via a base-catalysed mechanism for pH above the isoelectric point of silica (pH 2) and is acid catalysed for pH below the isoelectric point of silica [62]. A change in gelation pH is known to yield products ranging from weakly branched polymers to compact particulates [63]. A hydrolysis rate that is rapid compared with the condensation rate is expected to favour the formation of compact particulate structures [64] and it is reported that such conditions prevail under pH conditions between 2 to 4 [62]. Hence in this chapter, the effect of gelation at a pH of 3 and 5 on the structural characteristics of silica-alumina aerogels prepared by subcritical drying is discussed.

2.2.3 Experimental

Boehmite, (AlOOH) (99% purity, alumina content 70%, Condea Chemie, Germany) having BET surface area of 230 m^2/g and crystalline size 48-60 Å was used as the precursor for alumina and Tetraethoxysilane (TEOS) (98% purity, Fluka, Switzerland) for silica. Boehmite sol was prepared by dispersing 20 g of boehmite powder in 2 L water, by keeping under stirring while the pH was adjusted to 3.5 by addition of 20% HNO_3 (S.D. Fine Chemicals, India). The concentration of alumina in the stock boehmite sol was 0.0107 g/ml. For preparing silica sol, TEOS in isopropanol (S.D. Fine Chemicals, India) was hydrolysed with HCl (S.D. Fine Chemicals, India) (pH=1.54) in a molar ratio of 1: 4: 16 [18]. In a typical experiment for preparing 25 wt% alumina in silica, 3.884 g of TEOS in 4.475 g isopropanol was hydrolysed using 5.45g of H_2O

(pH=1.54, HCl). The clear sol was stirred for 30 min, 35 ml boehmite was added and the sol was again stirred for 30 min. Subsequently, the gelation pH was adjusted to 5 using 5% ammonia solution. Another batch of experiment was done by changing the gelation pH to 3. The visually homogeneous sol was then transferred to vials (2cm diameter) and kept at 50 °C for gelation. The gelation time was noted. The gels were aged for 5 to 6 h and then were transferred to water taken in a beaker and was kept for 24 h at 50 °C. The gels were then soaked in isopropanol and the isopropanol was changed five times within 24 h in order to remove water from the pores. During this process the gels were kept at 50 °C. This was followed by aging the gels in 80% TEOS for 48 h at 50 °C and finally solvent exchange with isopropanol was performed at the same temperature i.e. at 50 °C. The gels were then dried in tightly closed containers at 70 °C so that the porous structure is retained in the gels by the slow removal of solvent from the pore network. The aerogels obtained after drying at 70 °C were calcined for 3 h at 500 °C. The alumina content was varied from 5 to 25 wt%. The detailed experimental Flowchart is provided in Fig. 2.2.1.

Bulk density of the dried gels was calculated from the mass and volume and the volumes were obtained from the diameter and thickness of the gel. The BET surface area of calcined aerogels were determined by N_2 adsorption at 77K (Micromeritics, Gemini Model 2360, USA). For Transmission Electron Microscopy (TEM) studies, the gel samples were dispersed in acetone. A few drops were placed on to a carbon coated copper grid. After ensuring the evaporation of the solvent, the copper grid was mounted in a FEI High Resolution Transmission electron microscope (HRTEM) Technai 30G[2] S-TWIN. The X- ray powder diffraction patterns of the calcined samples were recorded in

Philips Diffractometer (PW 1710), Netherlands, using Ni filtered CuKα radiation. The samples were scanned from 0 to 60° (2θ values) with a step speed of 2.4°/ min.

```
┌─────────────────────────────────────┐
│   TEOS + isopropanol + 0.001 M HCl   │
└─────────────────────────────────────┘
                  │
                  ▼
┌──────────────────────┐        ┌──────────────┐
│  Silica precursor sol │ ◄───── │ Boehmite sol │
└──────────────────────┘        └──────────────┘
                  │  Adjusting the pH to 3 and 5
                  ▼
┌──────────────────────┐
│ Silica-Alumina gel rods │
└──────────────────────┘
                  │
                  ▼
┌──────────────────────────┐
│ Aging in water for 24 hours │
└──────────────────────────┘
                  │
                  ▼
┌──────────────────────────────┐
│ Solvent exchange (isopropanol) │
└──────────────────────────────┘
                  │
                  ▼
┌──────────────────────────┐
│   Silane aging (48 hours)  │
└──────────────────────────┘
                  │
                  ▼
┌──────────────────────────────┐
│ Solvent exchange (isopropanol) │
└──────────────────────────────┘
                  │
                  ▼
┌────────────────────┐        ┌──────────────────────┐
│   Drying at 70 °C   │ ─────► │ Calcining at 500 °C   │
└────────────────────┘        └──────────────────────┘
```
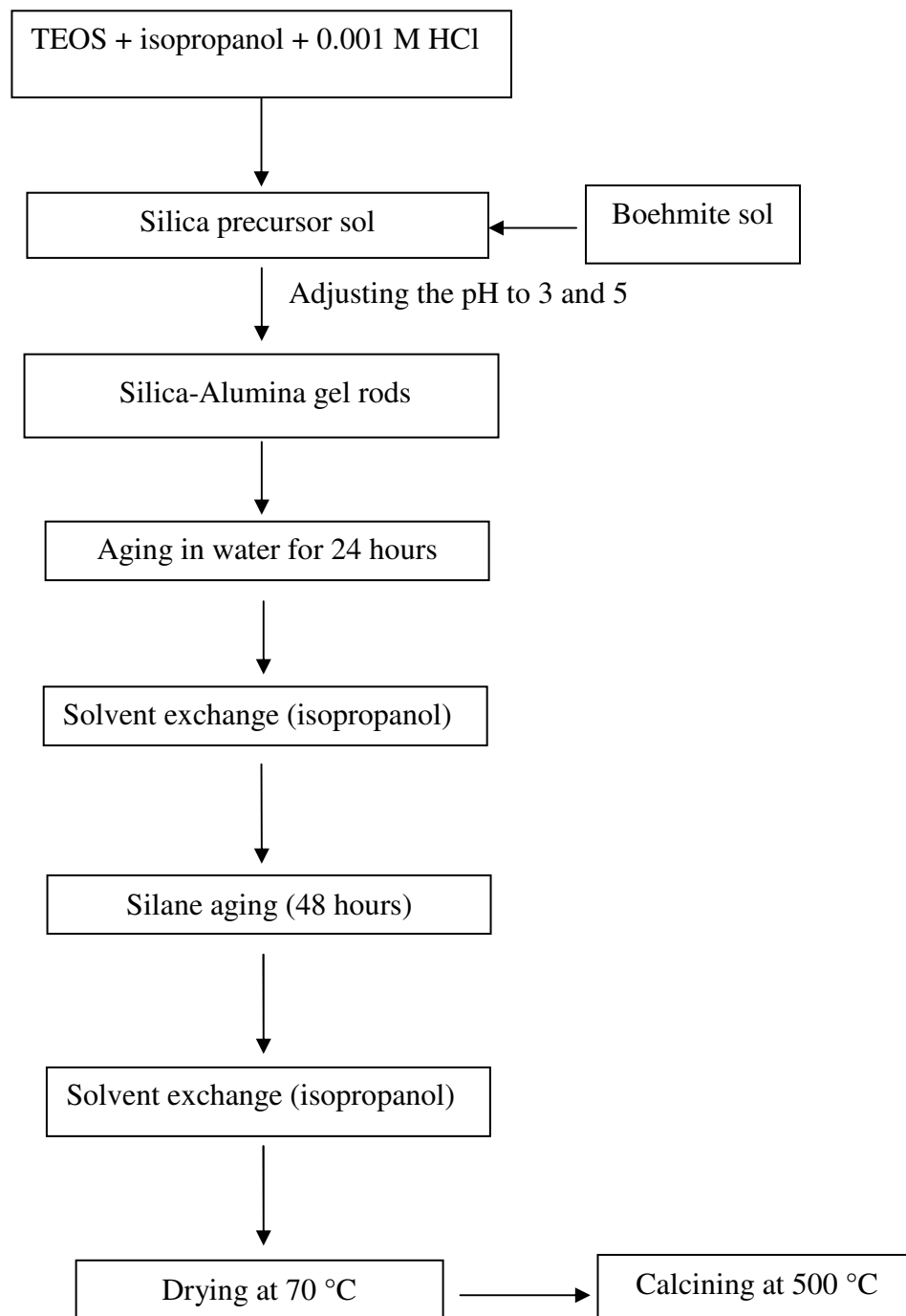
Fig. 2.2.1. Flowchart for the preparation of Silica-Alumina mixed oxide aerogels

2.2.4 Results and Discussion

The gelation time for silica as well as those containing various alumina compositions is provided in Table 2.2.1. As the alumina content increases the gelation time gets prolonged. Huang et al. found that increase of water content (as a reactant) would increase the gel time [51]. Here the TEOS: water was kept constant at 1:16, but to obtain higher loadings of alumina, a larger volume of boehmite sol was required compared with lower alumina compositions. When more and more of boehmite sol is added, water separates the condensation product and thereby decreases condensation rates. As the gelation pH is increased from 3 to 5, the gelation time is shortened. At pH 5 the hydrolysed species are consumed much faster than at pH 3 which should favour faster condensation to a three dimensional network. In the mixed system silanol groups undergo cross condensation with boehmite particles and result in a composite network structure upon gelation, with boehmite particles serving in the formation of the skeleton by a mechanism similar to that happens when silica soot is added to hydrolysed TEOS [65].

The photograph of aerogels synthesised in the present work is provided in Fig. 2.2.2. Usually the bulk density of aerogels ranges from 0.003 to 0.8 g/cm^3 with high surface area extending up to about 1500 m^2/g [66-68]. The density measurements of the as prepared silica-alumina aerogels and pure silica aerogel prepared are provided in Table 2.2.1. The adsorption isotherms of silica and mixed-oxide aerogels gelled at pH 3 and pH 5 are provided in Fig. 2.2.3.

Fig. 2.2.2. Photograph of silica-alumina mixed oxide aerogels
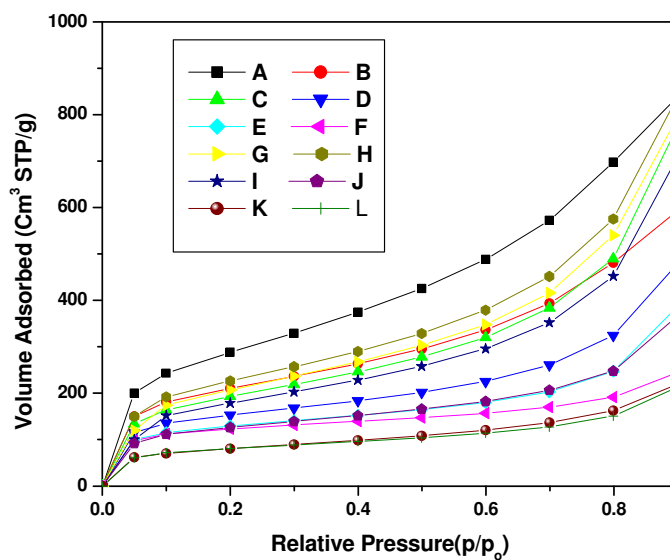
Fig. 2.2.3. Adsorption isotherms of (A) silica (pH 3) (B) 5 wt% (pH 3) (C) 10 wt% (pH 3) (D) 15 wt% (pH 3) (E) 20 wt% (pH 3) (F) 25 wt% alumina (pH 3) (G) silica (pH 5) (H) 5 wt% (pH 5) (I) 10 wt% (pH 5) (J) 15 wt% (pH 5) (K) 20 wt % (pH 5) and (L) 25 wt% (pH 5) alumina

The isotherms are Type IV which indicates that the aerogels are mesoporous. The amount of nitrogen adsorbed decreases as the percentage of alumina is increased. The decrease in the amount of nitrogen adsorbed indicates the decrease in the total pore volume and hence a decrease in the surface area. The surface area, total pore volume and pore diameter values of silica and silica-alumina mixed oxide gels prepared under gelation pH 3 and pH 5 are provided in Table 2.2.1.

F.M.A. Margaca et al. used the small angle neutron studies (SANS) to investigate the microstructure at nanoscale level, of silica gels at different processing stages [69]. The samples were prepared by the alkoxide route of the sol-gel process with different pH values. For gels prepared in strong acidic conditions, linear polymers were observed and an oxide network develops by means of a process that could be described by DLCCA (Diffusion Limited Cluster-Cluster Aggregation) model. In the case of gels produced in basic conditions, the scattering object growing in the sol has no similarity with a linear polymer and is observed to be particle like. The oxide network growth occurs through a process that can be described by the RLMCA model (Reaction Limited Monomer-Cluster Aggregation) [69]. J. Estella studied the simultaneous effect of pH, temperature, ethanol: TEOS and water: TEOS molar ratio on gelation time and textural and structural properties [70]. At pH 2.5, porous texture of gels is made up from ultramicropores, where as at pH 4.5 porous texture is in the range of supermicropores. Tamon et al. observed that the surface area and the pore radius of the aerogels were controlled by changing the molar ratio of ammonia to TMOS in sol-gel polymerization [3]. As the ratio increases, the radius decreases. In acidic conditions TEOS rapidly undergoes hydrolysis to form triethoxy silanol species. The alkoxy groups are proton donating and when alkoxy group

is removed, protonation of this silanol species will be less favourable and the second hydrolysis step will be slower. The condensation between partially hydrolysed monomers and silanol species plays a crutial role. The terminal Si (OC_2H_5) is reactive because of steric and inductive reasons and hence acid catalysed hydrolysis will lead to chain elongation and thereby formation of linear polymers [63, 69]. The entanglement of these linear polymers leads to dense gels with small pores [70]. This effect will be more marked for pH 3 than for pH 5. When pH is higher, condensation is faster when compared at pH 3 and the reaction at the central silicon atom of an oligomer is favoured. So the resulting network is characterised by big particles and large pores [67]. The aerogels which are prepared at a gelation pH of 3 have a higher surface area than the ones which are prepared at a gelation pH 5 which is due to fact that pH 3 gelled aerogels have larger pore volume compared to pH 5 gelled ones.

Transmission Electron Microscopy (TEM) studies confirmed that the prepared aerogel is meso/macro porous with a network structure. The Bright field TEM image of 5 wt% alumina-silica calcined at 500 °C (pH 5) (Fig. 2.2.3) and 25 wt% alumina-Silica aerogel calcined at 500 °C (pH 5) (Fig. 2.2.4) apparently exhibited meso-/macro-porous structure. The lighter area in the TEM is the several nanometer-sized pores. The selected area diffraction pattern (Fig. 2.2.3 and Fig. 2.2.4 inset- Top left) of 5% alumina calcined at 500 °C (pH 5) and 25 wt% alumina calcined at 500 °C (pH 5) indicates that the aerogel is amorphous. The elemental analysis employing EDAX of 5wt% alumina-silica calcined at 500 °C (pH 5) (Fig. 2.2.3. inset- Top right) and 25 wt% alumina-Silica aerogel calcined at 500 °C (pH 5) (Fig. 2.2.4 inset- Bottom right) shows the presence of Al. The silanol groups undergo cross condensation with boehmite particles and on

subsequent calcination, it will lead to the formation of Si-O-Al bonds. The Si-O-Al bond

formation starts from 400 °C and the samples are calcined at 500 °C.

Table 2.2.1. Surface area and pore volume of silica and silica-alumina aerogels prepared under gelation pH of 3 and 5 and calcined at 500 °C.

Alumina content in mixed oxide Sol (wt %)	Gelation pH	Gelation time (min)	Density (g/cm³)	Surface area (m²/g)	Pore volume (cm³/g)	Pore radius (Å)
0	pH 3	480	0.34	794	1.266	58
	pH 5	14	0.401	736	1.23	66
5	pH 3	960	0.423	744	1.3	51
	pH 5	25	0.400	796	0.94	65
10	pH 3	1875	0.516	676	1.18	65
	pH 5	70	0.54	618	1.09	69
15	pH 3	3300	0.65	506	0.74	49
	pH 5	110	0.63	420	0.57	53
20	pH 3	3840	Cracked gel	422	0.59	53
	pH 5	150	Cracked gel	272	0.34	57
25	pH 3	4800	Cracked gel	390	0.37	38
	pH 5	220	Cracked gel	266	0.33	49
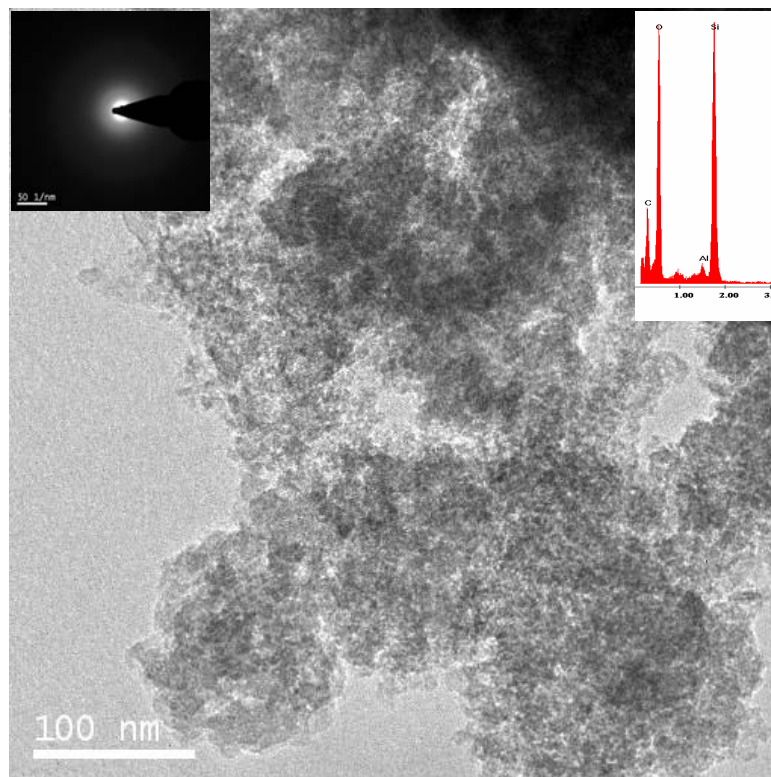
Fig. 2.2.3. Bright Field image of 5 wt% alumina aerogel calcined at 500 °C (pH 5),
Selected area diffraction pattern of (Inset-Top left) and EDAX spectrum (Inset-Top right)
of 5 wt% alumina aerogel.

Moreover Si-O-Al bond formation is a direct reflection of the structural homogeneity of
the aerogel. The absence of any crystalline phase, particularly α-alumina on calcination at
1200 °C, indicates that boehmite particles are homogeneously distributed through out the
aerogel without any segregation in the nanoscale.
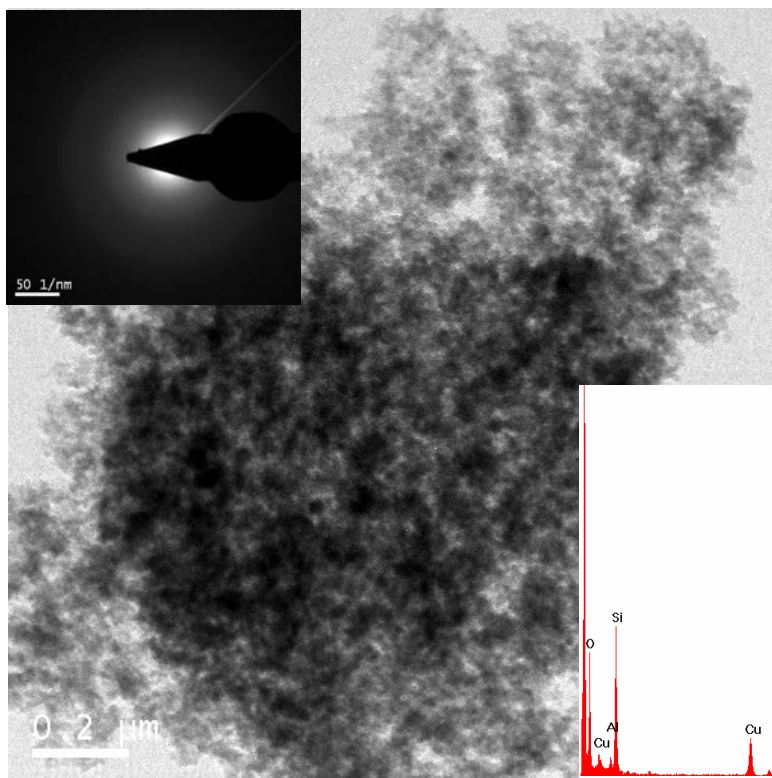
Fig. 2.2.4. Bright Field image of 25 wt% alumina aerogel calcined at 500 °C (pH 5), Selected area diffraction pattern of (Inset-Top left) and EDAX spectrum (Inset-Bottom right) of 25 wt% alumina aerogel.

2.2.5 Conclusion

A hybrid sol-gel route followed by subcritical drying was employed for the synthesis of silica-alumina mixed oxide aerogels. The gelation was carried out under pH of 3 and 5. The aerogels which were prepared by gelation at pH 3 had a higher surface area than the ones which were prepared at gelation pH 5. The reduction in surface area is attributed to the formation of larger pores. TEM microstructural analysis indicates that the aerogel is amorphous and absence of α-Al$_2$O$_3$ even after calcination at 1200 °C, is a direct consequence of alumina being homogeneously dispersed in the silica network which was confirmed using X-ray diffraction.

References

[1] Y. Matsumoto, K. Mita, K. Hashimoto, T. Tokoroyama, Appl. Catal. A: Gen. 131 (1995) L1-L6.

[2] Y. Matsumoto, K. Mita, K. Hashimoto, Tetrahedron 52 (1996) 9387.

[3] H. Tamaon, T. Sone, M. Mikami, M. Okazaki, J. Colloid Interface Sci. 188 (1997) 493.

[4] A. Carati, G. Ferraris, M. Guidotti, G. Moretti, R. Psaro, C. Rizzo, Catal. Today 77 (2003) 315.

[5] R.Takahashi, S. Sato, T. Sodesawa, M.Yabuki, J. Catal. 229(2005)24.

[6] R.Ochoa, H.V. Woert, W.H. Lee, R. Subramanian, E. Kugler, P.C. Eklund, Fuel Process. Technol. 49 (1996) 119.

[7] S.D. Jones, T.N. Pritchard, D.F. Lander**,** Micropor. Mater. 3 (1995) 419**.**

[8] A.C. Pierre*,* Ceram. Int. 23 *(*1997) 229.

[9] A. E. Gash, T.M. Tillotson, J.H. Satcher, L.W. Hrubesh, R.L. Simpson**,** J. Non-Cryst. Solids 285 (2001) 22**.**

[10] K. Okada, T. Tomita, A. Yasumori, J. Mater. Chem. 8 (1998) 2863.

[11] H. Schneider, K. Okada, J. A. Pask, Mullite and Mullite Ceramics; John Wiley: New York, 1994.

[12] A.R. Boccaccini, M. Bu¨cker, T.K. Kahlil, C.B. Ponton, J. Eur. Ceram. Soc. 19 (1999) 2613.

[13] S.S. Kistler, Nature 127 (1931) 741.

[14] J. Fricke, J. Non-Cryst. Solids 95 (1987) 1135.

[15] S.S. Prakash, C.J. Brinker, A.J. Hurd, S.M. Rao, Lett. Nature 374 (1995) 439.

[16] F. Schwertfeger, D. Frank, M. Schmidt, J. Non-Cryst. Solids, 225 (1998) 24.

[17] R. Deshpande, Duen-Wu-Hua, D.M. Smith, C.J. Brinker, J. Non-Cryst. Solids 225 (1992) 254.

[18] S. Rajesh Kumar, P. Krishna Pillai, K. G. K. Warrier, Polyhedron 17 (1998) 1699.

[19] A. Venkateswara Rao, E. Nilsen, M-A. Einarsrud, J. Non-Cryst. Solids 296 (2001) 165.

[20] P.J. Davis, C.J. Brinker, D.M. Smith, J. Non-Cryst. Solids 142 (1992) 189.

[21] P. J. Davis, C.J. Brinker, D.M. Smith, R. Assink, J. Non-Cryst. Solids 142 (1992) 197.

[22] M-A. Einarsrud, S. Haereid, J. Sol-Gel Sci. Technol. 2 (1994) 903.

[23] S. Haereid, M-A. Einarsrud, G. W. Scherrer, J. Sol-Gel Sci. Technol. 3 (1994) 199.

[24] S. Haereid, M. Dahle, S. Lima, M-A. Einarsrud, J. Non-Cryst. Solids 186 (1995) 96.

[25] S. Haereid, E. Nilsen, M-A. Einarsrud, J. Non-Cryst Solids 204 (1996) 228.

[26] M-A. Einarsrud and E. Nilsen, J. Non-Cryst. Solids 226 (1998) 122.

[27] R. Deshpande, D. Smith, C. J. Brinker. US patent No. 5, 565,142 issued 1996.

[28] D.M. Smith, D. Stein, J.M. Anderson, W. Ackerman, J. Non-Cryst. Solids 186 (1994) 104.

[29] C. J. Brinker, S.S. Prakash, US patent disclosure (1994).

[30] V.D. Land, T.M. Hareis, Dale C. Teeters, J. Non-Cryst. Solids 283 (2001) 11.

[31] G. S. Kim, S. H. Hyun, J. Mater. Sci. 38 (2003) 1961.

[32] T. Heinrich, R. Raether, O. Sportmann, J. Fricke, J. Appl. Cryst. 24 (1991) 788.

[33] T. Heinrich, F. Raether, J.Non-Cryst. Solids 147&148 (1992) 152.

[34] T. Heinrich, J. Non-Cryst. Solids 168 (1994) 14.

[35] J.C. Pouxviel J.P. Boilot, A. Dauger, A. Wright, J. Non-Cryst. Solids 103 (1988) 331.

[36] J .P. Boilot, J. C. Pouxviel, A. Dauger, A. Wright, in: Better Ceramics Through Chemistry III MRS Symposium, Vol.121 ed. C. J. Brinker, D. E. Clark and D. R. Ulrich (Materials Research Society, Pittsburg, PA, 1998) p. 22.

[37] S. Komerneni, R. Roy, J. Am. Ceram. Soc. 69 (1986) C42.

[38] P. Kansal, R. Laine, M.F. Baboneau, J. Am. Ceram.Soc.80 (1997) 2597.

[39] M.I. Nieto, G. Urretavizcaya, A.L. Cavalieri, P. Pena, Br. Ceram. Trans. 97 (1988) 17.

[40] J.A. Pask, A.P. Tomsia, J. Am. Ceram. Soc. 74 (1991) 2367.

[41] J.C. Huling, G.L. Messing, J. Am. Ceram. Soc. 74 (1991) 2374.

[42] D.X. Li, W.J. Thomas, J. Am. Ceram.Soc.74 (1991)2382.

[43] S. Sundaresan, I.A. Aksay, J. Am. Ceram. Soc. 74 (1991) 2388.

[44] K. Okada N. Otsuka in: S. Somiya, R. F. Davis, J. A. Pask (eds) Formation process of Mullite Ceramic Transaction, Mullite and Mullite Matrix Compositions, Vol, 6, American Ceramic Society 1990 p.375.

[45] Y. Suwa, R. Rou, S. Komarneni, J. Am. Ceram. Soc. 68 (1985) 238.

[46] M. Prassas, J. Phalippou and J. Zarzycki, Science of ceramic processing (Wiley, NewYork, 1986) Ch 17.

[47] W. Lenhard, Diploma thesis, University of Wurzburg, Report E21-0393 (1993).

[48] A. Emmerling, J. Gross, J. Gerlach, R. Goswin, G. Reichenauer, J. Fricke, H. G. Hanbolt, J. Non-Cryst. Solids, 125 (1992) 230.

[49] R. Saliger, T. Heinrich, T. Gleissner, J. Fricke, J. Non-Cryst. Solids, 186 (1995) 113.

[50] S. Rajesh kumar, PhD Thesis, "High Surface Area Porous Sol-Gel Silica and Mixed Oxide Aerogels Through Subcritical Drying: University of Kerala, 2002.

[51] Y.Y. Huang, K. –S. Chou, Ceram. Int. 29 (2003) 485.

[52] G. Zhang, A. Das, A. Rawashdeh, J. Thomas, J. A. Counsil, C. S- Leventis, E. F. Fabrizio, F. Ilhen, P. Varsilaras, D. A. Schaiman, L. Mc Corkle, A. Palzer, J. Chris Johnson, M. A. Meador, N. Leventis, J. Non-Cryst. Solids 35 (2004) 152.

[53] P. Padmaja, K.G.K. Warrier, M. Padmanabhan, W. Wunderlich, F. Berry, M. Mortimer, N.J. Creamer, Mat. Chem. Phy. 95 (2005) 56.

[54] A. Bertoluzza, C. Fagbabo, M.A. Morelli, V. Gottadri, M. Guglielmi, J. Non-Cryst. Solids 48 (1982) 117.

[55] D.R. Dunphy, S. Singer, A.W. Cook, B. Smarsly, D.A. Doshi, C.J. Brinker, Langmuir 19 (2003)10403.

[56] C. Hernandez, A.C. Pierre, Langmuir 1*6 (*2000) 530.

[57] K. Sinko, N. Hu¨sing, G. Goerigk, H. Peterlik, Langmuir 24 (2008) 949

[58] K. Balkis Ameen T. Rajasekharan, M.V. Rajasekharan J. Non-Cryst. Solids 352 (2006) 737.

[59] C.J. Brinker and G. W. Scherer, Sol-Gel Science: The Physics and Chemistry of Sol-Gel Processing, Academic Press, New York, 1989.

[60] B. Himmel, Th. Gerber, H. Burger, G. Holzhuter, A. Olbertz, J. Non-Cryst. Solids 186 (1995) 149.

[61] F. Cluzel, G. Larnac, J. Phalippou, J. Mater. Sci. 26 (1991) 5979.

[62] D.L. Meixner, P.N. Dyer, J. Sol-Gel Sci. Technol. 14 (1999) 223.

[63] C.J. Brinker, W.D. Drotning, G.W. Scherer, Mat. Res. Symp. Proc. 32 (1988) 25.

[64] L. Chu, M.I. Tejedar- Tejedar, M.A. Anderson, Micropor. Mater. 8 (1997) 207.

[65] M. J. Van Bommel, C.W. Den Engelsen and J.C. Van Miltenburg, J. Porous Mater., 4 (1997) 143.

[66] J. Frick, Sci. Am. 258 (1988) 92.

[67] N. Husing and U. Schubert, Angew. Chem. Int. Ed., 37 (1998) 22.

[68] A.C. Pierre and G.M. Pajonk, Chem. Rev., 102 (2002) 4243.

[69] F.M.A. Margace, I.M.M. Salvo, J. Teixeira, J. Non-Cryst. Solids, 258 (1999) 70.

[70] J. Estella, J.C. Echeverria, M. L. Laguna, J.J. Gaerido, J. Non-Cryst. Solids, 353 (2007) 286.

Chapter 3:   *Non-Supercritically Dried Silica-Silica Composite Aerogels and its Application for Confining Simulated Nuclear Wastes*

3.1 Synthesis and characterisation of non-supercritically dried Silica-Silica aerogels

3.1.1 Abstract

A simple non-supercritical drying approach has been used for the preparation of silica-silica composite aerogels (CA) and the efficiency of the process being demonstrated by testing the use of the aerogels for simulated high level nuclear waste confinement. Compositions of 5, 10, 20, 30, 40 & 50 wt% of silica (aerosil® 380) in silica- aerogel were prepared by introducing pyrogenic silica into silica sol derived by hydrolysis of Tetraethoxy silane (TEOS). The silica-silica composite aerogels (CA) possessed very high surface area and low bulk densities. The effectiveness of the prepared composite aerogels as precursor for high level nuclear waste immobilized glass is also presented. Neodymium nitrate dissolved in isopropanol is used to simulate +3 valent actinides. The stability of neodymium in the glass matrix has been found to be extremely high. Transmission Electron Microscopy (TEM) has been used to characterise the aerogels as well as neodymium incorporated sintered gels. X-ray diffraction (XRD) studies of the sintered samples reveal the formation of neodymium silicates.

3.1.2 Introduction

Aerogels are unique solid materials having extremely low densities (up to 95% of their volume is air), large open pores and high surface area. The pore sizes of aerogels lie

within the scale length of 1-100 nm, showing micro to macroporosity. Silica-Silica composite aerogel has much better permeability, improved pore size distribution and higher pore volume on comparison with classical aerogels. Generally Silica powder [aerosil ® (Degussa)] is used to prepare composite aerogels. Toki et al. [1] mixed aerosil OX 50 ® with hydrolysed TEOS, adjusted the pH to favour quick gelation, dried and subsequently sintered the dried gels to get glass. The resulting gels had larger pores (they were opaque white rather than clear, as alkoxide derived silica gels usually are) and larger samples could be dried much faster than gels not containing the particles. The advantage of larger pores is generally ascribed to the lower capillary pressure they produce and also results in much higher permeability. Aerosil particles also contribute to the strength of the gel.

The addition of aerosil soot to the hydrolysed solution of alkoxysilanes affects the fractal network which results from the aggregation mechanism of alkoxysilanes [2]. USAX showed that beside the fractal network built up by the organosiloxane, the silica soot is forming another fractal structure at a higher scale. For low aerosil content the aggregation mechanism of organosiloxane is preserved, but for high soot content a large part of TEOS is consumed and polymeric clusters cannot grow.

Different procedures have been adopted for the preparation of aerogels from the wet gel. The conventional approach is the high temperature supercritical drying where the pore liquid, usually alcohol, is dried above its critical point, avoiding shrinkage of the gel network. The supercitical drying is energy intensive, expensive and risky and attempts to find a suitable alternative to it is evident from earlier reports [3-5]. Two strategies are mainly employed for the preparation of aerogels by non-supercritical drying. One is

increasing the stiffness of the gel network by aging in a silane precursor [6-8] and the other is capping the surface silanol groups by alkyl groups so that the gel breaths back to shape after shrinkage due to repulsion between the alkyl groups [9, 10]. Non-supercritical/Subcritical drying approach which involves processes of solvent exchange, silane aging and drying under controlled conditions has evolved by virtue of various researchers into a competent alternative for the synthesis of silica aerogels [3-12].

Use of aerogels for confinement of radioactive wastes has gathered considerable attention in recent years [13-16]. The long life wastes are immobilised in a chemically durable matrix. Silica glass is the most important among them and sol-gel process is the best method to synthesise glasses at low temperature (~1000 °C). Waste is immobilized by chemical incorporation in to the structure of the glass matrix, so it is captured and is unable to escape. Silica glass has good mechanical strength and thermal shock resistance. Also high chemical durability and structural stability are achieved by high content of silica and low content of modifier oxides [17]. The silica aerogel is an appropriate precursor which can be converted into vitreous silica by short duration treatment at low temperature. The large pore volume of the silica aerogel is used as a sponge to incorporate chemical species [17]. T. Woignier et al. prepared Silica aerogels were by the hydrolysis of TEOS in acidic medium and the gels so obtained was supercritically dried in an autoclave [17]. Neodymium oxide was used to simulate the actinide oxide. The aerogel after simulation was dried and calcined at 600 °C in such a way to complete the drying and decomposition of the neodymium nitrate. Further heating at 1100 °C fully sinters the structure by viscous flow. The porous network features (mechanical strength, pore size) of the gel precursor to soak up simulating salts was also investigated. The

leaching studies were also performed on the simulated glass matrix using a conventional Soxhlet extractor. The percentage loading was found to be 10 wt%.

Use of silica aerogels for the purpose is limited by their brittleness in presence of water and also due to their low permeablity to nuclear waste [18-20]. Composite aerogels (CA) of the kind silica-pyrogenic silica (aerosil) is an alternative owing to their larger pore sizes and added mechanical strength [18-20]. T. Woignier et al. [18] prepared composite aerogels with tailored pore size and the aerogels thus prepared possess a much improved permeability compared with that of classical aerogels. The composite aerogels were prepared by the addition of fumed silica (aerosil) in the hydrolysed silica sol and then pH was adjusted to 4.5 which favours quick gelation. The supercritical drying of alcogels was carried out in an autoclave to produce the aerogels. The composite aerogels were then impregnated by neodymium salt solutions having different concentrations and the weight gain was measured after sintering the aerogels at 1100 °C. The isotopic linear shrinkage measurements and the bulk density by Archimedes principles were determined on the sintered aerogel. The leaching studies were also performed on the simulated glass matrix using a conventional Soxhlet extractor.

In a related work, Reynes et al. [19] prepared partially sintered composite aerogels and studied its permeability features. On comparison with classically sintered aerogels, pore size and pore volume of partially sintered composite aerogels (PSCA) was found to be larger and a weight loading close to 20 wt% was achieved.

T. Woignier [20] in another work studied the prospective use of different sets of silica aerogels (Classical, Partially densified aerogels and composite aerogels) as host matrices for chemical species. Mechanical properties and permeability measurements

were done on the above mentioned sets of aerogels in order to compare the advantages and drawback among the different sets of aerogels. The mechanical resistance was measured by static bending technique. Woignier tried to improve the mechanical properties by 1) increasing the monomer content, 2) by sintering and 3) by addition of oxide particles such as fumed silica. Different weight percentages of fumed silica were added to silica sol and the pH adjusted to 4.5 to favour quick gelation. The authors found that the mechanical features of composite aerogels with 0-40% aerosil content are quite constant and are analogous to that of polymeric classical aerogels. They also measured the permeability (D) by a method of impregnation based on Archimedes principle and found that the permeability was better than the classical aerogels. A high permeability is generally an advantage because it means that the fluid and thus the chemical species of interest migrate easily in the porous network and should field a homogeneous distribution of the chemical species. The composite aerogels were impregnated by neodymium salt solutions having different concentrations and the weight gain was measured after sintering the aerogels at 1100 °C. Waste loadings higher than 20 wt% was achieved by this method. The neodymium loaded samples present three different crystalline phases, neodymium sesquioxide (Nd_2O_3) and neodymium silicates (Nd_2SiO_5 and $Nd_2Si_2O_7$).

In this chapter, non-supercritical drying/subcritical drying technique employed for the preparation of silica-silica composite aerogels is presented. The effectiveness of the dried gels for nuclear waste confinement is also tested. A comparison of data available in literature shows that the prepared aerogels are at par with their supercritically dried counterparts for use as nuclear waste confinement media.

3.1.3 Experimental

Composite aerogels were synthesized by the hydrolysis of Tetraethoxysilane (TEOS), (Fluka, Switzerland) by acidified water in presence of isopropanol (S D Fine chemicals, India) as the solvent. Hydrolysis was carried out by maintaining the TEOS: Isopropanol: Acidified water ratio at 1:4:16. In a typical experiment, 2g of silica sol was prepared by hydrolyzing 6.91g of TEOS in 7.96g of isopropanol with 9.54g of 10^{-3} M HCl. The mixture was stirred using a magnetic stirrer for 1 hour. To this sol a definite weight of pyrogenic silica (aerosil® 380, Degussa, Average particle size of 7 nm) (weight % relative to the total silica content in the final aerogel), ie 5, 10, 20, 30, 40 or 50 % was added and stirring was continued for another half an hour. The pH of the visually homogeneous sol was adjusted to 5.5 by the addition of 2% ammonia solution. The sol was then immediately transferred into cylindrical vials and kept at 50 °C for gelation which was completed with in about 10 minutes. The composite gels were then aged in water for 24 hours. Solvent exchange with isopropanol was carried out five times within the next 24 hours. The gels were then kept for aging in 80% TEOS (in isopropanol) for 48 hours and then washed with isopropanol (5 times within 24 hours) and finally dried at 70 °C to obtain the composite aerogels.

Neodymium nitrate is usually employed to simulate experiments involving nuclear wastes [17]. The composite aerogels (i.e. 20, 30, 40 and 50 wt%) were immersed over a period of 4 hours in 30% neodymium nitrate solution (M/s Indian Rare Earths Ltd. India) in isopropanol maintained at 50 °C. The neodymium nitrate diffuses in to the porous network of the aerogel.

```
┌─────────────────────────────────────────┐
│   TEOS + isopropanol + 0.001 M HCl       │
└─────────────────────────────────────────┘
                    │
                    ▼
┌─────────────────────────┐        ┌──────────────────────┐
│   Silica precursor sol   │◄───────│   Pyrogenic silica    │
└─────────────────────────┘        └──────────────────────┘
                    │
                    ▼
┌─────────────────────────┐
│   Silica-Silica gel rods │
└─────────────────────────┘
                    │
                    ▼
┌─────────────────────────┐
│  Aging in water for 24 hours │
└─────────────────────────┘
                    │
                    ▼
┌─────────────────────────────┐
│  Solvent exchange (isopropanol) │
└─────────────────────────────┘
                    │
                    ▼
┌─────────────────────────┐
│   Silane aging (48 hours) │
└─────────────────────────┘
                    │
                    ▼
┌─────────────────────────────┐
│  Solvent exchange (isopropanol) │
└─────────────────────────────┘
                    │
                    ▼
┌─────────────────────────┐
│      Drying at 70°C      │
└─────────────────────────┘
                    │
                    ▼
┌─────────────────────────┐       ┌──────────────────────┐
│  Immersed in 5, 10, 20 & │──────►│  Drying and sintering at │
│   30% Nd (NO3)3          │       │       1200 °C         │
└─────────────────────────┘       └──────────────────────┘
```
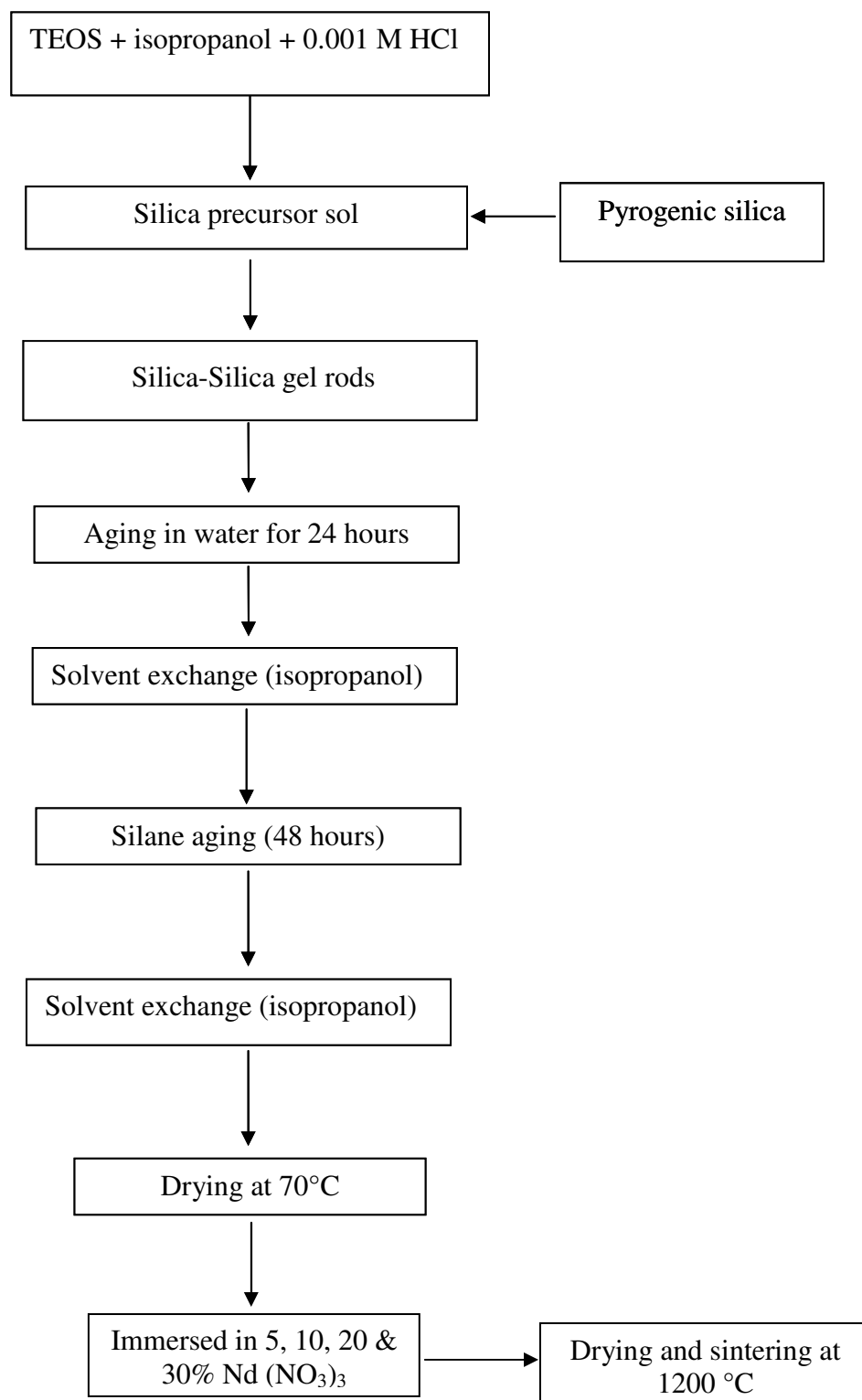
Fig. 3.1.1. Flowchart for the preparation of Silica-Silica aerogels

The neodymium loaded composite aerogels were then dried at 70 °C and subsequently sintered at 1200 °C. The percentage of loadings were calculated by simple weight difference of the sintered neodymium incorporated aerogel and that of the sintered aerogel without neodymium as reported by Woignier et al. [17]. The detailed flowchart is provided in Fig. 3.1.1.

The glass durability was measured using a conventional soxhlet device based on earlier reports [17]. Soxhlet device consists of a boiler containing 300ml of ultra pure water and a condenser system. A previously weighed neodymium incorporated aerogel sintered at 1200 °C was placed in a sample boat into which condensed steam was passed continuously. The test was conducted at about 60-70 °C. The samples were dried and the weight of the sintered sample was periodically noted after 10, 20, 30, 40 & finally after 51 hours.

Bulk density of the dried gels (cylindrical samples) was calculated from their mass and volume. The BET surface areas of calcined aerogels were determined by N_2 adsorption at 77K (Micromeritics, Gemini Model 2360, USA). The calcined samples were preheated in a flow of nitrogen for 5 hours at 200 °C to remove all the volatiles and chemically adsorbed water from the surface. Adsorption studies were carried out at liquid nitrogen temperature.

The specific surface area was determined using the BET equation with an accuracy of ± 10 m^2/g. The total pore volume was calculated as,

$$\text{Pore volume, } V = Va* D$$

Where V_a = volume adsorbed at P/P_0 0.99, D = density conversion factor (0.0015468 for nitrogen as adsorbate gas). The pore size distribution was obtained using the Barrette-

Joynere-Halenda (BJH) method. Assuming that the pores are cylindrical and open at both ends, the average pore size of a given sample is calculated using the equation,

$$\text{Average pore size} = 4V_{total}/S_{BET}$$

For Transmission electron microscopy studies (HRTEM) the gel powder was dispersed in acetone. A few drops were placed on carbon coated copper grids. After ensuring the evaporation of the solvent, the copper grid was mounted on a FEI High Resolution Transmission electron microscope (HRTEM) Technai $30\,G^2$ S-TWIN. The X-ray powder diffraction patterns of the calcined samples were recorded on a Philips Diffractometer (PW 1710)-The Netherlands, using Ni filtered CuKα radiation. The samples were scanned from 0 to 60 °, 2θ values with a step speed of 2.4°/ min.

### 3.1.4 Results and Discussion

The non-supercritical/subcritical drying approach presented here involves careful and systematic process of solvent exchange, silane aging and drying under controlled conditions. A high water/alkoxide ratio is used here since it results in porous gels having high surface area [11]. Cross condensation between silanol groups of pyrogenic silica and polymeric silesqueoxane particles formed by the hydrolysis condensation reactions of tetraethylorthosilane result in a composite network structure upon gelation, with particles from pyrogenic silica precursor also serving in the formation of the silica skeleton. The wet composite gels were then solvent exchanged with isopropanol since liquids of low surface tension and high molecular volume favour the production of gels having high surface area [11]. The aging process in 80% silane solution for 48 h provides strength to the gel network by dissolution and reprecipitation of silica on the gel network. The structural strength of the composite aerogel is attributed to the participation of pyrogenic

Chapter 3

silica particles in the formation of aerogel skeleton [21]. A composite polymeric –
particulate network would be more adaptive towards subcritical drying rather than a
polymeric network. This is the underlying principle to the success in the preparation of
composite silica-silica aerogels by subcritical drying.
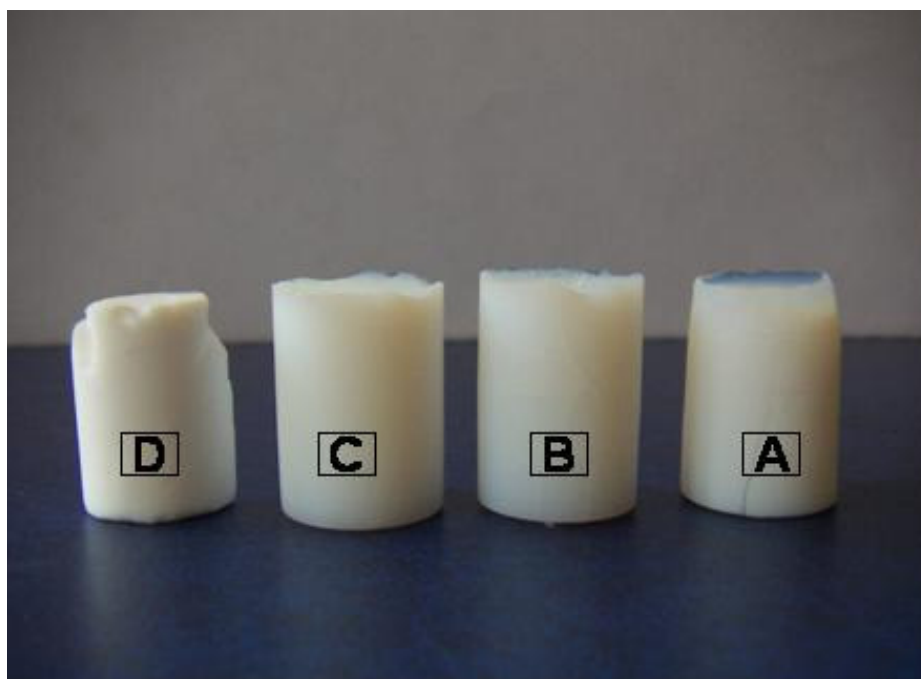
Fig. 3.1.2. Photograph of composite aerogel prepared by subcritical Drying (A) 20 wt %
(B) 30 wt % (C) 40 wt % and (D) 50 wt% Composite aerogels

Crack free monoliths prepared by employing the subcritical drying technique
described are shown in the photograph provided in Fig. 3.1.2. The bulk density of silica-
silica composite aerogels (CA) and that of silica aerogel prepared under similar
conditions is provided in Table 3.1.1.
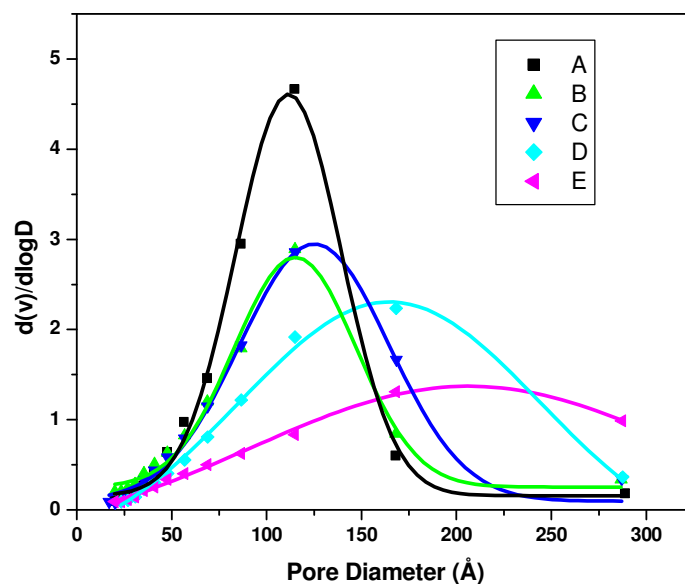
Fig. 3.1.3. Pore size distribution of (A) 5 wt% (B) 20 wt% (C) 30 wt% (D) 40 wt% & (E) 50 wt% composte aerogels.

Aerogel properties are observed in the density range 0.003 g/cm^3 to 0.8 g/cm^3, and surface area extending upto 1500 m^2/g [22-24]. The silica aerogel has a density of 0.40 g/cm^3 and the 5 wt% composite aerogel has a density of 0.36 g/cm^3. The density does not change much (except for 50 wt% CA) as the weight percentage of pyrogenic silica content is increased. This must be due to the fact that larger pores are formed on aerosil addition. At lower concentration, the pyrogenic silica particle acts as seeds for polymeric cluster formation, but as its concentration increases, the network of pyrogenic silica particles is formed with polymeric clusters surrounding the pyrogenic silica particles acting as links [25]. Compared to the polymeric network arising from the TEOS precursor a network of the larger pyrogenic silica particles will have larger pore sizes. Pore size distribution curves obtained for the samples is provided in Fig. 3.1.3 and pore volumes of silica and composite aerogels are summarised in Table 3.1.1. The pore size

distribution extends up to the 200 Å regions for the compositions containing low aerosil content and extends up to 300 Å for samples with higher aerosil content. The pore size distribution shifts towards larger diameters as the percentage of pyrogenic content is increased.

Table 3.1.1. Density and BET Surface area measurements of Composite aerogels

Sample	Density (g/cm³)	Pore volume (cm³/g)	Surface area(m²/g)	Pore diameter (Å)
Silica aerogel	0.40	1.15	764	60
5% CA	0.36	1.57	801	78
10% CA	0.36	1.48	804	73
20% CA	0.40	1.28	734	70
30% CA	0.43	1.18	651	72
40% CA	0.47	1.11	625	71
50% CA	0.63	0.71	493	57

Silica soot are dense particles and the increase in its ratio is expected to decrease the total pore volume. The total pore volume obtained for 5 wt% composite aerogel is 1.57 cm³/g and it decreases to 0.71 cm³/g for the 50 wt% composite aerogel. Comparing with the silica aerogels prepared under the same conditions, the total pore volume and surface area are higher for the 5 and 10 wt% composite aerogels with a corresponding decrease in density. The capillary pressure Pc, which is responsible for the drying stress is propotional to $1/r_p$, where r_p is the pore radius. Hence the composite aerogels are

subjected to lesser drying stress during drying due to their larger pore radius. The decrease in drying stress due to larger pore sizes and increased strength of a composite polymeric-particulate network ensures better properties for composite aerogels with lower aerosil content while the competing increase in density due to higher ratio of denser aerosil particles becomes detrimental for the composite aerogels with higher aerosil content. When the shrinkage becomes less the densities will be low. The lower shrinkage of the composite aerogels is evident from the total pore volume.

The adsorption-desorption isotherms of the silica and silica-silica composite aerogels (CA) are provided in Fig. 3.1.4. The isotherm is of Type IV which is characteristic of mesoporous materials. The BET surface area results are provided in Table 3.1.1. As the percentage of pyrogenic silica content increases the volume of nitrogen adsorbed decreases as a consequence of the reduced total pore volume. The 5 wt% composite aerogel has surface area of 801 m^2/g and for 10 wt% composite aerogel the surface area is 804 m^2/g**.** For 5 and 10 wt% CA, the increase in surface area when compared with pure silica system may be attributed to larger pore volume resulting from the reduced shrinkage. The surface area for 30, 40 & 50 wt % composite aerogels is 651, 625 & 493 m^2/g respectively. The decrease in the surface area values as the aerosil content is increased beyond 10 wt% is due to the decrease in the total pore volume and can be attributed to the removal of porosity by the increasing presence of denser pyrogenic aerosil particles.
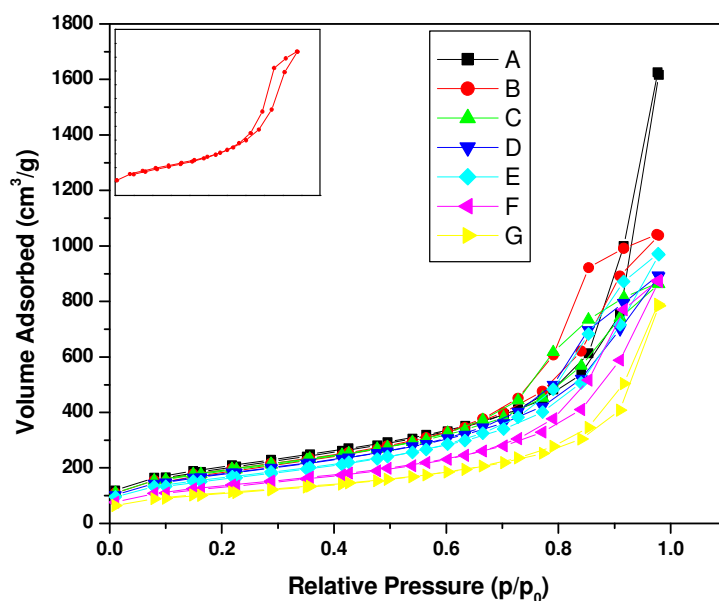
Fig. 3.1.4. Adsorption-Desorption Isotherms of (A) Silica (B) 5 wt% (C) 10 wt% (D) 20 wt% (E) 30 wt% (F) 40 wt% & (G) 50 wt% composite aerogels. (Inset-The adsorption-desorption isotherm of 5 wt% composite aerogel).

Transmission Electron Microscopy (TEM) studies confirmed that the prepared aerogel is nanoporous with a network structure. The Bright field image of 40 wt% and 10 wt% silica-silica composite aerogel is provided in Fig. 3.1.5 and Fig. 3.1.6 respectively. The lighter area in the TEM is the nanopore inside the prepared aerogel with dark particles of the minority phase A (aerosil particle) and brighter particles of the rest B (silica condensed from TEOS). The TEM micrograph of 10 wt% composite aerogels reveal that the pyrogenic silica (marked A in the Fig. 3.1.6) is uniformerly distributed in the silica matrix.
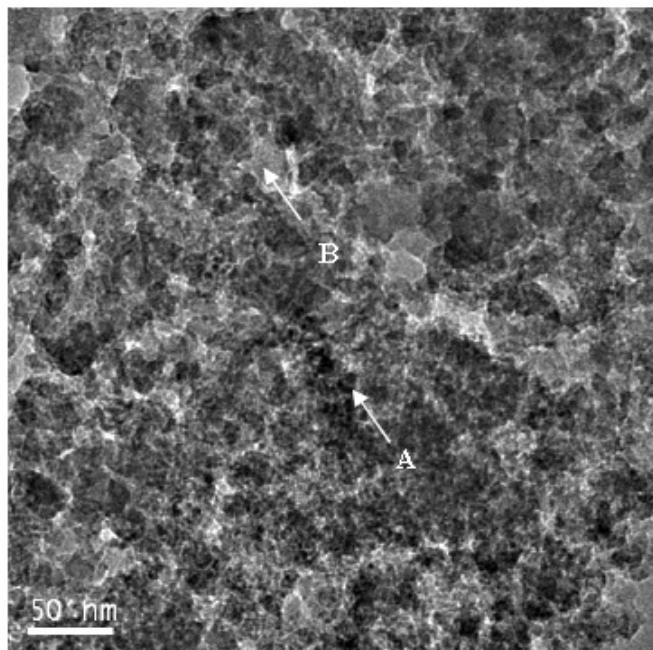
Fig. 3.1.5. TEM micrograph of 40 wt% Composite aerogel. A is the pyrogenic silica particle and B is the Silica particles condensed from TEOS
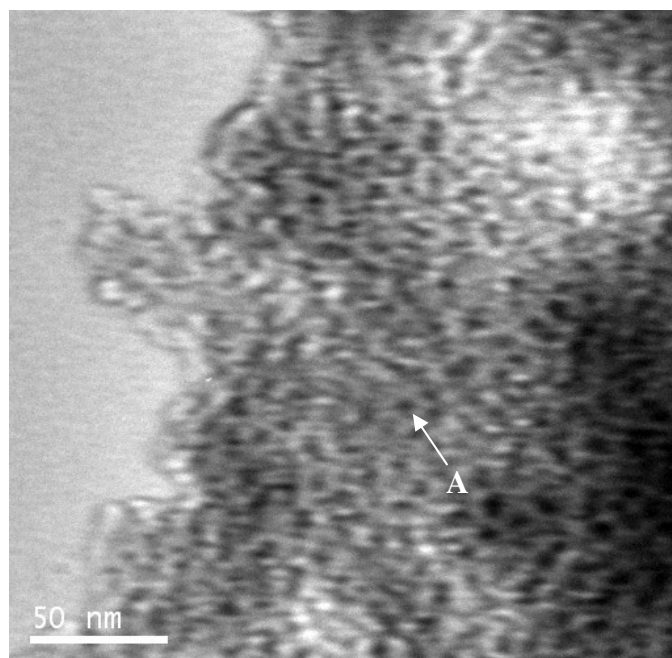
Fig. 3.1.6. TEM micrograph of 10 wt% Composite aerogel. 'A' is the pyrogenic silica particle.
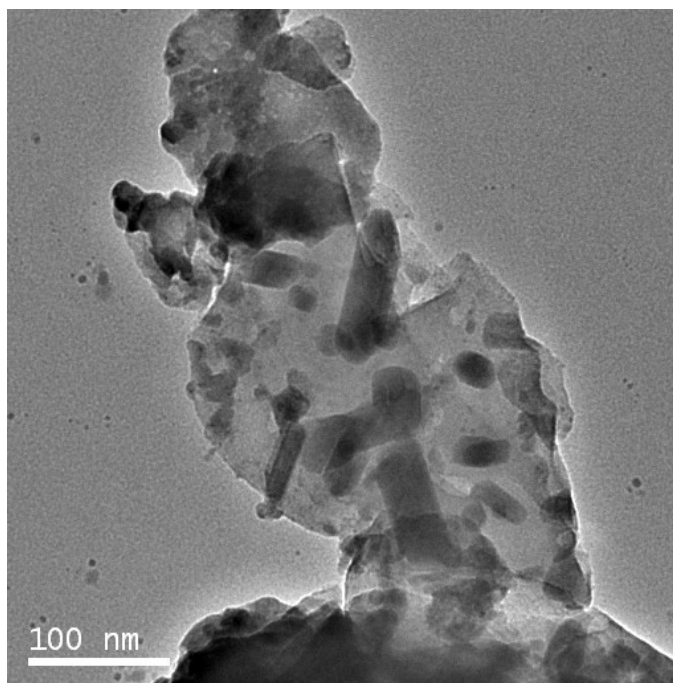
Fig. 3.1.7. TEM micrograph of 40 wt% Composite aerogel incorporated with neodymium nitrate and sintered at 1200 °C
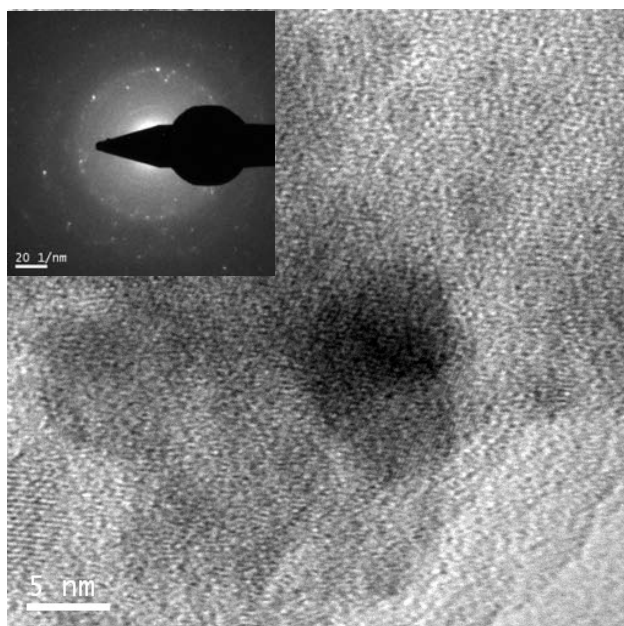
Fig. 3.1.8. HRTEM micrograph of 40 wt% Composite aerogel in coorporated with neodymium nitrate and sintered at 1200 °C (Inset picture electron diffraction pattern)

The increased pore size of the composite aerogels increases its permeablity compared to pure silica aerogels and the increased strength owing to the composite network can improve the ability of the aerogels to function as a nuclear waste absorbant. The silica-silica composite aerogels were soaked in simulated waste solution and were sintered at 1200 °C to confine the wastes. The percentage of loading was calculated by the usual weight difference method [17]. The 20 wt% composite aerogels gave a loading of 51 % and for 50 wt% composite aerogel the percentage of loading was 39 %. The 30 wt% composite aerogel was almost crack free when immersed in neodymium nitrate solution and a loading of 47% was obtained. The total pore volume for the 20 wt% CA is slightly higher than that of 30 wt% CA and must be the reason for the slightly increased capacity of the 20 wt% CA to confine neodymium even when average pore diameter is close to that of the 30 wt% CA. The closeness in values for the loading and average pore diameter suggests the similar pore size distributions actually observed (Fig. 3.1.3). The percentage of loadings observed are much higher than those previously reported by other researchers employing supercritically dried aerogels [17-20].

TEM micrograph (Fig. 3.1.7) indicates that the Neodymium ions are confined as silicates in the silica matrix after calcining at 1200 °C. HRTEM image shown in Fig. 3.1.8 also confirms the confinement of neodymium silicate in the silica matrix. The electron diffraction pattern (in set of Fig. 3.1.8) indicates that the nano crystals are constituted of neodymium silicate. The X-ray diffraction pattern of the sintered composite aerogel, provided in Fig. 3.1.9 reveal that they were crystalline and consists of neodymium silicate ($Nd_2Si_2O_7$).
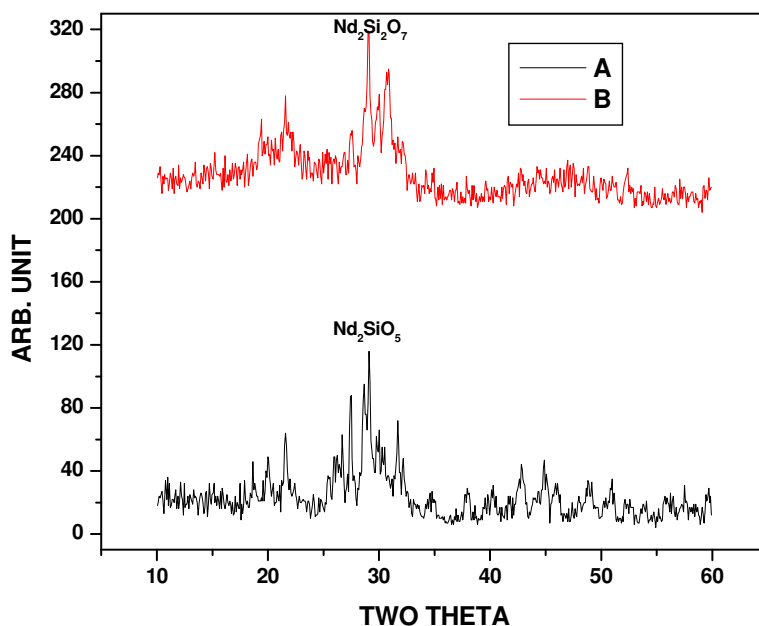
Fig. 3.1.9. XRD pattern of (A) 30 wt% and (B) 40 wt% composite aerogels immersed in 30 % solution of Nd $(NO_3)_3$ solution and sintered at 1200 °C.

The results of leaching studies are presented in Fig. 3.1.10. For the study 0.208 g of 20% composite aerogel and 0.373 g of 50% composite aerogel after neodymium incorporation and subsequent sintering were placed in a soxhlet extractor [17] and were leached with water for a total period of 51 hours. The samples were withdrawn periodically, dried and weighed to measure the weight loss. Measurements were done at an interval of 10 hours. There is no weight change after leaching for 51 h and confirms the stability of the matrix. The leachability tests indicate that the present approach is very effective in confining actinide ions in aerogel structure.
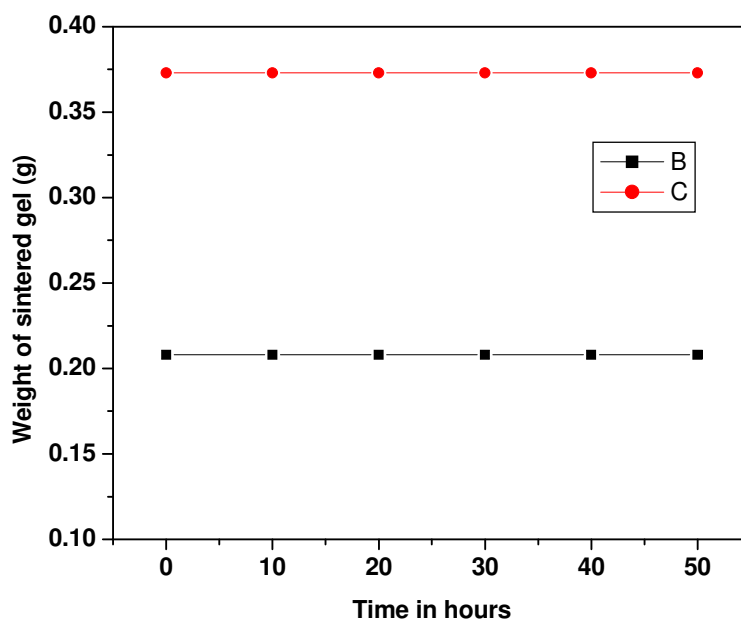
Fig. 3.1.10. Results of leaching experiments with respect to composite aerogels after neodymium incorporation and subsequent sintering (B) 20% Composite aerogel (C) 50% composite aerogel

3.1.5 Conclusion

A simpler and safer non-supercritical drying technique has been applied for the synthesis of silica-silica composite aerogels. The composite aerogels possess very high surface area as confirmed by BET surface area analysis. The application of composite aerogels as a precursor for high level nuclear waste immobilized glass was also tested. The percentage of loadings were high and the leaching studies confirmed the stability of the matrix. TEM observations revealed that the aerogels were porous and the micrograph of the sintered neodymium incorporated gel indicates the presence of neodymium silicate in the glass matrix. The XRD patterns also reveal the presence of neodymium silicate ($Nd_2Si_2O_7$) in the silica matrix.

3.2 Silica alcogels for possible nuclear waste confinement- A simulated study

3.2.1 Abstract

A new method for possible incorporation of nuclear wastes has been attempted here by using silica alcogels as a host precursor for confinement. The aerogels, classical or composite faces problem in that they are highly sensitive to moisture and cracks when exposed to water. Moreover the impregnation step is slow. Incorporation of wastes in the wet gel stage is an alternative that has received less attention. The large pore volume of the silica alcogel is used as a sponge to incorporate chemical species. Neodymium nitrate is used as a simulant for high level waste. The alcogels have been immersed in 5, 10, 20 & 30% neodymium nitrate solution and the resulting alcogels are dried under controlled conditions at 70 °C. The bulk density of the gels increases on absorption of neodymium nitrate. The BET analysis shows a decrease in surface area and total pore volume as the percentage of neodymium nitrate is increased. On sintering the gels at 1200 °C neodymium was confined which was confirmed by negative leachability. The percentage of loading has been found out by calculating the difference in weight of the neodymium incorporated gel before and after incorporation of neodymium. XRD studies of the sintered samples reveal the formation of neodymium silicates.

3.2.2 Introduction

Radioactive wastes remain an imposing problem before human race. Considerable efforts have been expended for their safe disposal. Immobilisation in a chemically durable matrix has been highlighted for the disposal of long lived wastes. Silicate glasses, borosilicate glass and phosphate glasses [26], silicate and oxide ceramics, [27], alumino borosilicate glass powders [28], Synroc [29], Titania ceramics [30], glass ceramics [31],

monazite ceramics [32], novel ceramic forms [33], cementitious waste forms [34] and iron phosphate glasses [35] are some of the prominent matrices used. Silica glass is the most important among them since it has good mechanical strength and thermal shock resistance and sol-gel process is the best method to synthesise glasses at low temperature. (~1000 °C). The silica aerogels are widely recognised as precursor which can be converted in to vitreous silica by short duration treatment at low temperature [17]. The large pore volume of the silica aerogel is used as a sponge to incorporate chemical species [17].

T. Woignier et al. [17] described the process in which porous partially sintered silica aerogel is used as a host matrix for actinides. Neodymium oxide was used to simulate the actinide oxide and the aerogel after simulation was heated at 1100 °C which results in fully sintered structure by viscous flow. But the silica aerogels have poor mechanical strength and permeability is also poor.

T. Woignier et al. [18] in another work prepared composite aerogels with tailored pore size and the aerogels thus prepared possess a much improved permeability and mechanical strength compared with that of classical aerogels. The composite aerogels were prepared by the addition of fumed silica (aerosil) and then were impregnated by neodymium salt solutions. In a related work, Reynes et al. [19] prepared partially sintered composite aerogels (PSCA) and studied its permeability features. The pore size and pore volume of partially sintered composite aerogels (PSCA) was found to be larger and a weight loading close to 20 wt% was achieved. Woignier et al. [20] in another work studied the prospective use of different sets of silica aerogels (Classical, Partially densified aerogels and composite aerogels) as host matrices for chemical species.

Incorporation of wastes into aerogels, classical or composite faces problem in that aerogels are highly sensitive to moisture and cracks when exposed to water, moreover the impregnation step is slow. Incorporation of wastes in the wet gel stage is an alternative that has received less attention. In this work we have attempted to incorporate the simulated waste in the wet gel stage i.e. in the silica alcogel. The impregnated alcogels were then dried under controlled conditions at 70 °C to prepare gel precursor. The bulk density of the neodymium incorporated gels was noted and the gels were also characterised by BET surface area measurements. The neodymium incorporated gels were then sintered at 1200 °C at the rate of 10 °C per minute so as to confine the simulated wastes. The glass durability is measured using a conventional soxhlet device [15] and the XRD studies of the sintered samples reveal the formation of neodymium silicates.

3.2.3 Experimental

3.2.3.1 Materials and Method

Silica alcogels were prepared by using Tetraethoxysilane (Fluka, Switzerland) as the precursor, isopropanol (S D Fine chemicals, India) as the solvent and acidified water (0.001M HCl) as the catalyst. Hydrolysis was carried by maintaining the TEOS: isopropanol: acidified water ratio 1:4:16 [11]. In a typical experiment 27.63 g of TEOS was mixed with 31.83 g of isopropanol. The mixture was stirred using a magnetic stirrer and 38.18 g of acidified water (0.001M HCl) was added drop wise. The stirring was continued till a transparent solution resulted. Five vials were taken and labeled A, B, C, D and E. 10 ml of the clear sol was transferred into each of the five cylindrical vials and kept for gelation at 50 °C. The silica alcogels thus obtained were aged in water for 24

hours, solvent exchange with isopropanol was carried five times within another 24 hours and then kept for silane aging in 80 % TEOS solution for 48 hours. The silane aged gels are taken for solvent exchange with isopropanol, five times within 24 hours. 5, 10, 20 and 30% of neodymium nitrate solution was prepared in isopropanol. The silica alcogels in B, C, D and E are immersed in 5, 10, 20 and 30 % neodymium nitrate solution respectively for 48 hours while maintaining the temperature at 50 °C. The alcogel labeled A was used as a standard to measure the percentage of loadings. The alcogels were then dried at 70°C to obtain aerogels and neodymium incorporated composite aerogels and were then subsequently sintered at 1200 °C. The detailed experimental procedure is given in Fig. 3.2.1. A duplicate experiment was also conducted.

The glass durability was measured using a conventional soxhlet device [15]. The experimental details are as follows. Soxhlet device consists of a boiler containing 300 ml of ultra pure water and a condenser system. A previously weighed sample (sintered at 1200 °C) was placed in the sample boat into which condensed steam was passed continuously. The test was conducted at about 60-70 °C. The samples were dried and the weight of the sintered samples was periodically noted after 10, 20, 30, 40 & finally after 51 hours. The percentage of loadings were calculated by simple weight difference of the sintered neodymium incorporated gel and that of the gel without neodymium.

3.2.3.2 Characterisation techniques

Bulk density of the dried gels was calculated after drying at 70 °C by measuring their mass and volume.

TEOS +isopropanol +0.001 M HCl

↓

Silica precursor sol

↓

Silica gel rods

↓

Aging in water for 24 hours

↓

Solvent exchange (isopropanol)

↓

Silane aging (48 hours)

↓

Solvent exchange (isopropanol)

↓

Immersed in 5, 10, 20 & 30% Nd $(NO_3)_3$

↓

Drying at 70 °C → Sintering at 1200 °C
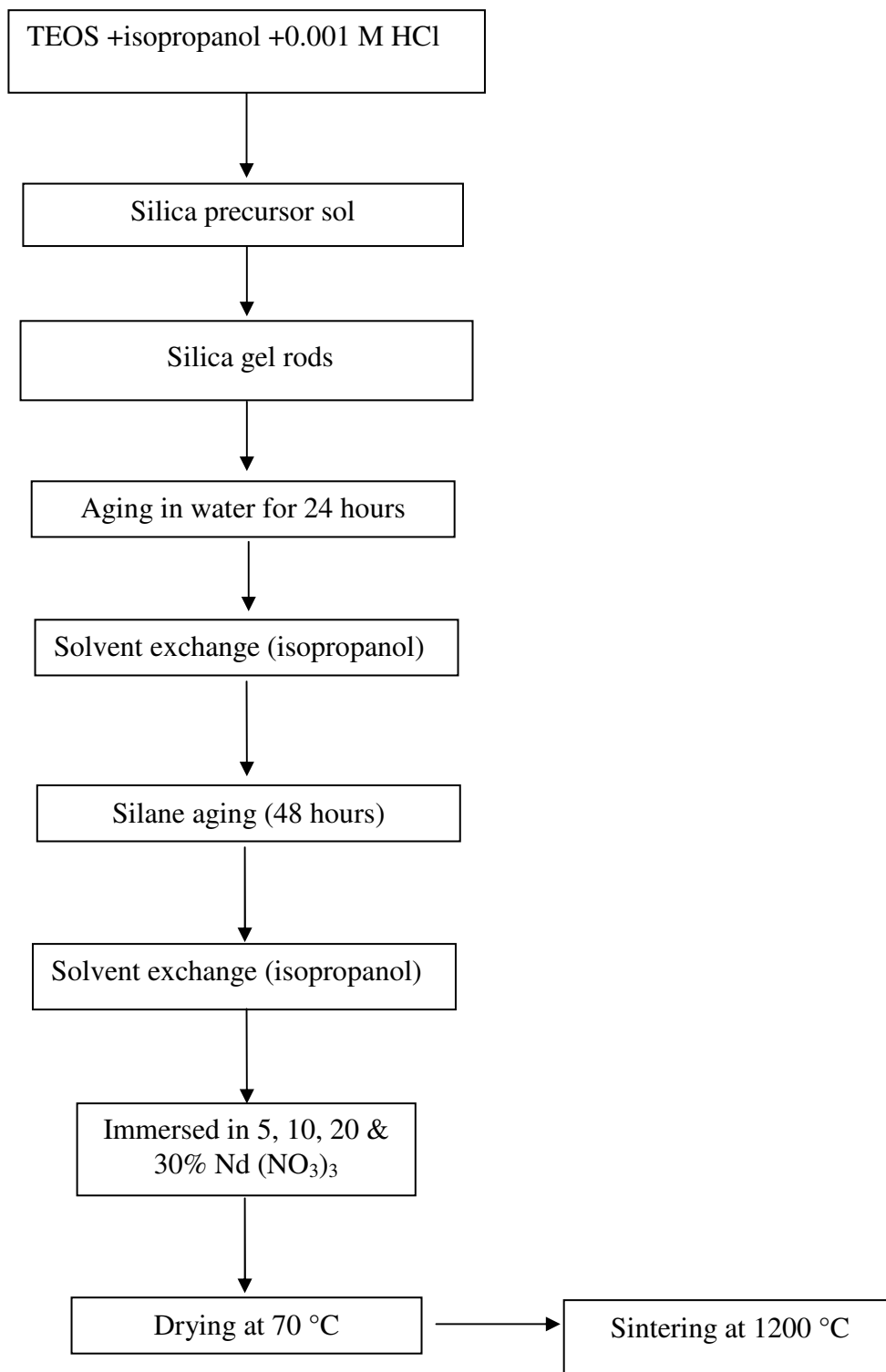
Fig. 3.2.1. Silica alcogels as a precursor for waste simulation

$$\text{Volume, V} = \pi d^2 I \Big/ 4$$

Where d is the diameter and I length of the gel.

$$\text{Bulk Density} = \text{Mass/Volume}$$

The BET surface areas of calcined aerogels were determined by N_2 adsorption at 77K (Micromeritics, Gemini Model 2360, USA). The calcined samples were preheated in a flow of nitrogen for 5 hours at 200 °C to remove all the volatiles and chemically adsorbed water from the surface. Adsorption studies were carried out at liquid nitrogen temperature.

The X- ray powder diffraction patterns of the calcined samples were recorded in Philips Diffractometer (PW 1710)-The Netherlands, using Ni filtered CuKα radiation. The samples were scanned from 0 to 60°, 2θ values with a step speed of 2.4°/ min.

3.2.4 Results & Discussion

The gels were immersed in water for 24 hours so as to hydrolyse any unreacted TEOS. Solvent exchange was done with isopropanol to remove water from the pores and was aged in 80% silane solution. The aging process provides strength to the gel network, since dissolution and reprecipitation of silica particles to the gel network takes place [36]. These gels were then solvent exchanged with isopropanol, since solvent exchange reduces capillary stresses [37] which favour the formation of crack free gels. The neodymium incorporated silica alcogels were then dried in controlled conditions at 70 °C to obtain crack free gels.

The density of the neodymium incorporated gels was measured and is provided in Fig. 3.2.2. The density of the silica aerogel was found to be 0.67 g/ cm^3 and the density of

the gels increased with increase in percentage of neodymium nitrate. The density of silica gel immersed in 30% neodymium nitrate solution was found to be as high as 1.63 g/ cm^3.
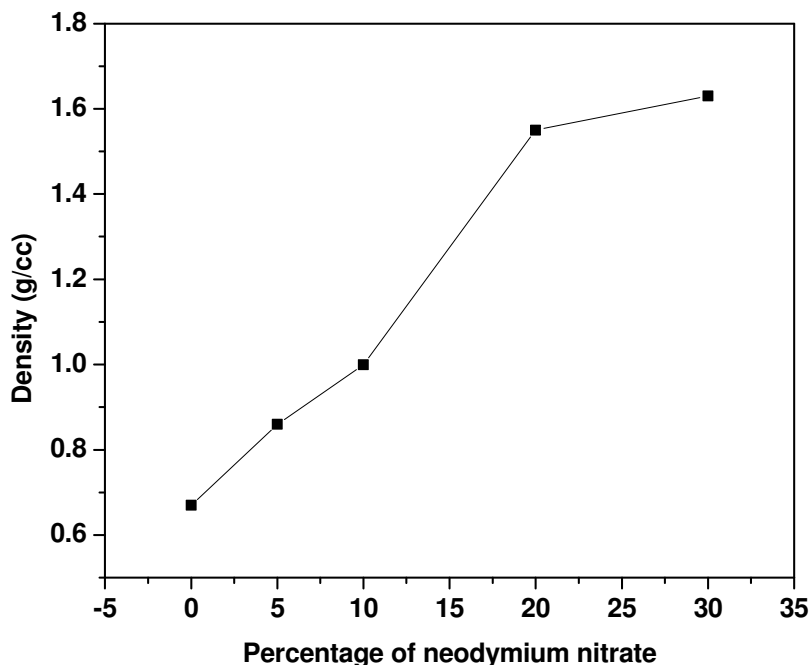
Fig. 3.2.2. Density of silica aerogel and neodymium incorporated silica gels

When the alcogel is immersed in neodymium nitrate solution the Nd $^{+3}$ and NO$_3$ $^-$ ions migrate in to the nano pores of the gel and hence an increase in the density of the aerogel.

The surface area and pore volume of the gel and neodymium incorporated gels are provided in Fig. 3.2.3. Silica aerogel with a density of 0.67 g/ cm^3 has a surface area of 1023 m^2/g with a pore volume of 1.3 cm^3/g. The 5% neodymium incorporated gel has a surface area of 481 m^2/g with a pore volume of 0.47 cm^3/g. The 30 % neodymium incorporated gel has a surface area of 61 m^2/g with a pore volume of 0.07 cm^3/g. The decrease in surface area of the gels with an increase in the percentage of neodymium

loadings is due to the decrease in the total pore volume. The total pore volume decreases as more and more Nd $^{+3}$ and NO_3^- ions migrate in to the pores of the gel with an increase in the concentration of immersing solution.
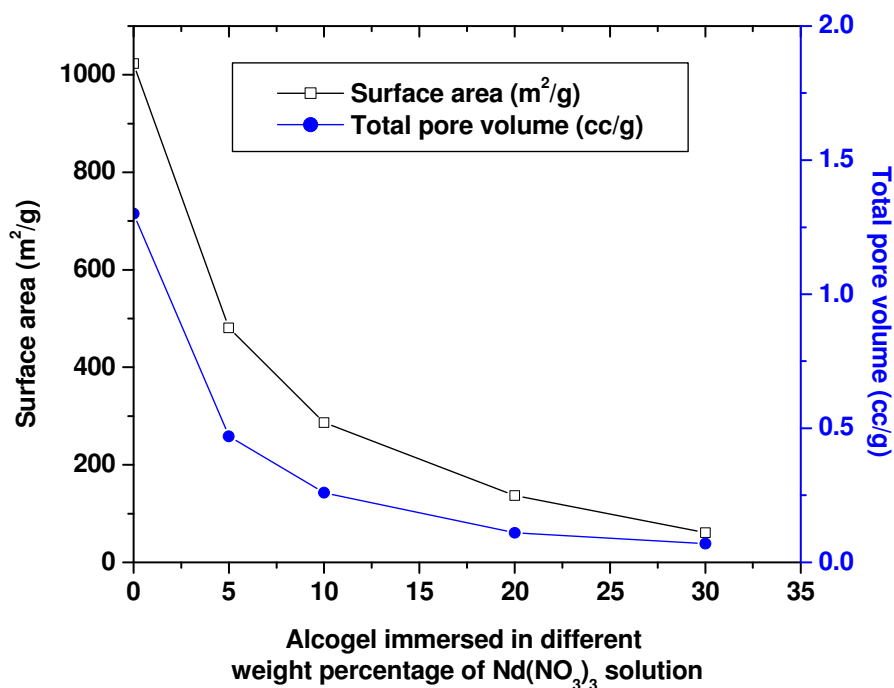
Fig. 3.2.3. The surface area results of the silica gel and neodymium incorporated gels.

The Weight incorporated per 100g of silica gel after sintering at 1200 °C for 3 hours is provided in Table 3.2.1. The gel immersed in 5% neodymium nitrate solution gave a loading of 15% and a maximum loading of 59% was obtained for gel immersed in 30% Nd $(NO_3)_3$ solution.

The leaching studies are provided in Fig. 3.2.4. 0.212 g of Sintered 20 % Neodymium incorporated gel and 0.308 g of Sintered 50% Neodymium incorporated gel were placed in a soxhlet extractor [17] and were leached with water for a total period of 51 hours.

Table 3.2.1. Percentage of loadings of gels after sintering at 1200°C for 3 hours

Sample	Weight of Nd $(NO_3)_3$ incorporated per 100g of silica gel
Gel immersed in 5% neodymium nitrate solution	15
Gel immersed in 10% neodymium nitrate solution	30
Gel immersed in 20% neodymium nitrate solution	41
Gel immersed in 30% neodymium nitrate solution	59

The samples were dried and the weight of the sintered samples was periodically noted after 10, 20, 30, 40 & finally after 51 hours. There is no appreciable weight change (0.001 g) after leaching and confirms the stability of the matrix.

It is reported by Woignier [17] that the neodymium loaded samples present three different crystalline phases, neodymium sesquioxide (Nd_2O_3), and neodymium silicates. ($Nd_2Si_2O_7$, Nd_2SiO_5). The XRD analysis of sintered neodymium incorporated composite aerogels is also present as neodymium silicates. ($Nd_2Si_2O_7$, $Nd_2Si_3O_9$)
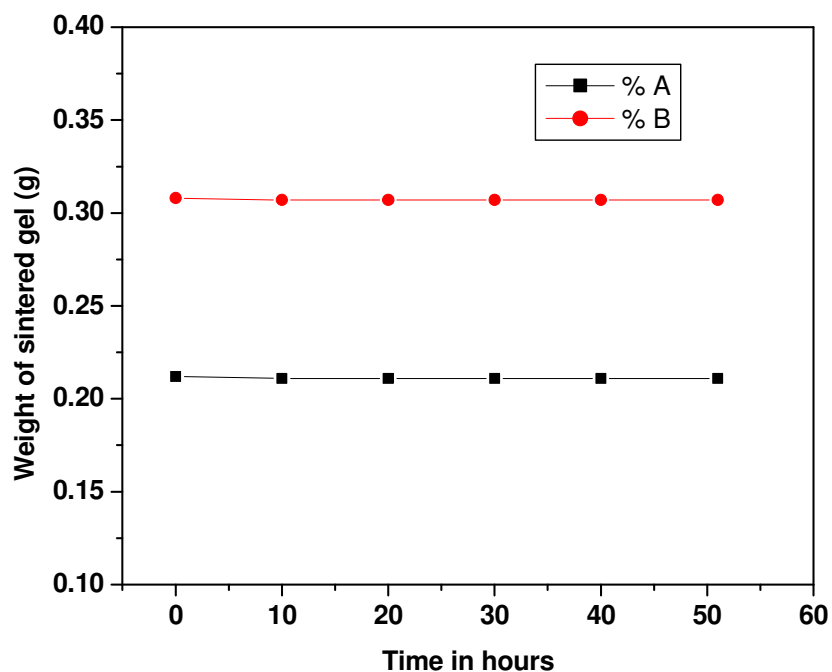
Fig. 3.2.4. Leaching studies on (A) Sintered 5% Neodymium incorporated gel & (B) Sintered 30% Neodymium incorporated sintered gels

3.2.5 Conclusion

1) Silica alcogel was used for the first time as a precursor for waste mobilisation

2) A much higher percentage of loading compared to earlier reports in similar systems was obtained using alcogels.

3) Maximum loading of 59% was obtained when the gel immersed in 30% solution of neodymium nitrate which was subsequently sintered.

4) The leachability tests proved the stability of the matrix.

5) Neodymium is immobilised as silicate in the silica matrix.

References

[1] M. Toki, S. Miyashita, T. Takeuchi, S. Kanbe and A. Kochi, J. Non-Cryst Solids. 100 (1988) 479.

[2] C. Marliere, T. Woignier, P. Dieudonne, J. Primere, M. Lamy, J. Phalippou, J. Non-Cryst. Solids 285 (2001) 175

[3] S.S. Prakash, C.J. Brinker, A.J. Hued, S.M. Rao, Lett. Nature 374 (1995) 439.

[4] F. Schwertfeger, D. Frank, M. Schmidt, J. Non-Cryst. solids 225 (1998) 24.

[5] F. Kirkbir, H. Murata, D. Meyers, S.R. Chaudhuri, J. Non-Cryst. Solids 225 (1998) 14.

[6] P.J. Davis, C.J. Brinker, D.M Smith, J. Non-Cryst. Solids 142 (1992)189.

[7] P.J. Davis, C.J. Brinker, D.M. Smith, R. J. Assink, J. Non-Cryst. Solids 142 (1992) 197.

[8] M-A Einarsrud, S. Haereid, J. Sol-Gel Sci. Technol. 2 (1994) 903.

[9] R. Deshpande, D. Smith, C.J. Brinker US patent No. 5, 565,142 issued 1996.

[10] C.J. Brinker, S.S. Prakash US patent disclosure (1994).

[11] S. Rajesh Kumar, P. Krishna Pillai, K.G.K. Warrier, Polyhedron 17 (1998) 1699.

[12] S. Dai, Y.H. Ju, H.J. Gao, J.S. Lin, S.J. Pennycook, C.E. Barnes, Chem. Comm. 3 (2000) 243.

[13] S.J. Coleman, P.R. Coronado, R.S. Maxwell, J.G. Reynolds, Environ. Sci. Technol. 37 (2003) 2286.

[14] M. Aparicio, M.O. Prado, A. Durán, J. Non-Cryst. Solids 352 (2006) 3478.

[15] E. Sizgek, J.R. Bartlett, M.P. Brungs, J. Sol-Gel Sci. Technol., 13 (1999) 1011.

[16] E.R. Vance, J. Mater. Sci. 21 (1986) 1413.

[17] T. Woignier, J. Reynes, J. Phalippou, J.L. Dussossoy, N.N. Jacquet-Francillon, J. Non-Cryst. Solids 225 (1998) 353.

[18] T. Woignier, J. Reynes, J. Phalippou, J.L. Dussossoy, J. Sol-Gel Sci. Technol. 19 (2000) 833.

[19] J. Reynes, T. Woignier, J. Phalippou, J. Non-Cryst. Solids 285 (2001) 323.

[20] T. Woignier, J. Primera, M. Lamy, C. Fehr, E. Anglaret, R. Sempere, J. Phalippou, J. Non-Cryst. Solids 350 (2004) 292.

[21] M.J. Van Bommel, C.W. Den Engelsen, J.C. Van Miltenburg, J. Porous Mater. 4 (1997) 14.

[22] N. Husing, U. Schubert, Angew. Chem. Int. Ed. 37 (1998) 22.

[23] J. Fricke, Sci. Am. 258 (1988) 92.

[24] A.C. Pierre, G.M. Pajonk, Chem. Rev. 102 (2002) 4243.

[25] C. Marliere, T. Woignier, P. Dieudonne, J. Primera, M. Lamy, J. Phalippou, J. Non-Cryst. Solids 285 (2001) 175.

[26] Lutze W, In: Radioactive waste forms for the future, ed. Lutze. W. and Ewing. R. C (North Holland Amsterdam, 1988) pp. 1

[27] Mc. Carthy G. J. , J. G. Pepin, Pfoertsch D. E. and Clarke D. R, Crystal chemistry of the synthetic minerals in current supercalcine ceramics. In: Ceramics in nuclear waste management, ed. Chikkala. T. D and Mendel. J. E, CONF-790420, National Technical Information Service, (Springfield, VA, 1979) pp 315

[28] M.A. Audero, A.M. Bevilacqua, Norma B. M. de Bernasconi, Diego. O. Russo, Marco E. Sterba, J. Nucl. Mater. 223 (1995)151.

[29] R.C. Ewing, W.J. Weber, F. W. Clinard, Jr, Prog. In: Nuc. Energy, 29 (1995) 63.

[30] Adelhelm.C, C. Bauer, Gahlert. S and G. Ondracek, TiO_2- A ceramic matrix In: Radioactive waste forms for the future, ed. Lutze. W and R. C. Ewing, (North Holland, Amsterdam, 1988) pp 393.

[31] P. J. Hayward Glass ceramics. In: Radioactive waste forms for the future, ed. Lutze. W. and Ewing R. C. (North Holland, Amsterdam, 1988) pp 427.

[32] L.A. Boatner and B.C. Sales Monazite In: Radioactive waste forms for the future, ed. Lutze. W and Ewing R. C (North Holland, Amsterdam, 1988) pp 495.

[33] Ewing R. C. (1988) Novel waste forms In: Radioactive waste forms for the future, ed. Lutze W. and Ewing R. C (North Holland, Amsterdam, 1988) pp 589.

[34] Jiang W, Wu X and Roy D. M, Alkali activated fly ash slag cement based nuclear waste forms. In: Scientific basis for Nuclear waste management XVI, Interrante, ed. C. G and Pabalan. R. T. Materials Research Society Symposium Proceedings, Vol. 294, (Materials Research Society, Pittsburg, 1993) pp 255.

[35] S.T. Reis, M. Karabult, D.E. Day, J. Nuc. Mat. 304 (2002) 87.

[36] T. Heinrich, J. Non- Cryst. Solids 168 (1994) 14.

[37] R. Deshpande, D.W. Hua, D.M. Smith, C.J. Brinker, J. Non-Cryst. Solids, 144 (1992) 32.

Chapter 4:   High Surface Area Silica-Titania Aerogels by Non-Supercritical Drying

4.1 Synthesis and Characterisation of non-supercritically dried Silica-Titania aerogels

4.1.1 Abstract

Non-supercritical drying has been carried out for the synthesis of silica-titania aerogels where the properties are nearly comparable with the supercritically dried ones. Stable titania sol was prepared by chelating Titanium Isopropoxide Ti $(O^iPr)_4$ with acetic acid and acetyl acetone. The aerogels thus prepared have densities in the range of 0.34 to 0.38 g/cm^3. The surface areas and pore volumes of mixed oxide aerogels are comparable to that of the supercritically dried ones. The surface area for 5 wt% titania aerogel has been found to be as high as 685 m^2/g with a pore volume of 2.34 cm^3/g and the 10 wt% titania aerogel possesses surface area of 620 m^2/g with a pore volume of 2.36 cm^3/g. The thermal pore stability of silica-titania gels derived from acetic acid chelated titania sols has also been studied. Silica-Titania gels were also prepared by impregnation. For impregnation the alcogels were soaked in chelated titanium isopropoxide [$(TiO^iPr)_4$] for 24 h. The photocatalytic property of mixed gels has been studied using methylene blue degradation. High Resolution Transmission Electron Microscopy (HRTEM) has been used to characterise the aerogels and Fourier Transmission Infrared (FT-IR) spectroscopy has been used to study the effect of titania addition to silica. X-ray diffraction (XRD) patterns were recorded to verify the molecular homogeneity of the aerogel.

4.1.2 Introduction

Significant interest has been generated for the application of aerogels ever since Kistler had synthesized it in 1931 with application areas shifting from thermal insulators to high energy particle collectors to recent solid state dye lasers [1-7]. Aerogels are unique among solid materials in having extremely low densities, large open porosities and high surface area. The removal of solvent from the three dimensional network with minimum shrinkage is the most crucial step for obtaining an aerogel in a sol-gel process. The three dimensional network collapses when gels are dried under ambient conditions due to the high capillary pressure exerted by the solvent on the gel network. Hence the wet gels are normally dried under supercritical conditions, where the surface tension (θ) of the solvent and hence the capillary pressure (P_r) will be reduced to zero thereby preserving network structure for the preparation of aerogels. The dried gels will hence be characterized by low densities and extremely high porosity [1, 8]. Search for suitable alternatives to the supercritical drying, which is generally considered energy intensive, hazardous and expensive [9, 10] are part of the growing aerogel technology by all means. The drying stress developed due to the capillary forces and the subsequent shrinkage during drying can be minimized by reducing the capillary force [11-13]. Mainly two strategies are used for preparation of aerogels by ambient pressure drying. One is increasing the stiffness of the gel network by aging in a silane precursor [14-20] and the other is capping the surface silanol groups by alkyl groups so that the gel breaths back to shape after shrinkage due to repulsion between the alkyl groups [10, 13, 21-25]. The adaptablity of a system to subcritical drying also seems to influence the success of the drying technique. The mixed oxide aerogels involving silica like silica-alumina, silica-zirconia and silica-titania are

reported to be excellent catalysts for numerous organic reactions. Silica–Titania mixed oxide aerogels have been reported to catalyse a number of reactions such as phenol amination [26], olefin epoxidation [27], ethene hydration [26], butene isomerisation [28, 29], cumene dealkylation [30], 2-propanol dehydration [30] and 1, 2-dichloro ethane decomposition [31].

The preparation of free standing titania-silica aerogels is more difficult due to the weaker Si-O-Ti network. The literature reports several strategies for preparing freestanding titania-silica aerogels. Yoda et al. impregnated silica alcogels with titanium precursor and obtained aerogels of good mechanical strength but with uneven distribution of titanium [32-35]. They reported that aerogel blocks prepared by this method exhibited less defects [32] and anatase titania were deposited on the surface of the silica network, thus promising a good catalytic activity [35, 36]. The slow diffusion of the titania precursor into the alcogel necessitated a long impregnation time and also resulted in a non-uniform deposition of titania. Kim and Hong used co-hydrolysis of titanium and silica precursors to obtain crack-free titania-silica aerogel with Ti/Si $\leq$ 1 by carefully matching the hydrolysis and condensation rates of two precursors [37]. Morris et al. suggested the use of about-to-gel silica sol as nanoglue to entrap particles in the aerogel network [38]. This approach was used to prepare titania crystals in silica aerogel [39]. In this study Degussa P25 was homogeneously dispersed into the silica precursor solution and trapped within the alcogel followed by rapid gelation. The hybrid aerogel displayed good mechanical strength, however the photocatalytic activity was poor as the titania surface was passivated by a layer of silica. Further Watson et al. also reported similar

poor performance of silica-titania gels with respect to photocatalytic deactivation of Ecoli in water [40].

Baiker et al. prepared titania-silica aerogels by co-hydrolysis of the titania and silica precursor under acidic conditions [41-43]. The more reactive titanium precursor condensed before the silica, thus concentrating the titanium in the bulk and creating a weaker aerogel network. Powders were obtained even after the use of strong chelating compounds to slow the hydrolysis and condensation of the titania precursor.

Cao et al. prepared Titania–silica aerogels by a two step procedure in an attempt to match the hydrolysis and condensation rates of the two alkoxide precursors [44]. The silica alkoxide was prehydrolysed at low pH to generate reactive monomers while chelating compounds was added to the titanium alkoxide to slow the reaction. The acidic silica precursor was rapidly mixed with chelated titanium alkoxide at an alkaline pH that further favours the rapid condensation of silica. The gels were supercritically dried by carbondioxide and ethanol supercritical drying. But the ethanol Supercritically dried aerogels were crystalline due to crystallisation of bulk titania.

During the preparation of mixed oxide sols from the respective alkoxide precursors involving silica, if the hydrolysis of the metal alkoxide is faster than that of silicon alkoxide, a non uniform sol results because sedimentation takes place before gelation. Due to this difference of reactivity of silicon and titanium alkoxides, various procedures such as modification of the titanium alkoxide by a chelating ligand [45-50], acidic hydrolysis [51], controlling the rate of addition of water [52], prehydrolysis of silicon alkoxide [47-56], or using single source precursor with pre-existing Si-O-Ti linkages [57] were employed. Titania-Silica aerogels are generally prepared by

employing supercritical or critical point drying (CPD) [58-63]. The collapse of the pore structure of titania-silica gels (xerogels) during drying was also reported to be effectively minimised either by washing with n-hexane and silylation of the gels before drying [51, 52], or by aging the wet gels for 10 days, then washing with n-heptane which is a low surface tension solvent and hence the capillary stress during drying is reduced [56].

In the present chapter, successful preparation of silica-titania mixed oxide aerogels utilising the subcritical drying technique involving careful and systematic process of solvent exchange, silane aging and drying under controlled conditions.The aerogels were then calcined at 200 °C and were characterized by BET, FT-IR & XRD measurements. The aerogels were also calcined at 500, 900 and 1200 °C to study the thermal pore stability. Acetyl acetone was also used as a chelating agent for Titanium isopropoxide and was later used for preparing silica-titania aerogels. Silica-Titania aerogels were also prepared by impregnation. Transmission Electron Microscopy (TEM) and X- ray diffraction (XRD) analysis have been performed to verify the homogeneity of the mixed oxide aerogel. The photocatalytic studies were also conducted on the prepared aerogels. The bulk density of the as prepared aerogels is also presented.

4.1.3 Experimental

Tetra ethoxy silane (TEOS) (Fluka, Switzerland), Ti $(O^iPr)_4$ (Aldrich), acetic acid (S.D. Fine chemicals, India) and isopropanol (S.D. Fine Chemicals, India) were used as received. Stable titania sol was prepared by method reported else where [64]. In a typical experiment for the preparation of 10 wt% titania in silica, 0.5336g titanium isopropoxide (Aldrich) in 1.12 ml acetic acid (S.D. Fine chemicals, India) was hydrolysed with 11.825 ml water. Simultaneously silica sol was prepared by hydrolysing

4.6617 g Tetraethoxysilane (TEOS) (Fluka, Switzerland) in 5.3704 g isopropanol (S.D. Fine Chemicals, India) with 6.4425 g water. The hydrolysis pH was maintained at 1.54 due to the difference of reactivity of silicon and titanium isopropoxide. The two sols were stirred for 3 hours each separately and then titania sol was added drop wise to silica sol. The mixed sol was then stirred for 1 hour and the gelation pH was adjusted to 5 using 5% ammonia solution.

To prepare acetyl acetone chelated titania sol, the ratio of isopropoxide: acetyl acetone was maintained at 1: 1. In a typical experiment for the preparation of 10 wt% titania in silica, 0.5336 g titanium isopropoxide (Aldrich) was mixed with 0.1877 g acetyl acetone (S.D. Fine chemicals, India) and stirred for 1 h. Simultaneously silica sol was prepared by hydrolysing 4.6617 g Tetraethoxy silane (TEOS) (Fluka, Switzerland) in 5.3704 g isopropanol (S.D. Fine Chemicals, India) with 6.4425 g water and was stirred for 1 h. After 1 h of stirring, the titania sol was added to silica sol and was stirred for 2 h. The pH of the mixed sol was raised to 5 to favour quick gelation.

The visually homogeneous sol was then transferred to vials (2cm diameter) and kept at 50 °C for gelation. The gelation time was found to be 10 to 15 minutes for all compositions. The gels were kept for 24 hours at 50 °C, then transferred to water and was kept for 24 hours at 50 °C after which they were soaked in Isopropanol. The isopropanol was changed five times within 24 hours in order to remove water from pores. The whole soaking process of the gels was done at 50 °C. This is followed by aging the gels in 80% TEOS for 48 hours at 50 °C and the final solvent exchange with isopropanol maintaining the gels at the same temperature of 50 °C. The gels were then dried in airtight containers at 70°C so that the porous structure is retained in the gels by the slow removal of solvent

from the pore network. The aerogels obtained after drying at 70 °C were further heated for 3 hours at 200 °C. The titania content was varied from 2 to 20 wt%. The detailed flow chart is provided in Fig. 4.1.1.

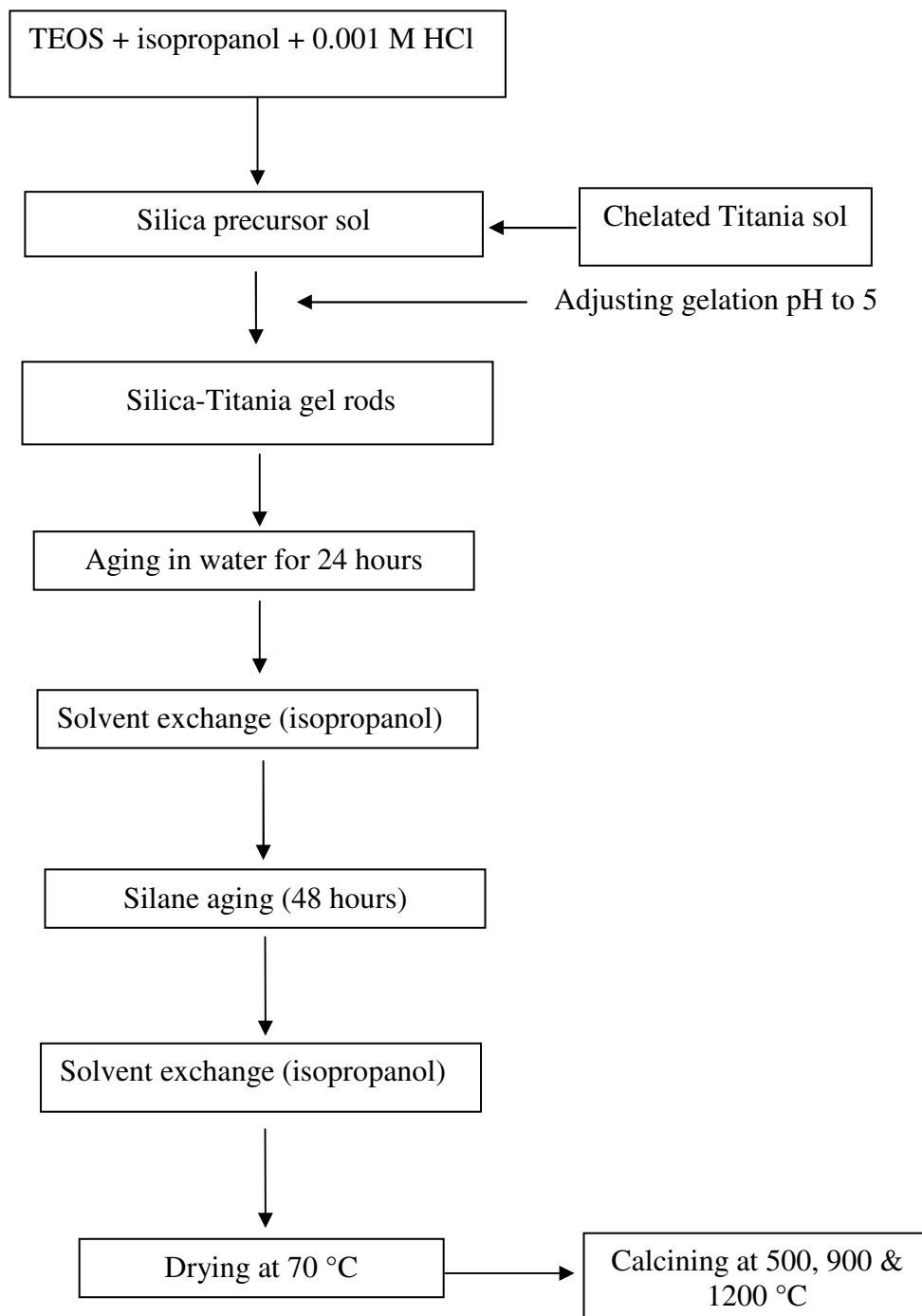For impregnation, the silica alcogels were immersed in acetyl acetone chelated titanium isopropoxide. The molar ratio of isopropoxide: acetyl acetone was maintained at 1:1. In a typical experiment for the preparation of 3 g silica, 10.3594 g TEOS in 11.9342 g isopropanol was hydrolysed with 14.321 g acidified water (pH 3). The clear sol was transferred into vials and kept for gelation at 50 °C. The gels were aged for 24 h and put in water for 24 h. Later solvent exchange with isoproponal was carried out to remove water from the pores. The solvent exchange was carried out five times within 24 hours. A 1:1 molar solution of isopropoxide: acetyl acetone was prepared by mixing 14.21 g titanium isopropoxide in 50 ml isoproponal. Then to this solution 25 g of acetyl acetone was added. The silica alcogels were soaked in chelated titanium isopropoxide solution for 24 h. After 24 h, excess chelated titania isopropoxide was washed with isopropanol and dried at 70 °C. The detailed flow chart is provided in Fig. 4.1.2.

Bulk density of the dried gels (cylindrical samples) was calculated from their mass and volume. The Fourier Transform Infrared Spectroscopy of the heated gels was recorded in Nicolet Magna-560-FT IR Spectrometer (USA) using pellets made out of KBr and dispersed gel powder. The BET surface areas of calcined aerogels were determined by N_2 adsorption at 77K (Micromeritics, Gemini Model 2360, USA). The calcined samples were preheated in a flow of nitrogen for 3 hours at 200 °C to remove all the volatiles and chemically adsorbed water from the surface.

```
                    ┌─────────────────────────────────────┐
                    │ TEOS + isopropanol + 0.001 M HCl     │
                    └─────────────────────────────────────┘
                                      │
                                      ▼
        ┌──────────────────────────┐          ┌──────────────────────┐
        │   Silica precursor sol   │◄─────────│ Chelated Titania sol │
        └──────────────────────────┘          └──────────────────────┘
                      │        ◄──────────────  Adjusting gelation pH to 5
                      ▼
        ┌──────────────────────────┐
        │  Silica-Titania gel rods │
        └──────────────────────────┘
                      │
                      ▼
        ┌──────────────────────────┐
        │ Aging in water for 24 hours │
        └──────────────────────────┘
                      │
                      ▼
        ┌──────────────────────────┐
        │ Solvent exchange (isopropanol) │
        └──────────────────────────┘
                      │
                      ▼
        ┌──────────────────────────┐
        │  Silane aging (48 hours) │
        └──────────────────────────┘
                      │
                      ▼
        ┌──────────────────────────┐
        │ Solvent exchange (isopropanol) │
        └──────────────────────────┘
                      │
                      ▼
        ┌──────────────────────┐       ┌──────────────────────────┐
        │  Drying at 70 °C     │──────►│ Calcining at 500, 900 &  │
        └──────────────────────┘       │        1200 °C            │
                                       └──────────────────────────┘
```

Fig. 4.1.1. Flowchart for the preparation of Silica-Titania mixed oxide aerogels

```
┌─────────────────────────────────────────┐
│   TEOS +isopropanol +0.001 M HCl         │
└─────────────────────────────────────────┘
                    │
                    ▼
┌─────────────────────────────────────────┐
│           Silica precursor sol           │
└─────────────────────────────────────────┘
                    │
                    ▼
┌─────────────────────────────────────────┐
│            Silica gel rods               │
└─────────────────────────────────────────┘
                    │
                    ▼
┌─────────────────────────────────────────┐
│        Aging in water for 24 hours       │
└─────────────────────────────────────────┘
                    │
                    ▼
┌─────────────────────────────────────────┐
│      Solvent exchange (isopropanol)      │
└─────────────────────────────────────────┘
                    │
                    ▼
┌─────────────────────────────────────────┐
│     Immersed in Chelated Ti (OiPr)₄      │
└─────────────────────────────────────────┘
                    │
                    ▼
┌─────────────────────────────────────────┐
│      Solvent exchange (isopropanol)      │
└─────────────────────────────────────────┘
                    │
                    ▼
┌──────────────────────┐        ┌──────────────────────┐
│   Drying at 70 °C    │ ─────▶ │  Calcining at 500 and │
│                      │        │        800 °C         │
└──────────────────────┘        └──────────────────────┘
```
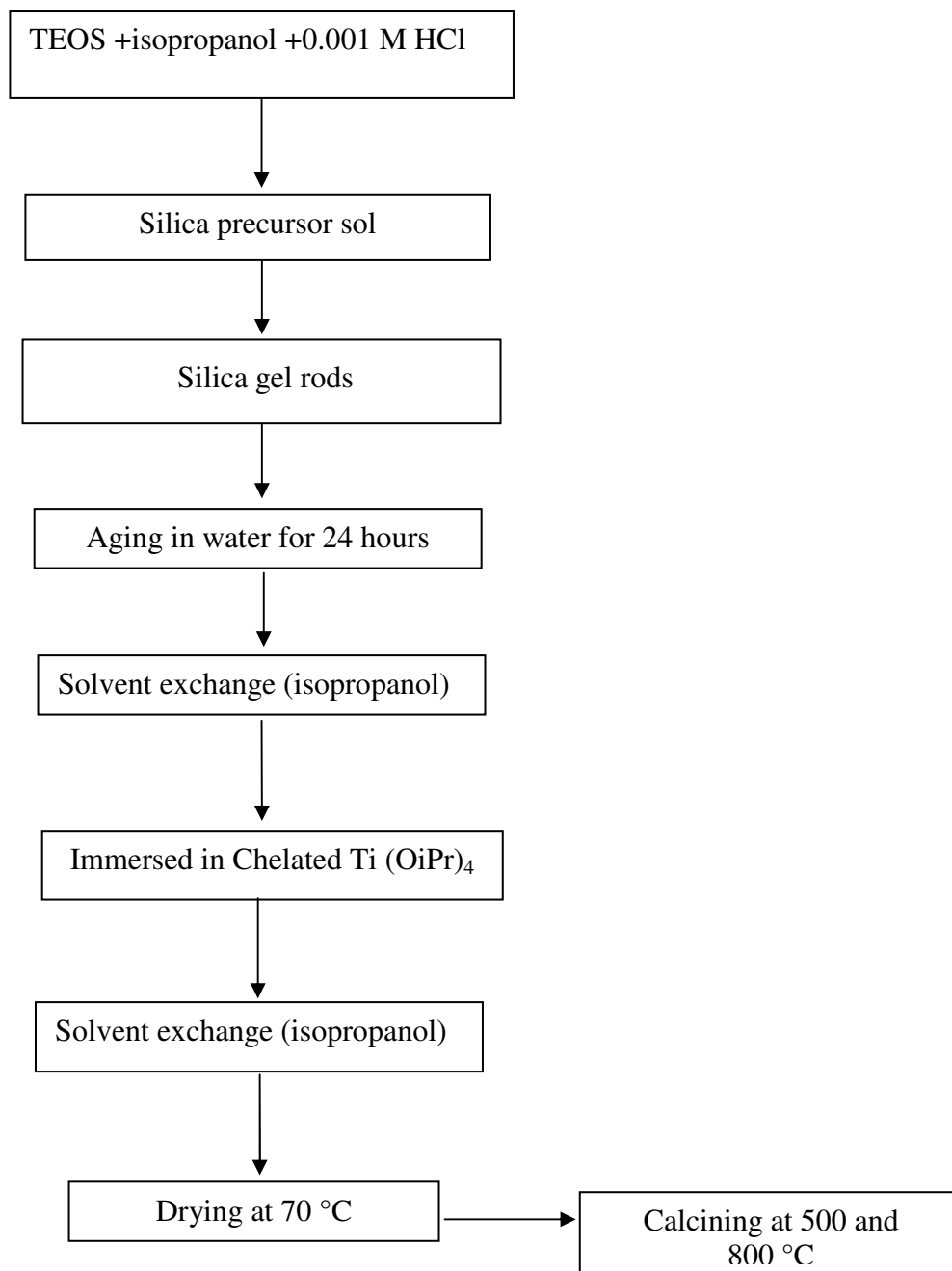
Fig. 4.1.2. Flowchart for the preparation of impregnated Silica-Titania mixed oxide aerogels

The specific surface area was determined using the BET equation with an accuracy of ± 10 m^2/g. The total pore volume was calculated as,

$$\text{Pore volume, } V = V_a * D$$

Where V_a = volume adsorbed at P/P_0 0.99, D = density conversion factor (0.0015468 for nitrogen as adsorbate gas). The pore size distribution was obtained using the Barrette-Joynere-Halenda (BJH) method. Assuming that the pores are cylindrical and open at both ends, the average pore size of a given sample is calculated using the equation,

$$\text{Average pore size} = 4V_{total} / S_{BET}$$

For Transmission electron microscopy studies (HRTEM) the gel powder was dispersed in acetone. A few drops were placed on carbon coated copper grids. After ensuring the evaporation of the solvent, the copper grid was mounted in a FEI High Resolution Transmission Electron Microscope (HRTEM) Technai 30 G^2 S-TWIN. The X-ray powder diffraction patterns of the calcined sample were recorded in Philips Diffractometer (PW 1710), Netherlands, using Ni filtered CuKα radiation. The samples were scanned from 0 to 60° (2θ values) with a step speed of 2.4°/ min.

The photocatalytic activity of mixed oxide gels was studied by measuring the amount of methylene blue degraded under UV radiation. For the methylene blue degradation studies aliquotes were prepared by dispersing 0.1 g of aerogel powder in 250 ml of 6.4 x 10^{-9} mol l^{-1} methylene blue solution (AR grade, Qualigens Fine Chemicals, India Ltd). The peak between 640 nm and 680 nm in the UV spectrum of methylene blue was used for determining the concentration. The suspension was then irradiated with UV

using a Rayonet Photoreactor (Netherlands) with constant stirring. The UV source was fifteen 15 W tubes (Philips G15 T8) arranged in circular fashion emitting radiation in the ragion 200-400 nm. The degradation of the dye was monitored using UV-visible spectrometer (Shimadzu, Japan, UV-2401 PC).

4.1.4. Results and Discussion

Ambient pressure drying process has evolved as a suitable alternative to supercritical method by virtue of many researchers [9-25]. Crack free monoliths prepared by employing the ambient pressure drying technique described is shown in the photograph provided as Fig. 4.1.3.
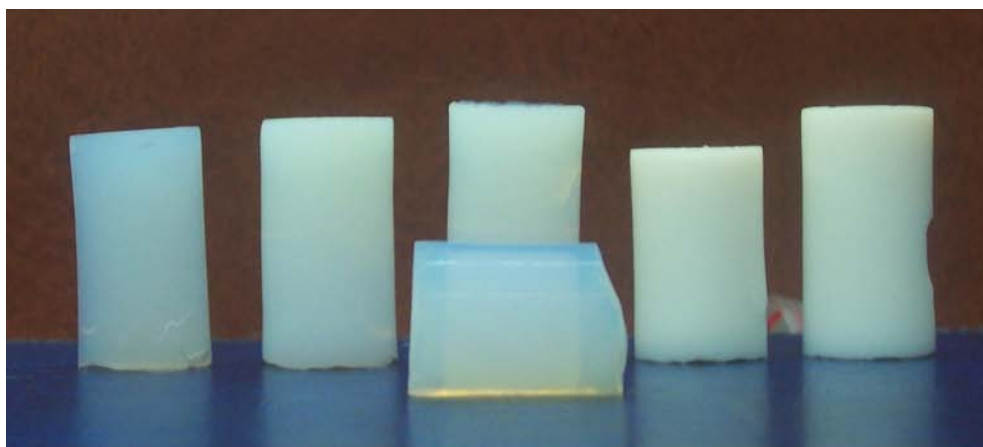
Fig. 4.1.3. Photographs of Silica-titania aerogels

The bulk density of aerogels is provided in Table 4.1.1. Usually aerogels possess densities in the range of 0.003 to 0.8 g/cm^3, with high surface area extending up to 1500 m^2/g [65, 66]. Silica aerogels prepared under ambient conditions has a density of 0.34 g/cm^3 and the 2, 5 and 10 wt% titania aerogel possess densities of 0.36, 0.38 and 0.35 g/cm^3 respectively.
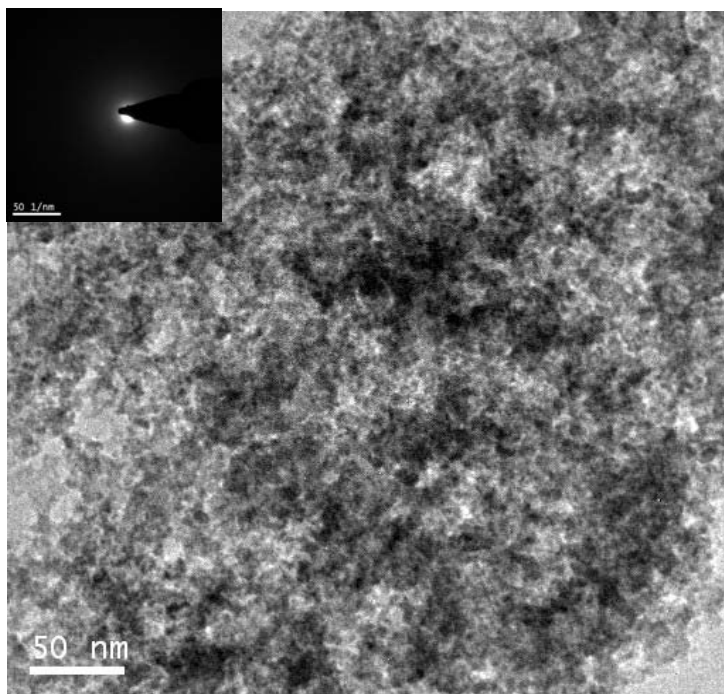
Fig. 4.1.4. TEM micrograph of 10 wt % Titania-silica aerogel. The selected area diffraction pattern is provided in the inset.
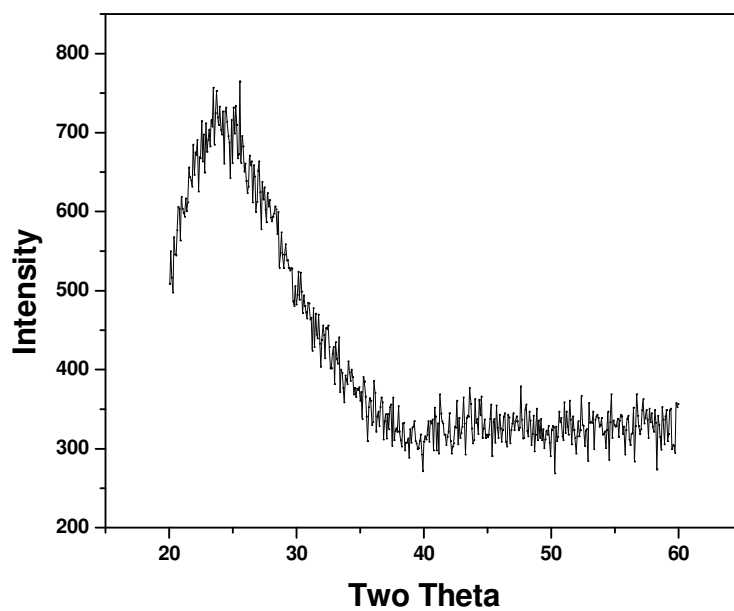

Fig. 4.1.5. XRD spectrum of 20% titania calcined at 600 °C.

Transmission Electron Microscopy (TEM) studies (Fig. 4.1.4) of 10 wt% titania-silica aerogel confirmed that the prepared aerogel is nanoporous with a network structure. The selected area electron diffraction pattern (inset of Fig. 4.1.4) indicates that the aerogel is amorphous which is direct evidence to the structural homogeneity of titania distribution [41]. This was confirmed by X-ray diffraction (XRD) where there was no peak corresponding to crystalline titania. The XRD patterns (Fig. 4.1.5) of the samples with even 20% titania did not show any peaks corresponding to crystalline titania even after calcination at 600 °C which confirms that there is no segregation or agglomeration of silica and titania and the advantageous structure developed during sol-gel process is preserved.
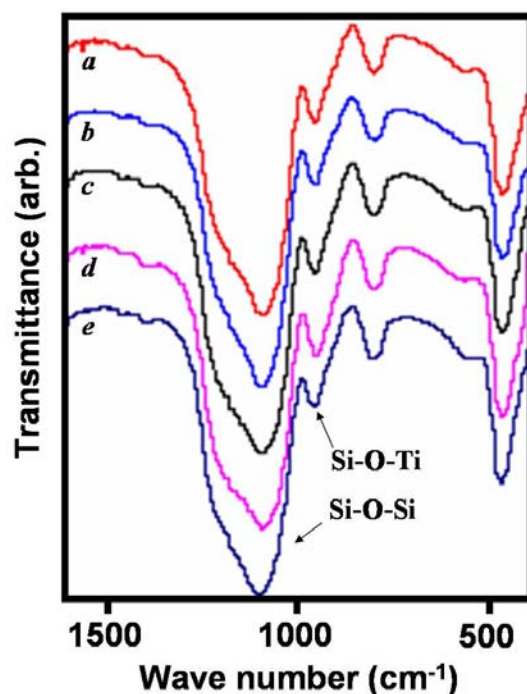
Fig. 4.1.6. FT-IR spectra of (a) 2 wt% Titania (b) 5 wt% Titania (c) 10 wt% Titania (d) 15 wt% Titania (e) 20 wt% silica-titania aerogels.

FTIR of the aerogels calcined at 200 °C, Fig. 4.1.6 has Si-O-Ti vibrations at 940 cm^{-1} [41]. This indicates good mixing of Ti and Si at the atomic level which is a crucial factor in catalytic applications.
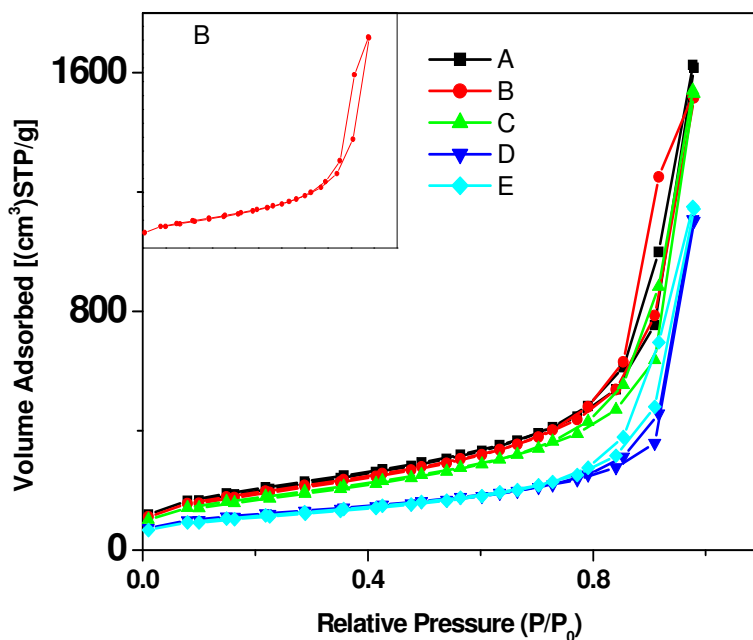
Fig. 4.1.7. Adsorption isotherms of (A) 2 wt% Titania (B) 5 wt % Titania (C) 10 wt% Titania (D) 15 wt% Titania (E) 20 wt% Titania-Silica (Isotherm B is given in the inset for clarity)

The adsorption-desorption isotherms of silica-titania aerogels are provided in Fig. 4.1.7. The presence of a hysterisis loop indicates Type IV behaviour, exclusive of mesoporous nature. The 5 wt% sample has the maximum area under the hysterisis loop indicating that it has the maximum pore size distribution in the mesopore region. The adsorption isotherms of the 15 and 20 wt% samples lie below indicating the lower pore volume, but has a similar pattern as that observed for the 2 wt% and 10 wt% samples.

Table 4.1.1. Density and BET surface area results of silica-titania aerogels

Sample	Density (g/cm^3)	Surface area (m^2/g)	Totalpore volume (cm^3/g)	Pore diameter (Å)
Silica	0.34	895	2.07	92
2% Titania	0.36	726	2.5	137
5% Titania	0.38	685	2.34	136
10% Titania	0.35	620	2.36	152
15% Titania	Cracked gel	412	1.74	165
20% Titania	Cracked gel	399	1.76	176

Microporosity, which is manifested as the non linear rise in adsorption at very low pressures (<0.1 P/P_0) is comparable for the samples with titania weight percentages <15 wt% and similar for 15 wt% and 20 wt% samples. Microporosity is considered to reside within primary particles in aerogels. The added titania particle becomes part of the primary particles in the mixed oxide system and reduces the micropore volume on increasing content. Details of the BET surface area analysis are given in Table 4.1.1. Dutoit et al. has reported exhaustive structural characterization of xerogels, supercritically dried high temperature and low temperature silica-titania aerogels [41]. The surface areas of the gels dried under different conditions are comparable. But the aerogels have very large pore volumes in comparison with their xerogel counterpart. The

ambient pressure dried aerogels have surface areas and pore volumes comparable with the ones reported by Dutoit et al. [41]. Moreover the prepared aerogels have very high pore volume, advantageous for catalytic applications.

The surface area of silica-titania aerogels decreases as the percentage of titania is increased. D.R. Dunphy et al. prepared surfactant templated silica-alumina thin films by doping alumina into the pore walls during material synthesis or grafting on to the pore surface of preformed mesophases [67]. There was a decrease in total porosity and surface area with Al doping. On the basis of refractive index data, this decrease was attributed to reduction in pore accessibility and not pore collapse. Similar decrease in surface area was also reported by Hernandez et al. [68]. The authors studied the relationship between the porous texture, the co-ordination number of Al atoms, the type of surface acidity and the sol-gel acidic synthesis conditions at two pH values (pH≈ 2 and pH ≈ 0) in silica-alumina aerogels made with molar Si to Al ratio r $_{Si/Al}$ =100. K. Sinko et al. prepared alumino-silicate aerogels under various conditions and compared with respect to their nanostructures and porosity [69]. The authors found that the Al incorporation into the silicate network did not decrease the porosity in these series. The highly bonded Al content, the loose fractal structure and the very small elementary units derived from gelation of aluminium nitrate or isopropoxide and TEOS guarantee good porosity property and hence a high surface area.

B. Ameen et al. prepared silver nanoparticles in silica aerogel matrix by subcritical drying [70]. On increasing the silver concentration, the specific surface area decreased from 845 m^2/g to 307 m^2/g. The concomitant decrease in surface area with increase in silver concentration showed that fine silver particles crystallises within the

pores of the aerogel matrix. Moreover the largest pore volume was obtained for 1% Ag and it subsequently decreased as percentage of silver is increased. This characteristic was attributed to the partial replacement of silicon by silver atom in the silica framework and the associated vacancy created for the charge compensation. With increasing silver concentration, the silver atoms get crystallised in the pores of the aerogel matrix, reducing the total pore volume.

The pore size distribution curves obtained for silica-titania aerogels is provided in Fig. 4.1.8. The pore size distribution extends from 20 to 300 Å which confirms that the mesoporous gel network is preserved after ambient drying.
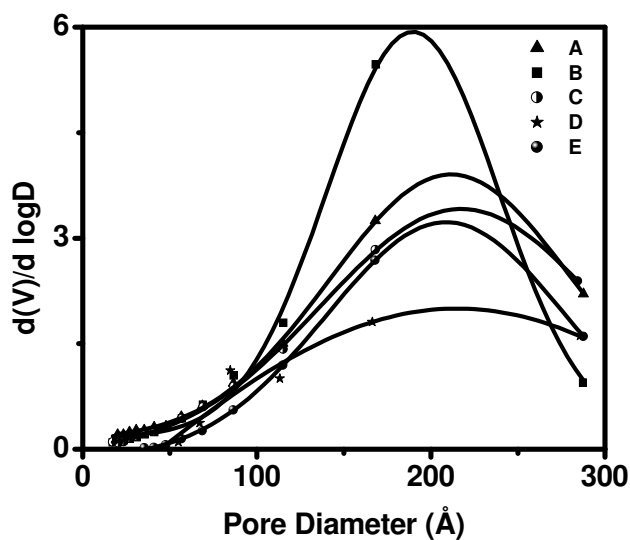

Fig. 4.1.8. Pore size distribution of (A) 2 wt% Titania (B) 5 wt % Titania (C) 10 wt% Titania (D) 15 wt% Titania (E) 20 wt% Titania-Silica

The adsorption-desorption isotherm of silica-titania gels calcined at 500 °C is presented in Fig. 4.1.9. The presence of a hysterisis loop indicates Type IV behaviour, exclusive of mesoporous nature and the hysterisis loop is due to capillary condensation in the pores of the aerogels. The adsorption-desorption isotherms of silica-titania gels

calcined at 900 °C is presented in Fig. 4.1.10. The aerogels are mesoporous as evidenced

from the presence of hysterisis loop characteristic of mesoporous material.
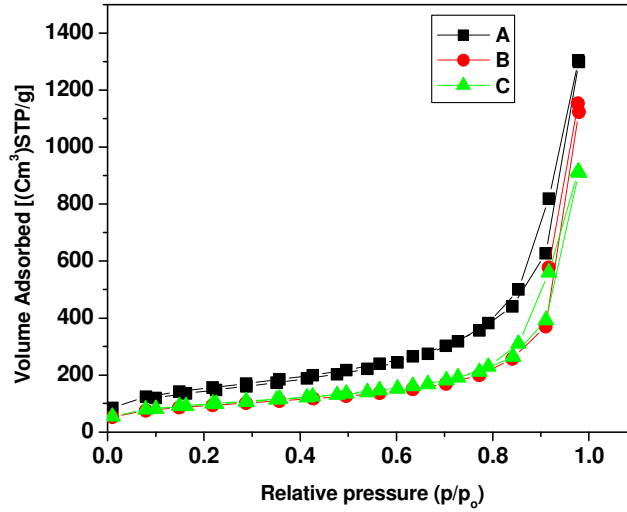
Fig. 4.1.9. Adsorption isotherms of (A) 5 wt% Titania (B) 15 wt % Titania (C) 20 wt%
Titania calcined at 500 °C.
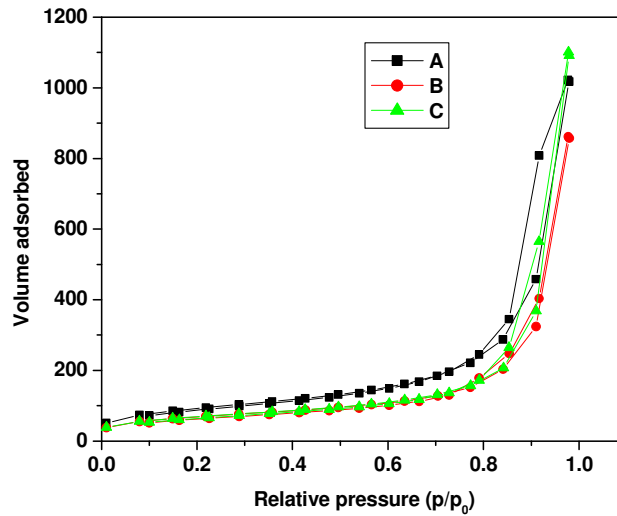
Fig. 4.1.10. Adsorption isotherms of (A) 5 wt% Titania (B) 15 wt % Titania (C) 20 wt%
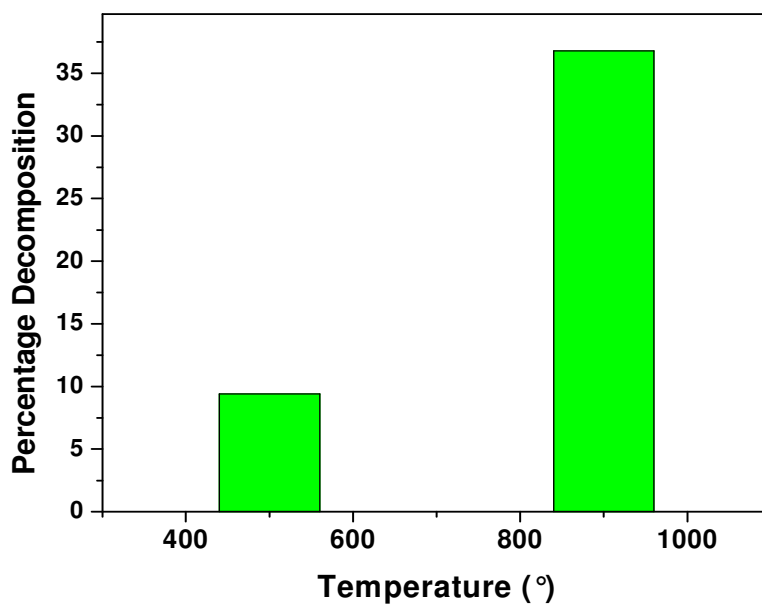Titania calcined at 900 °C.

Surface area and pore volume of silica and silica-titania aerogels calcined at 500, 900 and 1200 °C are provided in Table 4.1.2. The incorporation of aluminium atoms into the silica network has a significant influence on the macroscopic properties of the aerogels.

Table 4.1.2. Surface area and pore volume of silica and silica-titania aerogels calcined at 500, 900 and 1200 °C.

Titania content in mixed oxide Sol (wt %)	Calcination temp. (°C)	Surface area (m^2/g)	Pore volume (cm^3/g)	Pore radius (Å)
0	500	736	1.23	66
	900	415	0.73	70
	1200	nil		
5	500	536	2.0	149
	900	328	1.57	191
	1200	nil		
15	500	319	1.73	217
	900	232	1.32	220
	1200	nil		
20	500	340	1.68	165
	900	242	1.4	278
	1200	nil		

Himmel et al. prepared SiO_2-Al_2O_3 aerogels and characterized by X-ray scattering at small and large angles as well as by electron diffraction and transmission electron microscopy [71]. The authors also investigated the dependence of linear shrinkage on heat treatment and found that the shrinkage of the aerogel was influenced by the presence of alumina. The linear shrinkage of silica aerogel was found to be approximately 48% while for that of $70Al_2O_3$-$30SiO_2$ was only 25%. Pure silica aerogels calcined at 1200 °C has a surface area much below the value one, (nearly no adsorption). But the addition of titania has little effect on the thermal stability of silica aerogels. By the incorporation of 15 and 20 wt% of titania, the surface area was not affected and the thermal pore stability was not increased with respect to silica. The densification of secondary particles leading to pore collapse is not prevented by the presence of titania and this is due to the weaker Si-O-Ti network [44]. This is different from the case of silica-alumina system which was discussed earlier.

The photocatalytic studies were tested by methylene blue decolourisation. 20% Titania-Silica aerogel was calcined at 500 °C and 900 °C and were subjected to degradation studies. J. Wang et al. added transition metal salts to aerogels of Titania – Silica mixtures and the resulting mixtures had very high surface areas [72]. The aerogels were active towards photocatalysis for acetaldehyde oxidation to carbon dioxide in presence of visible light [72]. The percentage decomposition (Fig. 4.1.11) of methylene blue for 900 °C calcined aerogel was found to be 36.8 % while for 500 °C calcined aerogel the percentage decomposition was found to be only 9.4% after 3.5 hours of U.V irradiation. The photograph of 900° C and 500 °C aerogels before and after irradiation is provided in Fig. 4.1.12.

Fig. 4.1.11. Percentage decomposition of Methylene blue as a function of temperature.
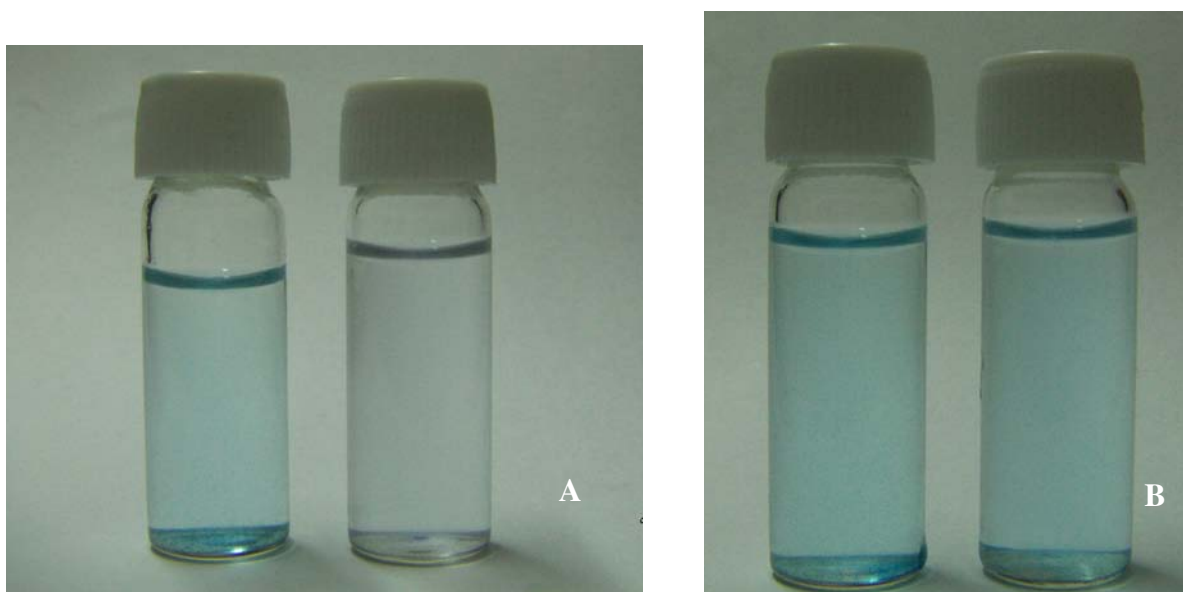
Fig. 4.1.12. Photograph of before and after UV irradiation of (A) 20% Titania-Silica aerogel calcined at 900 °C and (B) 20% Titania-Silica aerogel calcined at 500 °C aerogel.

4.1.4.1 Aerogels derived from Titania chelated with acetyl acetone

The silica-titania aerogels derived from acetic acid chelation contains considerable amount of water since Titanium isopropoxide is chelated with acetic acid and is hydrolysed with water in the molar ratio of 1:10:350. M. Stolarski et al. found that the amount of water used at hydrolysis step was found to have a significant effect on the texture of silica aerogels [73]. The effect of water concentrations was examined for the samples prepared at precursor concentrations: 25 wt%, hydrolysis pH: 3.0, and gelation pH.7.0. The highest surface area (935 m^2/ g) was obtained using stoichiometric amount of water. Both deficiency and excess of water led to a reduction of surface area by 200±300 m^2/g.
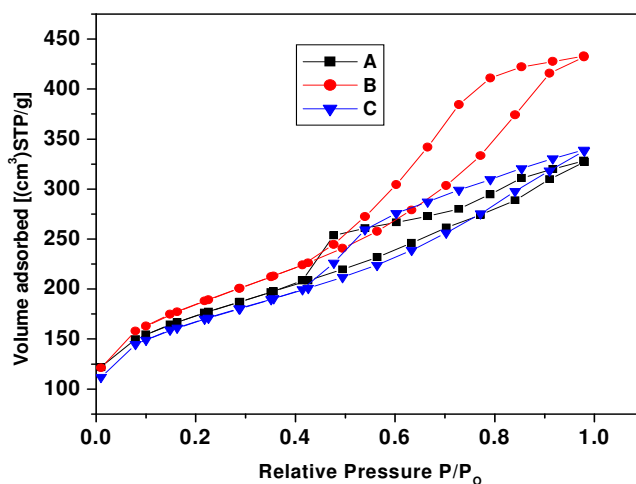

Fig. 4.1.13. Adsorption isotherms of (A) 5 wt% Titania (B) 10 wt % Titania (C) 20 wt% Titania

The adsorption-desorption isotherms of Silica-titania, derived from chelated titania using acetyl acetone is provided in Fig. 4.1.13. The isotherms clearly indicate that the aerogels are mesoporous, which is confirmed by hysterysis loop due to the capillary condensation.

The surface area, pore volume and pore diameters are provided in Table 4.1.3. The acetyl acetone chelated 15 wt% and 20 wt% titania aerogels possess a surface area of 513 and 557 m^2/g while the acetic acid chelated gels possess surface areas of 412 and 399 m^2/g respectively. The surface areas do not change much as the percentage of titania is increased from 5 to 20%. This may be due to the fact that in the acetic acid derived aerogels, we used water to hydrolyse chelated titania and as the percentage of titania increases more and more of water is required to hydrolyse the same. In the case of acetyl acetone chelated gels, the titania gets hydrolysed in presence of excess water remaining after the hydrolysis of silica sol.

Table 4.1.3. Surface area and pore volume of silica and silica-titania aerogels

Sample	Surface area (m^2/g)	Totalpore volume (cm^3/g)	Pore diameter (Å)
Silica	895	2.07	92
5 % Titania	577	0.507	35
10 % Titania	621	0.668	42
15 % Titania	513	0.294	22
20 % Titania	557	0.522	37
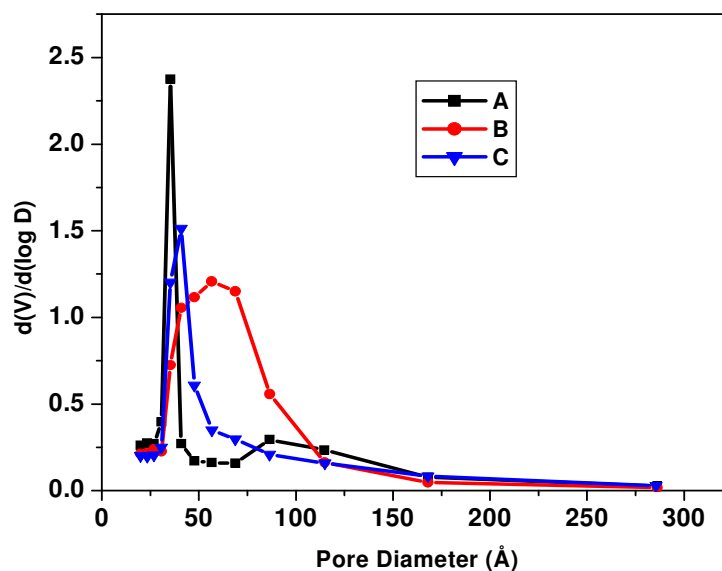
Fig. 4.1.14. Pore size distribution of (A) 5 wt% Titania (B) 10 wt % Titania (C)

20 wt% Titania

The pore size distribution of Silica-Titania gels prepared from acetyl acetone chelated titania sol is provided in Fig. 4.1.14. The pore size distribution extends from 20 Å to 200 Å which confirms that the mesoporous gel network is preserved after ambient drying.
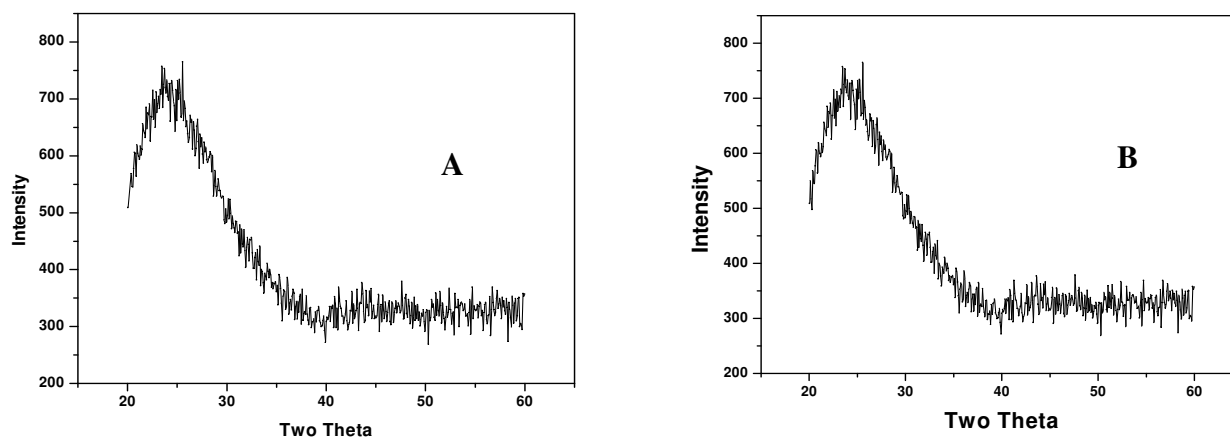
4.1.4.2 Silica-Titania aerogels by impregnation

Titanium alkoxide modified with acetyl acetone (TPAA) was prepared by mixing titaniumtetraisopropoxide with acetyl acetone in the molar ratio of 1:1. The silanol groups react with the isopropoxide to form Si-O-Ti bonds. Although silanol groups can react with both isopropoxide and acetylacetonato groups, Sanchez et al. confirmed that isopropoxyl groups react first [74]. S. Yoda et al. prepared silica-titania aerogels by impregnating titanium tetraisopropoxide modified with acetylacetone into silica alcogels followed by supercritical drying [32-36]. Moreover their application to the removal of

benzene from air was also attempted by the authors [35]. Titania conjugated on silica gel support was prepared by means of impregnation method using cyclohexane solution of tetrabutyl titanate by Hu Chun et al. [75]. The photocatalytic degradation of reactive 15 (R 15) was also tested.

Fig. 4.1. 15. Photograph of Silica-Titania aerogel prepared by impregnation

Fig. 4.1.16. XRD Spectrum of Impregnated Silica-Titania Calcined at (A) 500 °C and (B) 800 °C
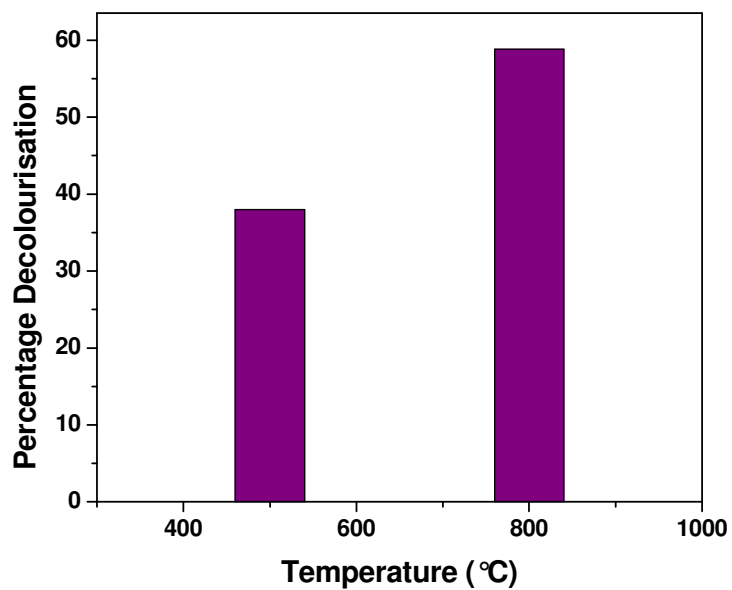
Fig. 4.1.17. Percentage decomposition of Methylene blue as a function of temperature.

Fig. 4.1.18. Photograph of before and after UV irradiation of (A) 900 °C aerogel and (B) 500 °C aerogel

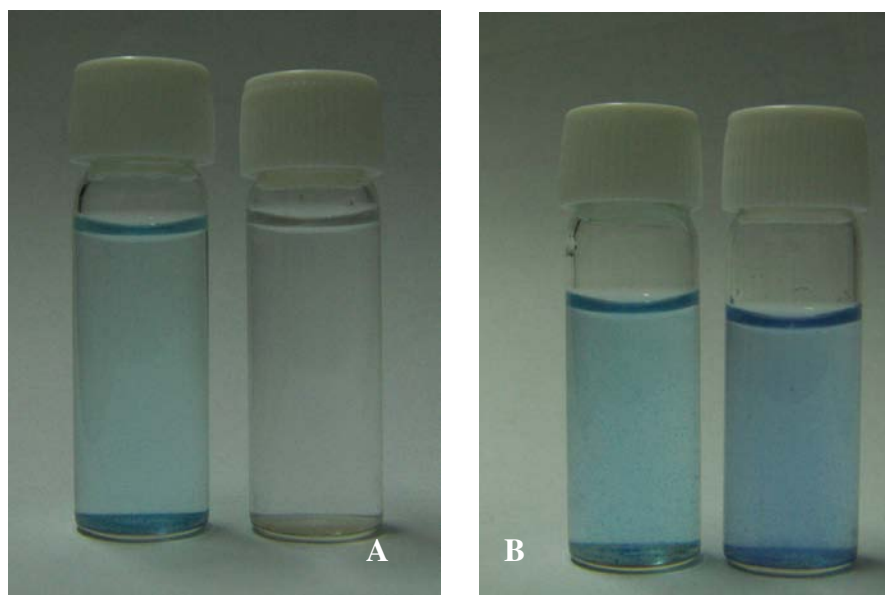The photograph of the Silica-titania gels prepared by impregnation is provided in Fig. 4.1.15. The XRD spectrum of impregnated aerogels calcined at 500 and 800 °C is provided in Fig. 4.1.16 which confirms that the aerogels are amorphous. Z. Zhang et al. investigated the photocatalytic activity of hydrated amorphous titania in the splitting of water [76]. Metal oxides typically show a decreasing band-gap size with increasing particle size or with phase change, such as amorphous to anatase to rutile [76]. The band gap sizes reach a maximum in the amorphous samples, and which likely leads to higher conduction band levels for reduction of water. The nanocrystalline and amorphous hydrated forms of titania therefore do not suffer from this limitation, and which makes high rates of hydrogen evolution possible. The photocatalytic studies were performed on 500 and 800 °C calcined aerogels. The percentage decomposition as a function of time is plotted in Fig. 4.1.17. 58.82 % of the dye is getting degraded in 2.5 hours when tested with 800 °C calcined aerogel, while only 38% is degraded when subjected to 500 °C aerogel. The photograph of 900 °C and 500 °C aerogels before and after irradiation with methylene blue solution is provided in Fig. 4.1.18.

4.1.5 Conclusion

In conclusion silica-titania aerogels were synthesised by adopting an ambient pressure/non-supercritical drying technique. The aerogels are homogeneous and possess large surface areas and mesopore volumes ideal for catalytic applications. The mixed oxide aerogels thus prepared had densities in the range of 0.34 g/cm^3 to 0.38 g/cm^3. TEM studies indicated that the aerogels were nanoporous with a networked structure and the selected area diffraction patterns proved that the aerogels were amorphous. The absence of anatase peak in the XRD pattern even after calcining at 600 °C confirmed molecular scale

dispersion of titania in silica. The surface area for 5 wt% titania aerogel was as high as 685 m^2/g with a pore volume of 2.34 cm^3/g. The FTIR studies indicated the presence of Si-O-Ti bonds in the mixed oxide system. The thermal stability of silica-titania aerogels derived from acetic acid chelated titania sols were also investigated.

Silica-Titania aerogels were also prepared from acetyl acetone chelated titania sol. The aerogels possess high surface areas and the surface area does not change much as the percentage of titania is increased.

Photocatalytic studies were performed on acetic acid derived aerogels and it was found that the 900 °C calcined aerogel gave better activity compared to 500 °C calcined aerogel. The percentage decomposition for 900 °C aerogel was found to be 36% while for 500 °C aerogel was found to be only 9%. Silica-Titania aerogels were prepared by impregnation and the photocatalytic studies were performed. It was found that the 800 °C (60%) calcined aerogel gave better activity compared to 500 °C (38%) calcined aerogel.

4.2 Synthesis and Characterisation of non-supercritically derived Hydrophobic Silica-Titania aerogels

4.2.1 Abstract

Hydrophobic Silica-Titania aerogels have been prepared by non-supercritical method by surface treatment of gels with TMCS (Trimethylchlorosilane) and MTMS (Methyltrimethoxysilane). The surface modification has been achieved by Derivatisation method. The modification of the surface was confirmed by FT-IR (Fourier Infrared) spectroscopy. The surface modified aerogels had very high surface area and thermal stability as high as 520 °C. Nitrogen sorption studies indicate that the hydrophobic mixed oxide aerogels are mesoporous in nature. The pore size distribution of the aerogels indicated preservation of the aerogel structure.

4.2.2 Introduction

Silica–Titania mixed oxide systems have attracted considerable academic and industrial attention owing to their application as catalyst [26-31]. The hydrophobicity/hydrophilicity of the mixed oxides has a major role in their performance as a catalyst. It is reported that no leaching of the active titanium species to the aqueous phase occurs when the catalyst is hydrophobic [55]. Moreover the hydroxyl groups of silica are strongly hydrophilic and hence the organic substrate has limited access to the surface [77].

The efficiency of silica-titania mixed oxide catalysts is also heavily dependent on the molecular scale dispersion of titanium atoms, high surface area and pore diameters in the mesoporous range i.e. large enough for the easy accessibility of reactants. While molecular scale dispersion is ensured by a sol-gel synthesis, the need for high surface area and porosity brings in the importance of drying conditions [41]. High surface area xerogels and aerogels have been one of the most investigated forms of these types of catalysts.

Conventional xerogels are microporous in nature. However, the effectiveness of these catalysts lies in the mesopore region. As a consequence, the xerogel forms are less effective due to the limited accessibility of active sites although they have high surface areas. Mesoporous catalysts are well synthesised by supercritical drying technique. But as observed by Dutoit the high temperature supercritical drying methods adopted in such cases induces considerable segregation and agglomeration of titania and silica disturbing the advantageous structure developed during sol-gel process and results in the dominance of titanium located in hardly active anatase particles [41]. The low temperature supercritical drying (using CO_2 as solvent) resulted in lower microporosity, higher surface areas (up to 700 m^2/g) and the mixed oxides were amorphous.

Finding a suitable alternative to the expensive and risky supercritical drying, has been part of growing aerogel technology as evident from various reports available in literature [9, 10]. The ambient pressure drying can be effectively employed for the synthesis of aerogels and this can be achieved by increasing the stiffness of the gel network by aging in a silane precursor [14] and by capping the surface silanol groups by alkyl groups so that the gel breaths back to shape after shrinkage due to repulsion between the alkyl groups [21].

The aim of the present study is to synthesise hydrophobic silica-titania gels through modified ambient pressure drying technique where careful and systematic process of solvent exchange, silane aging and drying under controlled conditions were employed. The gels were made hydrophobic by attaching organic groups to the silica-titania clusters using two hydrophobic reagents (HR) Trimethyl Chloro Silane (TMCS) and Methyl Trimethoxy Silane (MTMS). The hydrophobicity of the aerogels can be achieved by two methods i.e.
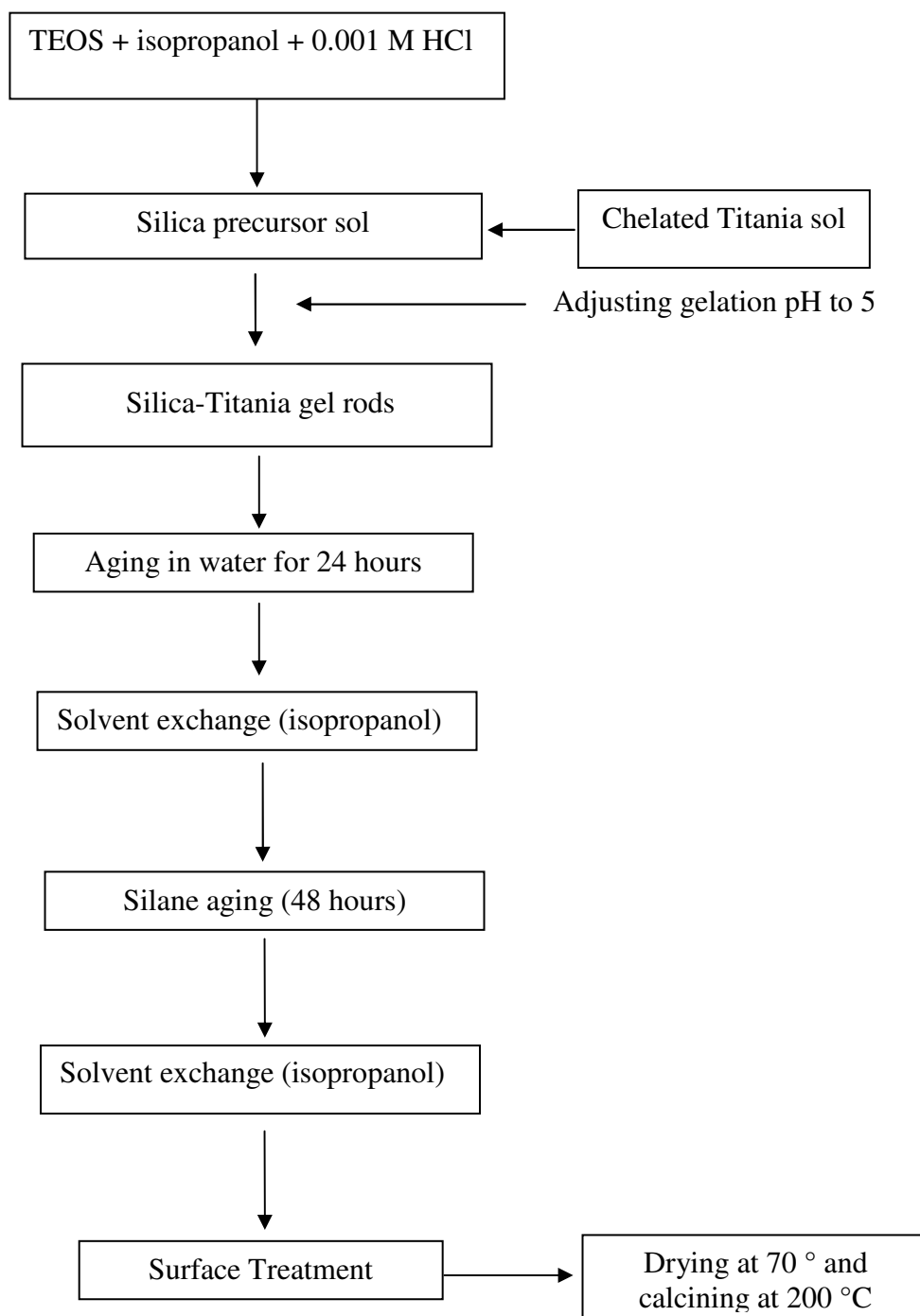
1) by co-precursor method [78] and 2) by derivatisation method [79]. We have adopted the derivatisation method where the alkyl groups graft to the clusters of the gel without affecting the gel network structure. To best of our knowledge, successful use of non-supercritical drying/subcritical drying in the preparation of hydrophobic silica-titania aerogels is presented here.

4.2.3 Experimental

Tetraethoxysilane (TEOS) (Fluka, Switzerland), Ti (O^{i}Pr)$_4$ (Aldrich), acetic acid (S.D. Fine chemicals, India) and isopropanol (S.D. Fine Chemicals, India) were used as received. Stable titania sol was prepared by the method reported else where [64]. In a typical experiment for the preparation of 10 wt% titania in silica, 0.5336 g titanium isopropoxide (Aldrich) in 1.12 ml acetic acid (S.D. Fine chemicals, India) was hydrolysed with 11.825 ml water. Simultaneously silica sol was prepared by hydrolysing 4.6617 g TEOS in 5.3704 g isopropanol with 6.4425 g water. The hydrolysis pH was maintained at 1.54 due to the difference of reactivity of silicon and titanium isopropoxide. The two sols were stirred for 3 hours each separately and then titania sol was added drop wise to the silica sol. The mixed sol was then stirred for 1 hour and the gelation pH adjusted to 5 using 5% ammonia solution.

The visually homogeneous sol was then transferred to vials (2 cm diameter) and kept at 50 °C for gelation. The gelation occurred within 15 minutes for all compositions. The gels were kept for 24 hours at 50 °C, and then aged in water for 24 hours at 50 °C. The gels were then solvent exchanged with isopropanol at 50°C. This was followed by

aging the gels in an 80% silane precursor solution for 48 hours at 50 °C and finally

solvent exchanged with isopropanol at 50 °C. To induce hydrophobicity, the 10 wt %

```
┌─────────────────────────────────────┐
│  TEOS + isopropanol + 0.001 M HCl    │
└─────────────────────────────────────┘
                  │
                  ▼
┌──────────────────────────┐      ┌──────────────────────┐
│    Silica precursor sol   │◄─────│  Chelated Titania sol │
└──────────────────────────┘      └──────────────────────┘
                  │
                  │◄───────────── Adjusting gelation pH to 5
                  ▼
┌──────────────────────────┐
│   Silica-Titania gel rods │
└──────────────────────────┘
                  │
                  ▼
┌──────────────────────────┐
│  Aging in water for 24 hours │
└──────────────────────────┘
                  │
                  ▼
┌──────────────────────────┐
│  Solvent exchange (isopropanol) │
└──────────────────────────┘
                  │
                  ▼
┌──────────────────────────┐
│   Silane aging (48 hours) │
└──────────────────────────┘
                  │
                  ▼
┌──────────────────────────┐
│  Solvent exchange (isopropanol) │
└──────────────────────────┘
                  │
                  ▼
┌──────────────────────┐      ┌──────────────────────┐
│   Surface Treatment   │─────►│  Drying at 70 ° and   │
└──────────────────────┘      │  calcining at 200 °C  │
                              └──────────────────────┘
```

Fig. 4.2.1. Flowchart for the preparation of Hydrophobic Silica-Titania mixed oxide

aerogels

titania-silica alcogels were immersed in 20, 30 and 40 vol % Trimethyl chloro silane

(TMCS) or Methyl Trimethoxy silane (MTMS) for 24 h at 50° C. The gels were washed

with Isopropanol prior to drying. The gels were then dried in airtight containers at 70 °C.

The containers were vented after a day. The aerogels obtained after drying at 70 °C were

further heated for 3 hours at 200 °C. Samples with titania content ranging from 2 to 20

wt% were prepared. The detailed experimental procedure is provided in Fig. 4.2.1. The

Fourier Transform Infrared Spectra of the heated gels was recorded in a Nicolet Magna-

560-IR Spectrometer (USA) (KBr pellets). The BET surface area of calcined aerogels

were determined by N_2 adsorption at 77K (Micromeritics, Gemini Model 2360, USA).

The calcined samples were preheated in a flow of nitrogen for 3 hours at 200 °C to

remove all the volatiles and chemically adsorbed water from the surface.

The specific surface area was determined using the BET equation with an

accuracy of ± 10 m^2/g. The total pore volume was calculated as,

$$\text{Pore volume, } V = V_a * D$$

Where V_a = volume adsorbed at P/P$_0$ 0.99, D = density conversion factor

(0.0015468 for nitrogen as adsorbate gas). The pore size distribution was obtained using

the Barrette-Joynere-Halenda (BJH) method.

Assuming that the pores are cylindrical and open at both ends, the average pore

size of a given sample is calculated using the equation,

$$\text{Average pore size} = 4V_{total} / S_{BET}$$

The DTA of the gel was carried out in Shimadzu 50H (Japan) Thermal analyzer in flowing nitrogen atmosphere. The contact angle measurements were done with a DCAT 11 Tensiometer, Dataphysics,Germany, using Washburn equation for powder contact angle measurements.

The contact angle measurement according to Washburn is done by the capillary rise of a liquid into a porous medium which implies the replacement of the solid-air interface by a solid-liquid interface. The Washburn equation defines the flow of a liquid through a capillary. A powder which is passed in a column can be described as a bundle of capillaries with some mean capillary radius r. A modified Washburn equation is used to calculate powder contact angle,

$$\frac{m^2}{t} = \frac{[(c*r)\,\xi^2(\pi)R^2]\,\rho\gamma_L\,Cos\theta}{2\,\eta}$$

where r, the radius of capillary, t, time of flow, γ_L, the surface tension of the liquid, η, the viscosity of liquid, m, the weight of the penetrating liquid, ρ, the density of measuring liquid, ξ, the relative porosity and R, the inner radius of the measuring tube.

4.2.4 Results and Discussion

A high water/alkoxide ratio of 16:1 was chosen for the hydrolysis of silica precursor since our earlier studies revealed that gels prepared under these conditions result in porous gels having high surface area [12]. Initial aging of the gel was done in water to allow the completion of the hydrolysis condensation reactions. The water aged gel was solvent exchanged with isopropanol prior to silane aging since silicon alkoxide is immiscible with water. Aging in silane solution results in the dissolution and

reprecipitation of silica particles on the gel network coarsening the smooth necks between the particles thereby strengthening the gel network [80]. An aging time of 48 hours and an aging solution having 80% silane concentration were used. These gels were then solvent exchanged with isopropanol as the drying solvent, since liquids of low surface tension and high molecular volume favour the production of gels having high surface area [12].

**Fig. 4.2.2.** Photograph of TMCS modified aerogel
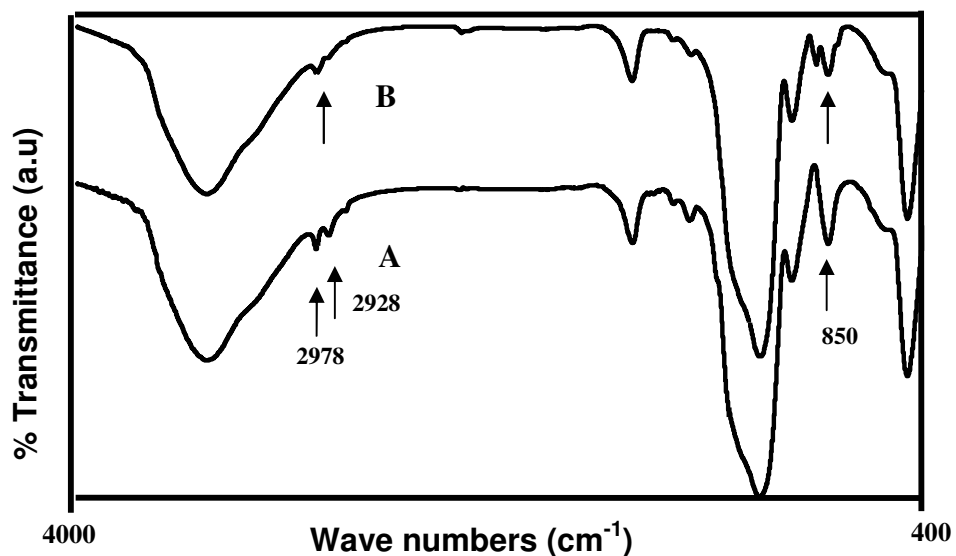
Fig. 4.2.3. FT-IR of surface modified aerogels (A) TMCS modified (B) MTMS modified aerogels

The photograph of aerogels synthesised is provided in Fig. 4.2.2. The Fig. 4.2.3 shows the FT-IR spectra of surface treated aerogels. The peaks at 2978 cm^{-1} and 2928 cm^{-1} corresponds to terminal –CH$_3$ groups. The peak at 850 cm^{-1} corresponds to Si-C bonding. This confirms that surface modification has taken place and as a consequence of this, the aerogels show hydrophobic behaviour.

The contact angle of the surface modified mixed oxide aerogels are provided in Fig. 4.2.4. The Trimethylchlorosilane treated aerogels possess a contact angle of 90°, while the Methyltrimethoxysilane modified aerogels have contact angles between 75-80°. The Trimethylchlorosilane treated gels have a higher contact angle in comparison with the Methyltrimethoxysilane modified gels. This is well in agreement with the expected results if we consider the R/Si ratio for the two hydrophobic reagents. The TMCS is having an R/Si ratio of 3 and the MTMS a ratio of 1. The larger the R/Si ratio, the better is the hydrophobic coverage yielding higher contact angle. Generally it has been observed that the aerogels retain their hydrophobic behaviour up to 320 °C and above this temperature they become hydrophilic. This may be attributed to the oxidation of surface – CH$_3$ groups, leaving behind the hydrophilicity. The Differential thermal analysis (DTA) of the surface treated gels is provided in Fig. 4.2.5. The thermal stability of chlorosilane modified aerogel is much higher (520 °C) than the methyltrimethoxysilane modified aerogel.

The specific surface area and porosity features of aerogels are provided in Table 4.2.1. The nitrogen Adsorption-Desorption isotherms are provided in Fig. 4.2.6. The figure suggests a Type IV isotherm which is characteristic feature of mesoporous

materials. The desorption cycle of the isotherms showed hysterisis loop which is attributed to the capillary condensation occurring in the mesopores.
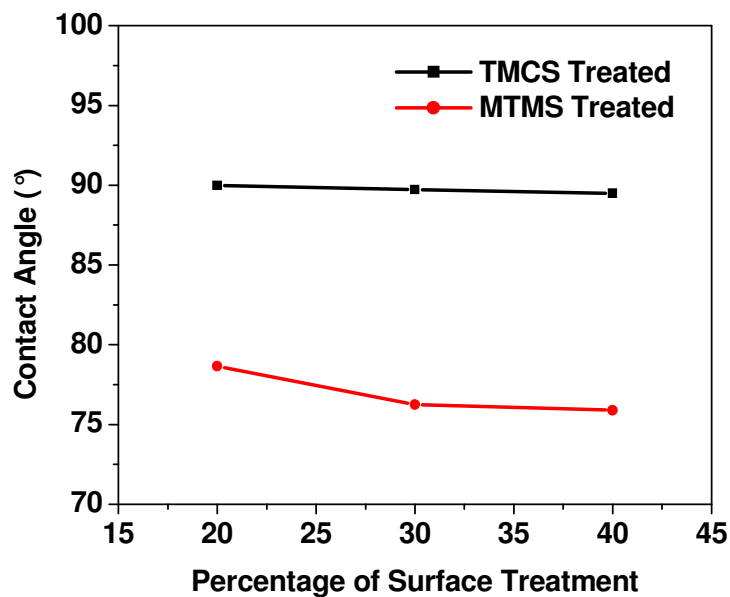

Fig. 4.2.4. Contact angle measurements of TMCS modified and MTMS modified aerogels
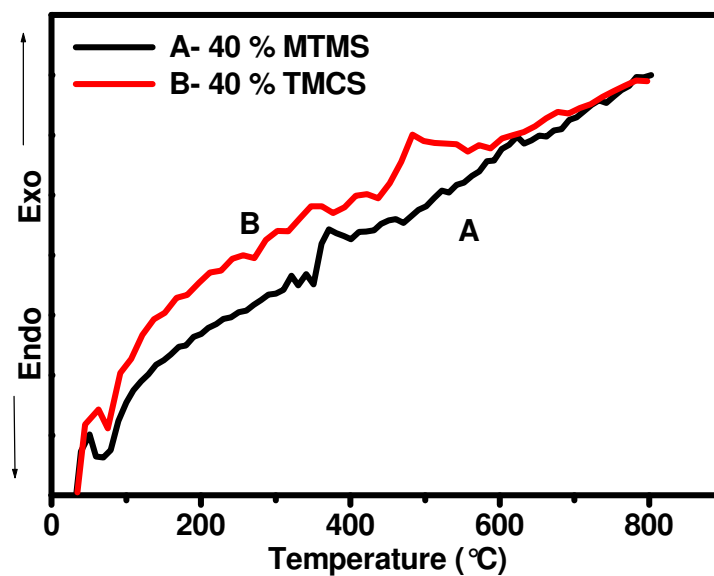
**Fig. 4.2.5.** DTA of (A) MTMS modified and (B) TMCS modified aerogels

Table 4.2.1. BET surface area results of surface modified aerogels

Surface modified aerogel	Surface area (m^2/g)	Total Pore Volume (Cm^3/g)	Pore Diameter $(\mathring{A})$
20% TMCS	540	1.52	112
30% TMCS	640	1.66	104
40% TMCS	610	0.61	40
20% MTMS	617	1.97	128
30% MTMS	582	2.02	138
40% MTMS	554	1.90	137
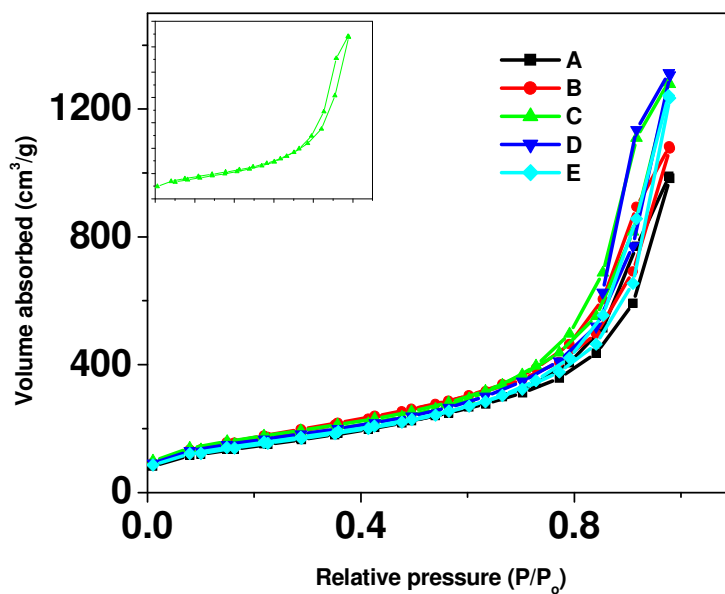
Fig. 4.2.6. Adsorption-Desorption isotherms of (A) 20% TMCS (B) 30% TMCS (C) 20% MTMS (also provided in inset for better clarity) (D) 30% MTMS and E) 40% MTMS

The pore size distribution of the hydrophobic aerogels is provided in Fig. 4.2.7. All the aerogels showed a pronounced peak in the mesoporous region (20- 300 Å). This confirms that the aerogel structure is preserved by drying at ambient temperature.
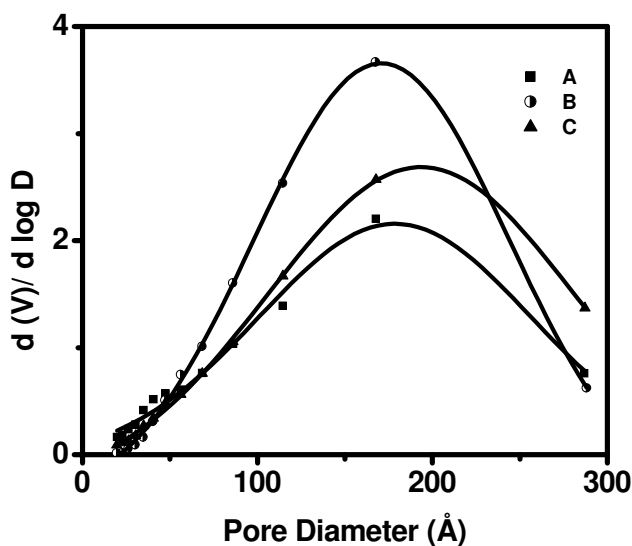
Fig. 4.2.7. Pore size distribution of (A) 20% TMCS B) 20% MTMS and (C) 40% MTMS

4.2.5 Conclusion

In summary a non-supercritical drying approach was adopted to synthesise silica-titania hydrophobic aerogels. The Trimethylchlorosilane treated aerogels possess a contact angle of 90°, while the Methyltrimethoxysilane modified aerogels have contact angles between 75-80°. The TMCS modified aerogels were more hydrophobic compared to MTMS modified ones. The thermal stability of chlorosilane modified aerogels was found to be 520 °C. The mixed oxide aerogels possess very high surface areas and pore volumes. The pore size distribution extends from 20-300 Å which confirms that the aerogels are mesoporous.

References

[1] S.S. Kistler, Nature 127 (1931) 741.

[2] M. Schmidt, F. Schwertfeger, J. Non-Cryst. Solids 225 (1998) 364.

[3] A.C. Pierre, G. M. Pajonk, Chem. Rev. 102 (2002) 4243.

[4] W.L. Hrubesh, J. Non-Cryst Solids 225 (1998) 335.

[5] G.M. Pajonk, Colloid polym. Sci. 281(2003) 637

[6] A. Costela, I. Garcia Moreno, C. Gomez, O. Garcia, R. Sastre, A. Roig, E. Molins, J. Phys. Chem. B. 109 (10) (2005) 4475.

[7] G.H. Negley, U.S Patent no. 7042020 dated May 9 2006.

[8] J.J. Fricke, J. Non-Cryst. Solids 95 (1987) 1135.

[9] S.S. Prakash, C.J. Brinker, A.J. Hurd, S. M. Rao, Lett. Nature 374 (1995) 439.

[10] F. Schwertfeger, D. Frank, M. Schmidt, J. Non-Cryst. Solids 225 (1998) 24.

[11] R. Deshpande, Duen-Wu-Hua, D. M. Smith, C.J. Brinker, J. Non-Cryst solids 225 (1992) 254.

[12] S. Rajesh Kumar, P. Krishna Pillai, K.G.K. Warrier, Polyhedron 17 (1998) 1699.

[13] A. Venkateswara Rao, E. Nilsen, M-A. Einarsrud, J. Non-cryst. Solids 296, 2001, 165.

[14] P.J. Davis, C.J. Brinker, D.M. Smith, J. Non-Cryst solids 142 (1992) 189.

[15] P.J. Davis, C.J. Brinker, D.M. Smith, R.J. Assink, Non-Cryst. Solids 142 (1992) 197.

[16] M-A. Einarsrud, S. Haereid, J. Sol-Gel Sci. Technol. 2 (1994) 903.

[17] S. Haereid, M-A. Einarsrud, G. W. Scherrer, J. Sol-Gel Sci. Technol. 3 (1994) 199.

[18] S. Haereid, M. Dahle, S. Lima, M-A. Einarsrud, J. Non-Cryst. Solids 186 (1995) 96.

[19] S. Haereid, E. Nilsen, M-A. Einarsrud, J. Non-Cryst. Solids 204 (1996) 228.

[20] M-A. Einarsrud, E. Nilsen, J. Non-Cryst. Solids 226 (1998) 122.

[21] R. Deshpande, D. Smith, C. J. Brinker, US patent No. 5, 565,142 issued 1996.

[22] D.M. Smith, D. Stein, J.M. Anderson, W.J. Ackerman, J. Non-Cryst. Solids 186 (1994) 104.

[23] C.J. Brinker, S.S. Prakash, US patent disclosure (1994).

[24] V.D. Land, T.M. Hareis, D.C. Teeters, J. Non-Cryst Solids 283 (2001) 11.

[25] G. S. Kim, S. H. Hyun, J. Mater. Sci. 38 (2003) 1961.

[26] M. Itoh, H. K. Hattori, K. J. Tanabe, J. Catal. 35 (1974) 225.

[27] R. Hutter, T. Mallet, A. Baiker, J. Catal. 153 (1995) 177.

[28] E.I. Ko, J. P. Chen, J. G. Weassman, J. Catal. 105 (1987) 511.

[29] H. Nakabayashi, Bull. Chem. Soc. Jpn. 65 (3) (1992) 914.

[30] J.R. Sohn, H.J. Jang, J. Catal. 132 (1991) 563.

[31] S. Imamura, H. Tarumoto, S. Ishida, Ind. Eng. Chem. Res. 28 (1989) 1449.

[32] S. Yoda, K. Ohtake, Y. Takebayashi, T. Sugeta, T. Sako, J Sol-Gel Sci. Technol. 19 (2000) 719

[33] S. Yoda, Y. Tasaka, K. Uchida, A. Kawai, S. Ohshima, F. Ikazaki, J. Non-Cryst. Solids 225 (1998) 105

[34] S. Yoda, K. Otake, Y. Takebayashi, T. Sugeta, T Sato, J. Non-Cryst. Solids 285 (2001) 8.

[35] S. Yoda, K. Ohtake, Y. Takebayashi, T. Sugeta, T. Sako, T. Sato, J. Mater. Chem. 10 (2000) 2151.

[36] S. Yoda, D.J. Suh, T. Sato, J. Sol-Gel Sci. Technol. 22 (2001) 75.

[37] W. Kim, I.K. Hong, J. Ind. Eng. Chem. 9 (2003) 728.

[38] C.A. Morris, M.L. Anderson, R.M. Stroud, C.I. Merzbacher, D.R. Rolison Science 284 (1999) 622.

[39] S. Cao, K.L. Yeung, P.L. Yue, Appl Catal. B: Environ. 68 (2006) 99.

[40] J.M. Watson, A.T. Cooper, J.R.V. Flora, Environ. Eng. Sci. 22 (2005) 666.

[41] D.C.M. Dutoit, M. Schneider, A. Baiker, J. Catal. 153 (1995) 165.

[42] D.C.M. Dutoit, M. Schneider, R. Hutter, A. Baiker, J. Catal. 161 (1996) 651.

[43] D.C.M. Dutoit, U. Gobel, M. Schneider, A. Baiker, J. Catal. 164 (1996) 433.

[44] C.H. Lee, T.S. Lin, C.Y. Mou, J. Phys. Chem. C 111(2007) 3873.

[45] M. Aizawa, Y. Nosaka N. Fujii, J. Non-Cryst. Solids 128 (1991) 77.

[46] C. Sanchez, J. Livage, M. Henry, F. Babonneau, J. Non-Cryst. Solids 100 (1988) 65.

[47] C. A. Muller, M. Maciejewski, T. Mallet, A. Baiker, J. Catal. 184 (1999) 280.

[48] C. A. Muller, M. Schneider, T. Mallet and A. Baiker, Appl. Catal. A: Gen. 189 (2000) 221.

[49] S. Klein, W. F. Maier, Angew. Chem. Int. Ed. Engl. 35 (1996) 2230.

[50] Z. F. Liu, R. J. Davis, J. Phys. Chem. 98 (1994) 1253.

[51] R. Mariscal, M. Lopez-Granador, J. L. G. Fierro, J. L. Sotelo, C. Martos, R. Van Grieken, Langmuir 16 (2000) 9460.

[52] J.L. Sotelo, R. Van Grieken, C. Marcos, Chem. Comm. 1999, 549.

[53] M. F. Best, R. A. Condrate, J. Mater. Sci. Lett. 4 (1985) 994.

[54] B. E. Yoldas, J. Mater. Sci. 21 (1986) 1086.

[55] H. Kochkar, F. Figueras, J. Catal. 171 (1997) 420.

[56] M. A. Holland, D. M. Pickup, G. Mountjoy, E. S. C. Tsang, G. W. Wallidge, R. J. Newport, M. E. Smith, J. Mater. Chem. 10 (2000) 2495.

[57] J. B. Miller, L. J. Mathers, E. I. Ko, J. Mater. Chem. 5 (1995) 1759.

[58] R. Hutter, T. Mallet, A. Baiker J. Catal. 153 (1995) 665.

[59] R. Hutter, T. Mallet, A. Peterhans, A. Baiker J. Catal. 172 (1997) 427.

[60] M. Dusi, T. Mallet and A. Baiker, J. Mol. Catal. A 138 (1999) 15.

[61] C. A. Muller, M. Schneider, T. Mallet, A. Baiker, Appl. Catal. A: Gen. 201 (2000) 253.

[62] M. Dusi, T. Mallet, A. Baiker, J. Catal. 184 (1999) 280.

[63] C.A. Muller, R. Deck, T. Mallet, A. Baiker, Top. Catal. 11/12 (2000) 369.

[64] C.P. Sibu, S. Rajesh Kumar, P. Mukundan, K.G.K. Warrier, Chem. Mater. 14 (2002) 2876.

[65] N. Husing, U. Schubert, Angew. Chem. Int. Ed. 37 (1998) 22.

[66] J. Fricke, Sci. Am. (May) (1988) 92.

[67] D.R. Dunphy, S. Singer, A.W. Cook, B. Smarsly, D.A. Doshi, C.J. Brinker, Langmuir, 19 (2003) 10403.

[68] C. Hernandez, A.C. Pierre, Langmuir 1*6* (2000) 530.

[69] K. Sinko, N. Hu¨sing, G. Goerigk, H. Peterlik, Langmuir 24 (2008) 949

[70] K. Balkis Ameen T. Rajasekharan, M.V. Rajasekharan J. Non-Cryst. Solids 352 (2006) 737.

[71] B. Himmel, Th. Gerber, H. Burger, G. Holzhuter, A. Olbertz, J. Non-Cryst. Solids 186 (1995) 149.

[72] J. Wang , S. Uma and K.J. Klabunde, Appl. Catal. B: Environ. 48 (2004) 151.

[73] M. Stolarski, J. Walendziewski, M. Steininger B. Pniak, Applied Catalysis A: General 177 (1999) 139.

[74] C. Sanchez, J. Livage, M. Henry, F. Babonneau, J. Non-Cryst. Solids 100 (1998) 65.

[75] H. Chun, W. Yizhong, T. Hongxiao, Appl. Catal. B : Environ. 30 (2001) 277.

[76] Z. Zhang, P.A. Maggard, J. Photochem. Photobiol. A: Chem. 186 (2007) 8.

[77] S. Klein, S. Thorimbert, W.F. Meir, J. Catal. 163 (1995) 476.

[78] F. Schwertfeger, A. Emmerling, J. Gross, U. Schubert, J. Fricke in: Y.A. Attia (Ed.), Sol-Gel Processing and Applications, Plenum, New York, 1994, p. 343.

[79] H. Yokogawa, M. Yokoyama, J. Non-Cryst. Solids, 186 (1995) 23.

[80] S. Rajesh kumar, "High Surface Area Porous Sol-Gel Silica and Mixed Oxide Aerogels Through Subcritical Drying": PhD Thesis, University of Kerala, 2002.

Summary

Aerogels are unique solid materials since they have extremely low densities (up to 95% of their volume is air), large open pores of 1-100 nm range and high surface area. The increasing industrial application of aerogels in the fields of catalysts, thermal and acoustic insulators, dielectric substrates and in space applications have generated considerable interest in developing aerogels through novel methods in addition to supercritical drying. The thesis entitled "**Mixed Oxide Silica Aerogels Synthesised Through Non-Supercritical Route for Functional Applications"** investigates two salient features of aerogels such as a novel synthesis technique involving non-supercritical drying and new mixed oxide aerogels having improved thermal pore stability and functionality.

The present thesis describes a sol-gel route followed by non-supercritical drying, typically subcritical drying or controlled solvent exchange at ambient temperature and pressures. The mixed oxide gels were silica-alumina, silica-silica and silica-titania. The aerogels which were calcined at different temperatures were characterised by Nitrogen sorption studies. The FTIR studies indicated the presence of Si-O-Al bonds in the silica-alumina system after calcining it at 500 °C. The resultant silica-alumina aerogel with an alumina content of 5 wt% showed surface area of 796 m^2/g at 500 °C. The surface area decreases as the percentage of alumina is increased beyond 5wt%. The initial increase in specific surface area is due to aluminium ions getting in to the structure of silica. With the incorporation of 15 wt% and 25 wt% alumina the thermal pore stability of silica aerogel was retained to as high a temperature as of 1200 °C**.** The aluminium sites shield adjacent Si-OH…OH-Si groups thus preventing the dehydroxylation and silanol

condensation and also reduce the number of hydrogen bonds. The densification of secondary particles leading to pore collapse is prevented by the presence of alumina. Thermo Mechanical Analysis (TMA) indicated that the linear shrinkage (%) of 25 wt% alumina-silica gel was only 15% when compared with that of silica which had shrinkage of 30%. Temperature-programmed desorption studies revealed that aerogel with 10 wt% alumina showed higher acidity compared to silica gels. The alumina phase appears to be very homogeneously distributed in the silica matrix in the present method since there was no α-Al_2O_3 peak in the XRD pattern even after calcining at 1200 °C.

For the synthesis of Silica-Alumina aerogels, the gelation was carried out under pH 3 and 5. The aerogels which were prepared by gelation at pH 3 had a higher surface area than the ones which were prepared at gelation pH 5. The reduction in surface area is attributed to the formation of larger pores. TEM microstructural analysis indicates that the aerogel is amorphous and absence of α-Al_2O_3 even after calcination at 1200 °C, is a direct consequence of alumina being homogeneously dispersed in the silica network which was confirmed using X-ray diffraction. Crystallisation of aerogels means the character of porous texture is lost which is not taking place even at 1200 °C.

Non-supercritical drying technique was applied for the synthesis of silica-silica composite aerogels. The composite aerogels possess very high surface area as confirmed by BET surface area analysis. The possible application of composite aerogels as a precursor for high level nuclear waste immobilized glass was also experimented. The percentage of loadings were high and the leaching studies confirmed the stability of the matrix. TEM observations revealed that the aerogels were porous and the micrograph of the sintered neodymium incorporated gel indicates the presence of neodymium silicate in

170

the glass matrix. The XRD patterns also reveal the presence of neodymium silicate ($Nd_2Si_2O_7$) in the matrix. Silica alcogel was also tested as a matrix and a maximum loading of 59% was obtained when the gel immersed in 30% solution of neodymium nitrate.

An ambient pressure/non-supercritical drying technique for the synthesis of silica-titania mixed oxide aerogels was also conducted. The aerogels are homogeneous and possess large surface areas and mesopore volumes ideal for catalytic applications. The mixed oxide aerogels thus prepared had densities in the range of 0.34 g/cm^3 to 0.38 g/cm^3. TEM studies indicated that the aerogels were nanoporous with a networked structure and the selected area diffraction patterns proved that the aerogels were amorphous. The absence of anatase peak in the XRD pattern even after calcining at 600 °C confirmed molecular scale dispersion of titania in silica. The surface area for 5wt% titania aerogel was as high as 685 m^2/g with a pore volume of 2.34 cm^3/g. The FTIR studies indicated the presence of Si-O-Ti bonds in the mixed oxide system. The thermal stability of silica-titania aerogels derived from acetic acid chelated titania sols were also investigated. The addition of titania has little effect on the thermal stability of silica aerogels because of the weak Si-O-Ti linkages. By the incorporation of 15 wt% and 20 wt% of titania, the surface area was not affected and the thermal pore stability was not increased with respect to silica The densification of secondary particles leading to pore collapse is not prevented by the presence of titania and this is due to the weaker Si-O-Ti network. Silica-Titania aerogels were also prepared from acetyl acetone chelated titania sol since the acetic acid chelated silica-titania systems contains considerable amount of water. The aerogels possess high surface areas and the surface area does not change much as the percentage of titania is

increased. The presence of water is reported to have significant effect on the texture of aerogels and both deficiencies and excess of water leads to reduction in surface areas by ± 200 m^2/g.

Photocatalytic studies were performed on acetic acid derived aerogels and it was found that the 900 °C calcined aerogel gave better activity compared to 500 °C calcined aerogel. The percentage decomposition for 900 °C calcined aerogel was found to be 36% while for 500 °C calcined aerogel, it was found to be only 9%. Silica-Titania aerogels were prepared by impregnation and the photocatalytic studies were performed. It was found that for the 800 °C calcined aerogel, the percentage decomposition was found to be 60% compared to the 500 °C calcined aerogel where the activity was only 38%. The mixed oxide aerogels were also made hydrophobic by surface treatments with TMCS and MTMS. The TMCS modified aerogels were more hydrophobic compared to MTMS modified ones. The thermal stability of chlorosilane modified aerogels was found to be 520 °C. The mixed oxide aerogels possess very high surface areas and pore volumes. The pore size distribution extends from 20-300Å which confirms that the aerogels are mesoporous.

The present study on the synthesis of silica and mixed oxide aerogels by ambient pressure drying has shown possibility of further developing mesoporous materials having high temperature pore stability and functionality by following simple and less expensive sol-gel route.

List of Publications

1. **P. R. Aravind**, P. Shajesh, P. Mukundan, P. Krishna Pillai, K.G.K. Warrier "Non-Supercritically Dried Silica-Silica Composite Aerogel and its Possible Application for Confining Simulated Nuclear Wastes", *Journal of Sol-Gel Science and Technology,* 46 (2) (2008) 146.

2. **Parakkulam Ramaswamy Aravind**, Palantavida Shajesh, Sashidharan Smitha, Poothayil Mukundan, Krishna Gopakumar Warrier, "Non-Supercritically Dried Silica-Alumina Aerogels-Effect of Gelation pH" *Journal of the American Ceramic Society,* 91 (4) (2008) 1326.

3. **P.R. Aravind**, L. Sithara, P. Mukundan, P. Krishna Pillai and K.G.K. Warrier, "Silica alcogels for possible nuclear waste confinement- A simulated study", *Materials Letters*, 61 (2007) 2398.

4. **P. R. Aravind**, P. Mukundan, P. Krishna Pillai, K.G.K. Warrier, "Mesoporous silica-alumina aerogels with high thermal pore stability through hybrid sol-gel route followed by Subcritical drying", *Microporous and Mesoporous Materials*, 96 (2006) 14.

5. S. Smitha, P. Shajesh, **P.R. Aravind**, S. Rajesh Kumar, P. Krishna Pillai and K.G.K. Warrier, "Effect of aging time and concentration of aging solution on the porosity characteristics of subcritically dried silica aerogels", *Microporous and Mesoporous Materials*, 91 (2006) 286.

6. **P. R. Aravind**, P. Shajesh, P. Mukundan, P. Krishna Pillai, K.G.K. Warrier, "High Surface Area Silica-Titania Gels by Ambient Pressure Drying For Potential Use as Catalyst" (*Communicated*).

Presentations and Posters at symposia

1. Smitha Sasidharan**,** S. Abhijit, *P. R. Aravind*, P. Shajesh, P. Krishna Pillai, P. Mukundan and K. G. K. Warrier, "Ultra Low Density Silica Aerogels for Various Applications in Fuel Gas Storage and as Electronic Substrates", International conference, 58th Annual Technical Meeting, IIM, Trivandrum, November 17-19, 2004.

2. Smitha Sasidharan**,** *P. R. Aravind*, P. Mukundan and K.G.K. Warrier, "Mesoporous Surface Modified Silica Aerogel Microspheres for Functional Applications", International conference of Indian Ceramic Society, Mumbai, December 21-24, 2004.

3. S. Smitha, P. Shajesh, *P.R. Aravind*, S. Rajesh Kumar and K.G.K. Warrier, "Optimization of aging time and concentration of aging solution in a subcritical drying technique for preparation of silica aerogels", International conference, 58th Annual Technical Meeting, IIM, Trivandrum, November 17-19, 2004.

4. *P.R. Aravind*, S.R. Abhijit, P. Mukundan, P. Krishna Pillai and K.G.K. Warrier "Low Density Silica Aerogel Composites For Possible Gas Storage And Dielectric Substrates" at Indian Ceramic Society (ICS) Seminar (ICCP-2004) held at Mumbal during December 21-24, 2004. **(Got the best poster award)**

5. *P.R. Aravind*, P. Shajesh, P. Mukundan, P. Krishna Pillai**,** K. G. K. Warrier "Preparation of composite aerogels by subcritical drying and its possible application as precursor for high level nuclear waste confinement." At Indian Ceramic Society (ICS) seminar "Ceratec-2007" held in Vishakapatnam. **(Got the best poster award)**